



**TECHNIQUES FOR IMPROVING THE PETROPHYSICAL
EVALUATION OF THE PATCHAWARRA FORMATION
IN THE TOOLACHEE FIELD, COOPER BASIN,
SOUTH AUSTRALIA**

by

ABBAS KHAKSAR
BSc in Mining Engineering
University of Tehran, Iran

OCTOBER 1994

This thesis is submitted in partial fulfilment of the requirements for the
Master of Science Degree in Petroleum Geology and Geophysics
at The University of Adelaide, South Australia.

For Adeleh And Sina

ABSTRACT

The Toolachee Field is the largest liquid-rich gas field in the southern Cooper Basin, South Australia. Due to the extensive depletion of the field, many challenges exist to exploit the remaining reserves in this area.

The objectives of this thesis are: to improve the current formation evaluation methods to explore the bypassed potential gas pays in existing wells, and to investigate the relationship between log-derived porosity and formation pressure in the Patchawarra Formation in the Toolachee Field.

Conventional log-derived lithology overlooks most of thin sandstone beds, leading to underestimation by up to 35 per cent of gross sandstone in each well through the Patchawarra Formation. A new method of log analysis for thin bedded shaly sandstone reservoirs has been successfully applied to commonly available log suites. Without the need for high resolution devices, the thin bed method is able to detect beds as thin as 6 inches. The method gives a more correct picture of reservoir rock distribution, indicating more potential pay than conventional log analysis. Further studies may be focused on petrophysical characteristics and hydrocarbon productivity of thin bedded sandstones in the Patchawarra Formation.

Existing information shows that there is an association between low sonic porosities and low formation pressures within the Patchawarra Formation. Combination of published experimental studies and the available data suggested that the anomalously low log-derived porosities observed in pressure depleted reservoirs are caused by the effect of reduced pore pressure on sonic tool response. The conventional method of porosity calculation from sonic log data in the Cooper Basin may lead to underestimation of the actual porosity of the reservoir rocks in a pressure depleted reservoir. Based on the available data an empirical equation has been derived which corrects the sonic log readings for the effects of formation pressure variation. This equation provides an approximate correction for the conventional sonic porosity in

partially depleted reservoirs in the study area. A detailed multidisciplinary study is required to derive a more correct correction.

The techniques developed in this thesis offer two routes toward maximising the production performance of the reservoirs in the Toolachee Field. These techniques are also likely to be useful in other gas fields within the Cooper Basin and indeed may find application in other basins.

TABLE OF CONTENTS

ABSTRACT	ii
TABLE OF CONTENTS	iv
LIST OF FIGURES	vii
DECLARATION	ix
ACKNOWLEDGMENT	x
CHAPTER ONE INTRODUCTION	1
1.1 Economic Background	1
1.2 Study Objectives	2
1.3 Study Area	3
1.4 Data Collection	3
1.5 Units Of Measurements And Symbols	5
CHAPTER TWO REGIONAL AND PETROLEUM GEOLOGY	6
2.1 Introduction	6
2.2 Stratigraphy	10
2.3 Structure	14
2.4 Exploration History	18
2.5 Reservoirs	19
2.6 Source Rocks	23
2.7 Traps and Seals	24

**CHAPTER THREE LOG-DERIVED LITHOLOGY INTERPRETATION
IMPROVEMENT 25**

3.1	Introduction	25
3.2	Conventional Log-Derived Lithology	27
3.3	Bed Thickness And Log Response	29
3.4	The Binary Lithology Method	34
3.5	Application Of The BLM In The Study Area	37
3.5.1	Process	37
3.5.1.1	Vsh And Filtering	37
3.5.1.2	Scaling Of ΔVsh Curve	40
3.5.2	Results	43
3.6	Reservoir Potential And Industrial Application Of Thin Beds	46

CHAPTER FOUR POROSITY AND PRESSURE DEPLETION 52

4.1	Introduction	52
4.2	Definitions	54
4.3	Pressure Conditions In The Toolachee Field	57
4.4	Data Availability And Limitation	59
4.5	General Observations	62

**CHAPTER FIVE AN INVESTIGATION OF THE RELATIONSHIP
BETWEEN APPARENT POROSITY DECREASE
AND PRESSURE DEPLETION 70**

5.1	Introduction	70
5.2	Porosity Reduction By Additional Compaction	71
5.2.1	Mechanical Compaction	71

5.2.2	Production And Additional Compaction	72
5.2.3	Rock Compressibility In The Cooper Basin	73
5.2.4	Depletion And Additional Compaction In The Study Area	74
5.3	Porosity Reduction Caused By Formation Damage	75
5.3.1	Formation Damage	75
5.3.2	Clay Minerals, Pore Texture And Formation Damage In The Study Area	76
5.4	Porosity Underestimation By The Sonic Log	78
5.4.1	Effect Of Various Factors On Wave Velocity	78
5.4.2	Differential Pressure And Velocity	82
5.4.2.1	Clean Sandstone	82
5.4.2.2	Low Porosity Rocks	86
5.4.2.3	Coal	88
5.4.3	Sonic Porosity And Depletion	89
5.4.3.1	Log-Derived Porosity	89
5.4.3.2	ΔT And RFT Data	90
5.4.3.3	ΔT And Water Saturation	90
5.5	Discussion	93
5.5.1	General	93
5.5.2	Comparison With The Berea Sandstone	94
5.6	Calibration Of The Sonic Log For Pore Pressure	97
5.6.1	General	97
5.6.2	ΔT -Pore Pressure Calibration	98
5.6.3	Notation	100
CHAPTER SIX CONCLUSIONS AND RECOMMENDATIONS		102
6.1	Conclusions	102
6.1.1	Log-Derived Lithology Interpretation Improvement	102
6.1.2	Sonic Porosity And Depletion	103

6.1.2	Sonic Porosity And Depletion	103
6.2	Recommendations	104
6.2.1	Thin Bed Log Analysis	104
6.2.2	Pressure Depletion And Formation Evaluation	104
6.2.2.1	Lithology And Field Control	104
6.2.2.2.	ΔT Calibration	106

REFERENCES	107
-------------------	------------

APPENDICES

ENCLOSURES

LIST OF FIGURES

Fig.		
1.1	Cooper and Eromanga Basins oil and gas fields	4
2.1	Cooper Basin location map	7
2.2	Schematic cross section on the Cooper Basin	9
2.3	Stratigraphic column	13
2.4	Major structural elements in the Cooper Basin	16
2.5	Depth structure map of the Toolachee Field	17
2.6	Well location map	21
3.1	Conventional log-derived lithology	28
3.2	Example of conventional log-derived lithology in Toolachee 6	30
3.3	Effect of minimum resolution on logs values	32
3.4	Effect of thin bed geometry on conductivity tool readings	33
3.5	Binary lithology method process	36
3.6	Cross plot of a and b values with zero monitor	42

3.7	Cross plot of monitor values versus gross sandstone	42
3.8	Comparison of thin bed and conventional methods in Toolachee 6	45
3.9	Hydrocarbon potential of thin beds in Toolachee 15	49
4.1	Sonic porosity data histogram	63
4.2	Pore pressure data histogram	63
4.3	Cross plot sonic porosity versus pore pressure	66
4.4	Cross plot averaged sonic porosity versus pore pressure	66
4.5	Cross plot sonic porosity versus pore pressure for the 73-0 reservoir	67
4.6	Cross plot sonic porosity versus pore pressure for the 73-5 reservoir	67
4.7	Cross plot sonic porosity versus pore pressure for the 74-4 reservoir	68
4.8	Cross plot sonic porosity versus pore pressure for the 74-6 reservoir	68
4.9	Cross plot sonic porosity versus pore pressure for the 75-5 ,6 reservoir	69
4.10	Cross plot sonic porosity versus pore pressure for the 76-4 reservoir	69
5.1	Various factors affecting rock velocity	79
5.2	Application of the sonic log to the estimation of overpressuring	80
5.3	Effect of gas saturation on rock velocity	81
5.4	Rock velocity and pressure (Wyllie et al. , 1958)	83
5.5	Rock velocity and pressure (King, 1966)	84
5.6	Rock velocity and pressure (Christensen and Wang, 1985)	84
5.7	Rock velocity and pressure in Chelmsford granite	86
5.8	Rock velocity and pressure in coal	88
5.9	Cross plot of sonic porosity versus sonic transit time	91
5.10	Cross plot of sonic transit time versus pore pressure	91
5.11	Cross plot of water saturation versus sonic transit time	92
5.12	Cross plot of water saturation versus pore pressure	92
5.13	Comparison effect of pore pressure on sonic transit time for the Berea Sandstone and the Patchawarra Formation reservoirs	95

DECLARATION

This thesis contains no material which has been accepted for the award of any other degree or diploma in any university and, to the best of the my knowledge and belief, the thesis contains no material previously published or written by any other person except where due reference is made in the text of the thesis. The author consents to the thesis being made available for photocopying and loan if accepted for the award of the degree.

Abbas Khaksar

19/10/1994

ACKNOWLEDGMENT

I am most grateful to the Iranian Ministry of Culture and Higher Education for the financial support that make my postgraduate study possible. I also indebted to Dr. William Stuart, the director of the National Centre for Petroleum Geology and Geophysics, for his help, encouragement and friendship during these past two years.

I say thank to the South Australian Department of Mines and Energy and staff at the Santos Ltd. in particular Rolf Schlichting, David Bowyer, Mitchell Chamalaun and the librarians for providing data and access to facilities for this thesis.

I would like to thank to Andrew Mitchell, my academic supervisor, for his assistance, criticism, encouragement and careful editing of the manuscript. I wish to thank to the academic staff and students at the National Centre for Petroleum Geology and Geophysics, especially Dr. Nick Lemon, Dr. Jorg Schulz-Rojahn, Dr. Sukru Apak and Sarah Ryan-Gregory for their advice and assistance throughout the course of this study.

I would especially like to thank to Graham and Vonni Blanchard for their warm friendship that make life easier for my family and myself during the past two years.

I am always indebted to my parents, brothers and sister for their support and encouragement in my education career. Finally, I particularly thank to my wife for her patience and strength throughout the course of this study.



CHAPTER ONE

INTRODUCTION

1.1 ECONOMIC BACKGROUND

The Cooper Basin, located in South Australia and Queensland, is one of the Australia's major petroleum provinces. To date 100 gas and 10 oil fields have been discovered in the Cooper Basin. These fields contain 6 TCF of sales gas and 300 MMSTB of oil and gas liquids (Laws, 1989). At present, two Australian states, South Australia and New South Wales, depend on gas supplies from the region.

The Toolachee Field is the largest liquid-rich gas field in the Cooper Basin, with 217 BCF of remaining recoverable raw gas reserves (as at 31/12/91). The combined liquid petroleum gas (LPG) and condensate production rate in this field is only exceeded by that from the Tirrawarra Field (Domato and Male, 1992).

Optimising development and hydrocarbon recovery from the Toolachee Field is extremely important to the operating companies in the Cooper Basin. Due to the

extensive depletion of the field (approximately two-thirds of the recoverable raw gas having now been produced) many challenges exist to fully exploit the remaining reserves. Development of unaccessed gas reserves in both existing and proposed additional wells is important in optimising the production performance of the field (Domato and Male, 1992).

Formation evaluation plays a crucial role in the identification and measurement of gas reserves. This thesis focuses on the limitations of, and possible improvements to, several aspects of formation evaluation, as currently practiced in the Toolachee Field. The techniques developed here using the Toolachee Field as a test site are also likely to be useful in other Cooper Basin gas fields, and indeed may find application in other basins.

1.2 STUDY OBJECTIVES

The aim of this study is to improve two aspects of the current formation evaluation routine in order to assess more accurately the gas reserves in the Patchawarra Formation in the Toolachee Field. More specifically the objectives are:

- I. To develop and test an algorithm for lithology interpretation from well logs to identify thin sandstones which are not recognised by conventional log analysis and hence may represent additional hydrocarbon pay.

II. To investigate the relationship between anomalously low log-derived porosity and decrease in reservoir pressure observed in depleted reservoirs, in order to improve formation evaluation in such reservoirs.

1.3 STUDY AREA

The study area encompasses the Toolachee Field in the south eastern Cooper Basin. The Toolachee Field is located approximately 60 km south east of the Moomba gas plant and covers an area of nearly 130 km² (Figure 1.1). It is a north-south oriented field situated on a structural high on the Toolachee Trend at the east end of the Tennapera Trough (Figure 2.4). The Toolachee Field is the fifth largest known gas field in South Australia. Gas production comes from the Patchawarra and Epsilon Formations.

1.4 DATA COLLECTION

The information used in this study consisted of digital wireline logs, composite well logs, core descriptions, drill stem and repeat formation test results and the output from conventional log analysis. Wells in the study area usually have only a limited suite of wireline logs, typically including the gamma ray, spontaneous potential (SP), shallow and deep resistivity, sonic and caliper logs.

The majority of the data, including wireline, composite and core logs, were already available in the library of the National Centre for Petroleum Geology and Geophysics (NCPGG). This information was gathered during previous studies on the porosity and

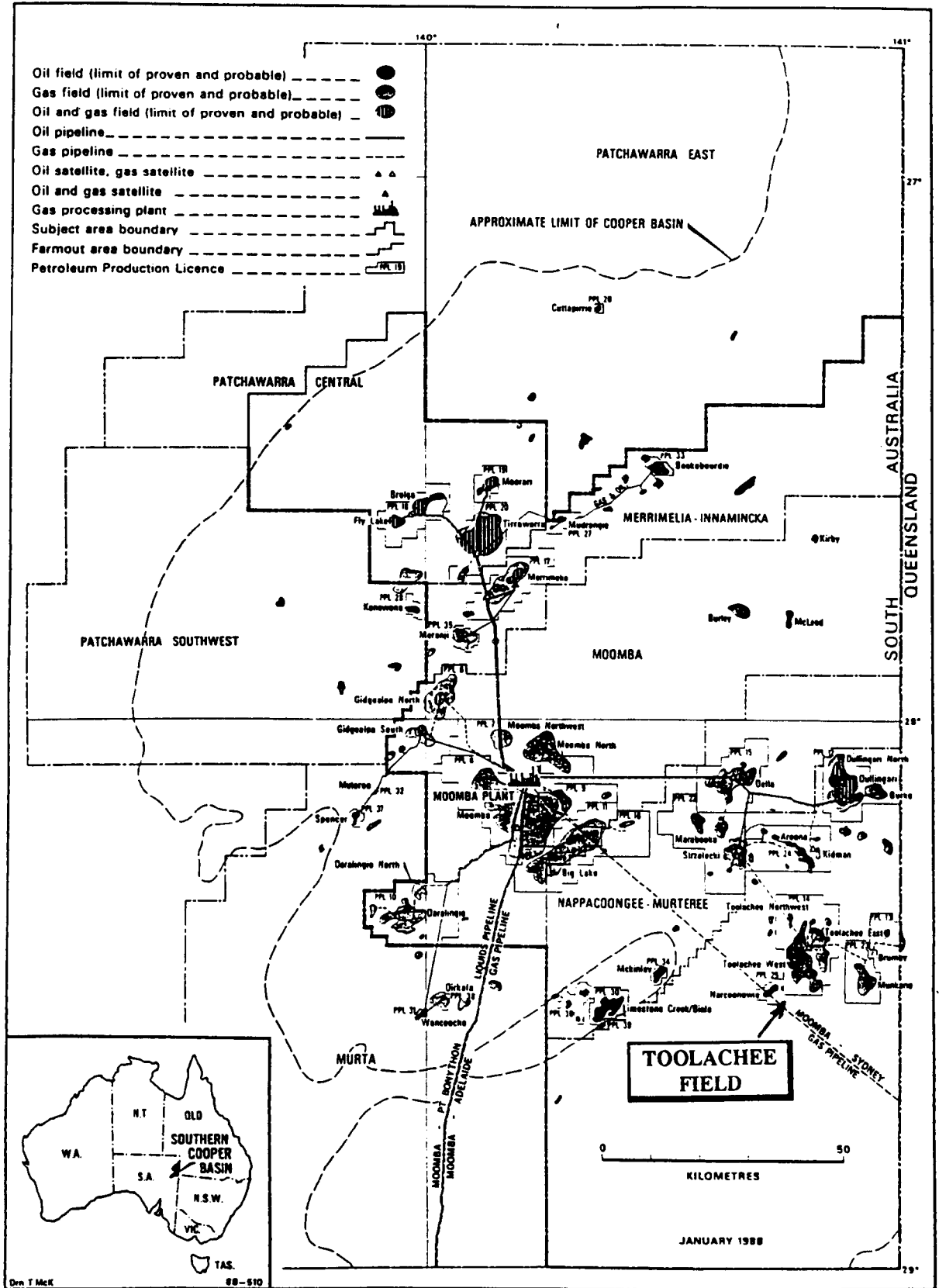


Figure 1.1 Oil and gas fields of the Cooper and Eromanga Basins, South Australia (from Northcott and McDonough, 1989).

permeability of Permian sandstones in the southern Cooper Basin undertaken by staff and students of the NCPGG in recent years. Additional digital wireline logs were donated by Wiltshire Geological Services. Drill stem and repeat formation test data and the results of conventional log analysis were obtained from Santos Ltd. and the Cooper Basin open file database in the library of the Department of and Mines and Energy, South Australia.

1.5 UNITS OF MEASUREMENTS AND SYMBOLS

Most of the data in the study area were measured using the British system of units. The traditional API units were also used particularly for hydrocarbon reserves and well logs, and metric units appear in some of the statistical data. These variations are reflected in the units of measurements quoted in the thesis. Appendix A lists abbreviations, symbols and conversion factors for these units.

CHAPTER TWO

REGIONAL AND PETROLEUM GEOLOGY

2.1 INTRODUCTION

The Cooper Basin is a northeast trending Permo-Triassic intracratonic basin in the north-east corner of South Australia and south-west of Queensland (Figure 2.1). The basin covers 130,000 km², of which about 50,000 km² is located in South Australia. It lies unconformably over the early Paleozoic sediments of the Warburton Basin and is overlain disconformably by the Early Jurassic to Late Cretaceous sediments of the central Eromanga Basin (Battersby, 1976) (Figure 2.2).

Three major depocentres, the Patchawarra, Nappamerri and Tennapera Troughs, are separated by the structurally high Gidgealpa-Merrimelia-Innamincka (GMI) and Nappacoongee-Murteree (MN) Trends. The troughs contain up to 8200 ft of sediments laid down during three non-marine megacycles which occurred between the Late

Carboniferous and the Early Triassic. The sediments consist of shales, siltstones, sandstones and coals deposited in glacial, fluvial and lacustrine environments (Kapel (1972), Thornton (1979)). Table 2.1 shows some key statistics for the Cooper Basin.

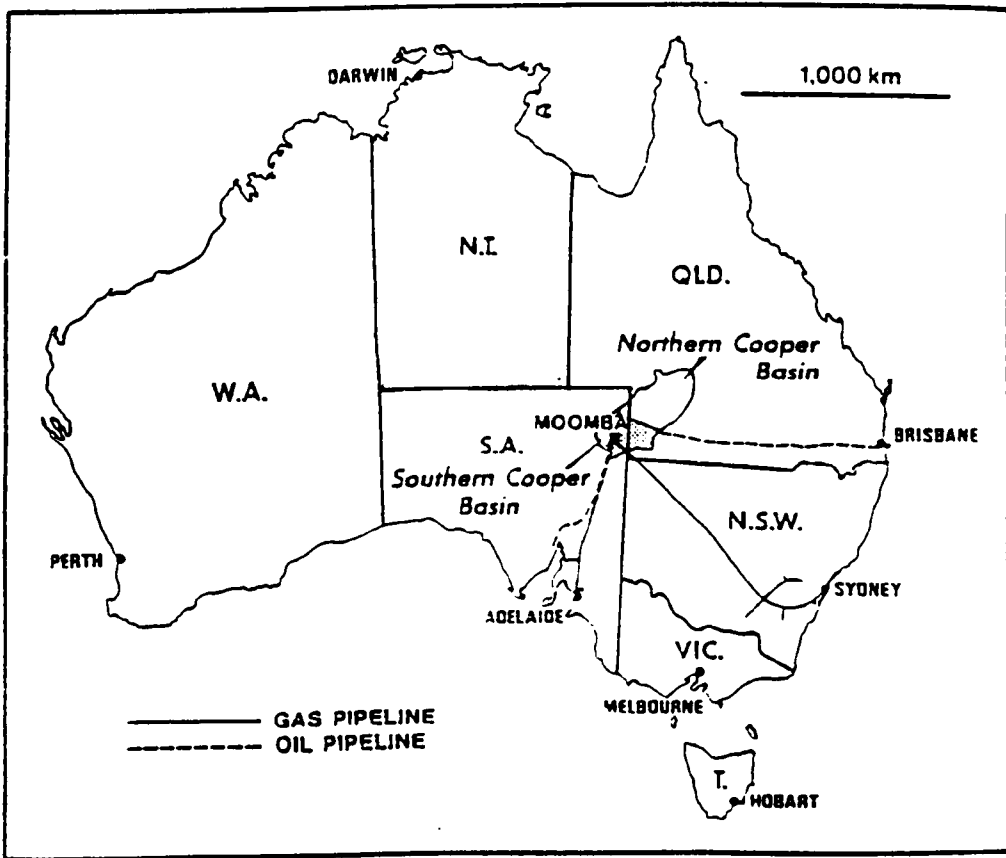


Figure 2.1 Location map of the Cooper Basin.

Age:	Permo-Triassic
Basin type:	Intracratonic
Depositional setting:	Non-marine
Reservoirs:	Non-marine sandstones
Major trap type:	Faulted anticlines
Seals:	Non-marine shale and thick coals (up to 100 ft)
Depth to target zones:	4100-12000 ft
Maximum thickness:	8200 ft
Area in South Australia:	50 000 km ²
Number of wells:	770
Seismic coverage:	71000 km total
Remaining reserves: (Santos Ltd. estimates as at 1/1/92, Cooper and Eromanga Basins)	2.58 TCF sales gas, 79 MMSTB LPG, 47 MMSTB condensate, 48.4 MMSTB crude oil, 230.8 BCF ethane
Undiscovered reserves (50% probability) (MESA estimates at 1/1/91, Cooper and Eromanga Basins)	1846 BCF sales gas, 166.7 MMSTB crude oil

Table 2.1 Cooper Basin key statistics (from MESA, 1992).

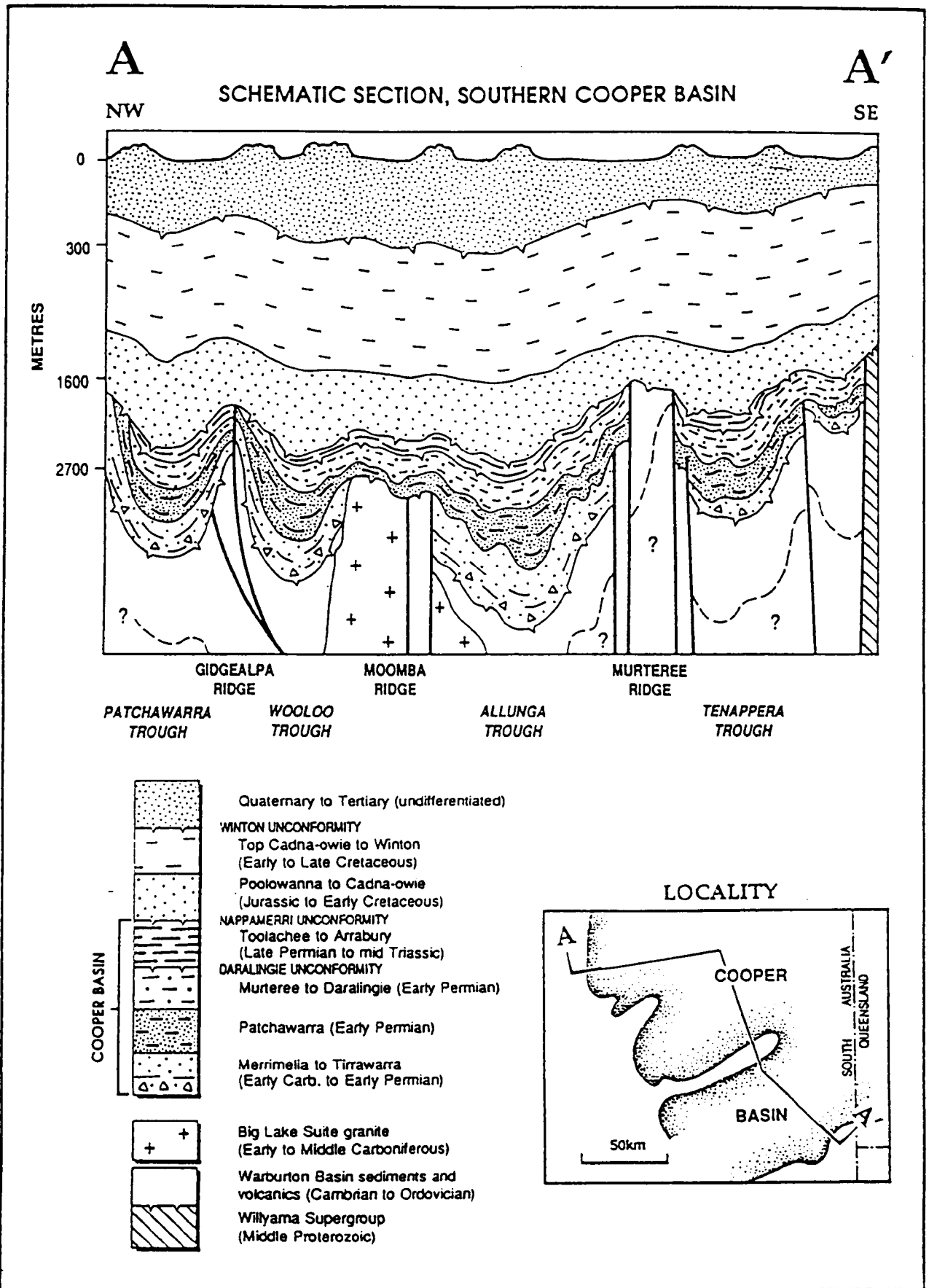


Figure 2.2 Schematic section across the Cooper Basin (From MESA, 1993).

2.2 STRATIGRAPHY

The Cooper Basin sequences range in age from the Late Carboniferous to Middle Triassic. They were deposited mostly in flood plain and lacustrine environments (Battersby, 1976). The Pre-Permian metasediments of the Warburton Basin underlie the Cooper Basin, and are generally considered to represent economic basement (Figure 2.2).

The Merrimelia Formation of Late Carboniferous age unconformably overlies the basement sediments (Figure 2.3). It consists of glacial, paraglacial and glacial-aeolian sediments (Williams et al. , 1985).

The Tirrawarra Sandstone of Early Permian age is thought to conformably overlie the Merrimelia Formation (Battersby, 1976) (Figure 2.3). It comprises quartz sandstone with minor intercalations of shale and coal (Thornton, 1979), which indicate a gradation from a braided to a meandering fluvial system. The Tirrawarra Sandstone is restricted to the south and southwestern parts of basin and it is not present in the Toolachee Field. Its absence is interpreted as being due to non-deposition over a pre-existing structure (Apak, 1994).

The Patchawarra Formation interfingers with sediments of the Tirrawarra Sandstone (Figure 2.3). It is composed of a rhythmic successions of sandstone, siltstone, shale and coal. Rocks of this formation were deposited in meandering stream, deltaic and lacustrine

environments (Thornton, 1979). Apak et al. (1993) recognised five chronostratigraphic units within the Patchawarra Formation.

In the Toolachee Field only the top two units of the Patchawarra Formation are present (Apak, 1994). The absence of the older units is due to onlap onto the fault-block highs, with additional section preserved progressively downflank as a result of synsedimentary faulting. The interbedded coals and shales with thin sandstones which make up unit 2 of the Patchawarra Formation in the Toolachee Field were deposited in an overbank environment. Unit 1 in the Toolachee Field consists of sandstones intercalated with silty shales and thin coals. These sediments are interpreted as having been deposited in distributaries, distributary mouth bars and shoreline environments (Apak, 1994).

The Murteree Shale is a thick-lacustrine unit, which conformably overlies the Patchawarra Formation (Figure 2.3) and comprises light to dark shales with interbedded micaceous siltstones (Thornton, 1979). It is interpreted to have been deposited in a permanent body of water fed by sediments from an deltaic alluvial plain (Thornton, 1979).

The Epsilon Formation conformably overlies the Murteree Shale (Figure 2.3) and is overlain by the Roseneath Shale (Thornton, 1979). The Epsilon Formation consists mainly of siltstone to fine sandstone with coarser-grained sandstone and coal deposited in flood plain to shoreline environments (Battersby, 1976). The Roseneath Shale has essentially the same lithological and paleo-environmental characteristics as the Murteree

Shale but the depositional basin was probably smaller than during deposition of the Murteree shale (Battersby, 1976 and Thornton, 1979).

Conformably overlying the Roseneath Shale is the Daralingie Formation (Figure 2.3). It comprises a succession of thin sandstones, siltstones, shales and coals which reflect a regressive environment similar to the lower part of the Epsilon Formation (Thornton, 1979). The upper part of the Daralingie Formation contains thicker sandstones and coals which were deposited in lower deltaic and flood plain environments (Battersby, 1976).

The Toolachee Formation unconformably overlies the Daralingie Formation (Figure 2.3) and consists of fresh water sandstones, siltstones, shales and coals (Battersby, 1976), deposited in fluvial, point bar, overbank and backswamp environments (Stuart (1976), Thornton (1979)).

The final phase of sedimentation within the Cooper Basin resulted in the deposition of the Nappamerri Group, which consists of sandstones, siltstones and shales deposited in fluvial and lacustrine conditions during the Early to Mid Triassic (Thornton, 1979).

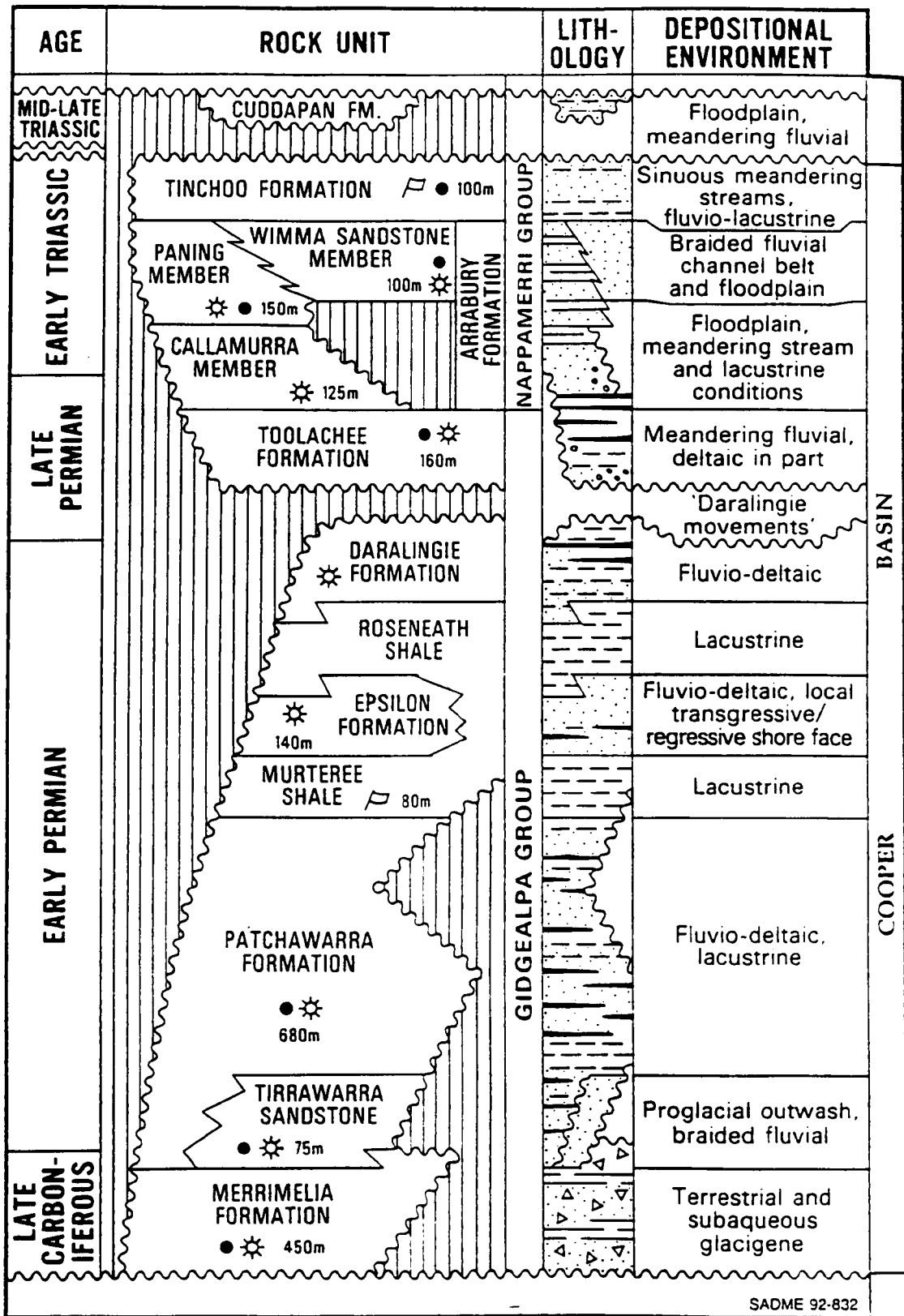


Figure 2.3 Cooper Basin stratigraphic nomenclature (from MESA, 1992).

2.3 STRUCTURE

In the southern part of the Cooper Basin the major structural elements are oriented northeast-southwest (Stuart, 1976). Based on geophysical studies six major structural zones have been recognised. These are the Gidgealpa-Merrimelia-Innamincka (GMI) and Murteree-Nappacoongee (MN) Anticlinal Trends, the Patchawarra, Nappamerri and Tennapera Troughs, and the Karmona Anticlinal Trend in the north east corner (Kapel (1966), Stuart (1976), Thornton (1979)) (Figure 2.4).

The GMI Anticlinal Trend is the most prominent positive feature in the basin, and comprises several structural culminations. It is very steep-sided, largely fault controlled and has a maximum relief of over 3280 ft (Figure 2.4). The MN Anticlinal Trend is S-shaped, plunging northeast and southwest from Murteree Ridge (Figure 2.2). It has a maximum relief of about 2600 ft northwest of the Della Field(Figure 1.1). The Karmona Anticlinal Trend separates the south and north parts of the Cooper Basin. Along its southern flank it is partly defined by a fault with a maximum throw of more than 1500 ft at the level of the 'P' Horizon (near top Toolachee Formation). This fault forms part of a major lineament that transects the Australian continent (Thornton, 1979).

The Nappamerri Syncline is nearly 300 km long and up to 100 km wide. The maximum proven thickness of Permian sediments in the Cooper Basin occurs in this structural province (Thornton, 1979). The Patchawarra Syncline runs sub-parallel to the GMI

Anticlinal Trend (Figure 2.4) and attains a maximum depth of 10500 ft below sea level at its northeastern extremity. Secondary asymmetrical fold structures such as that hosting the Tirrawarra Field occur near the axis of the trough (Stuart, 1976 and Thornton 1979). The Tennapera Trough is the main synclinal feature along the southern flank of the Cooper Basin, curving around the northern end of the Toolachee Anticlinal Trend; toward the northeast, the Tennapera Trough broadens and is subdivided by the Tickalara and Wolgolla Anticlinal Trends (Figure 2.4). It has a maximum depth of about 7200 ft below sea level (Thornton, 1979).

The major anticlinal structures are associated with faults, which become increasingly more abundant with depth. Rejuvenation of pre-existing basement structures is a pervasive characteristic of the Cooper Basin (Battersby (1976), Stuart (1976)). There were several phases of mild deformation prior to and during Permian times (Stuart, 1976). Structures within the basin show evidence of fold interference patterns, thrusting and compressional wrench tectonics, indicating that the structural style within the Cooper Basin is complicated and can not be explained by single tectonic regime (Apak, 1994).

Structure within the Toolachee Field is also complex and comprises at least five separate north-south trending anticlinal culminations covering an area of approximately 130 km². The structures are separated from each other at the seismic 'Z' horizon (near top of the Pre-Permian basement) by faults which were active throughout deposition of the lower part of the Patchawarra Formation (Figure 2.5).

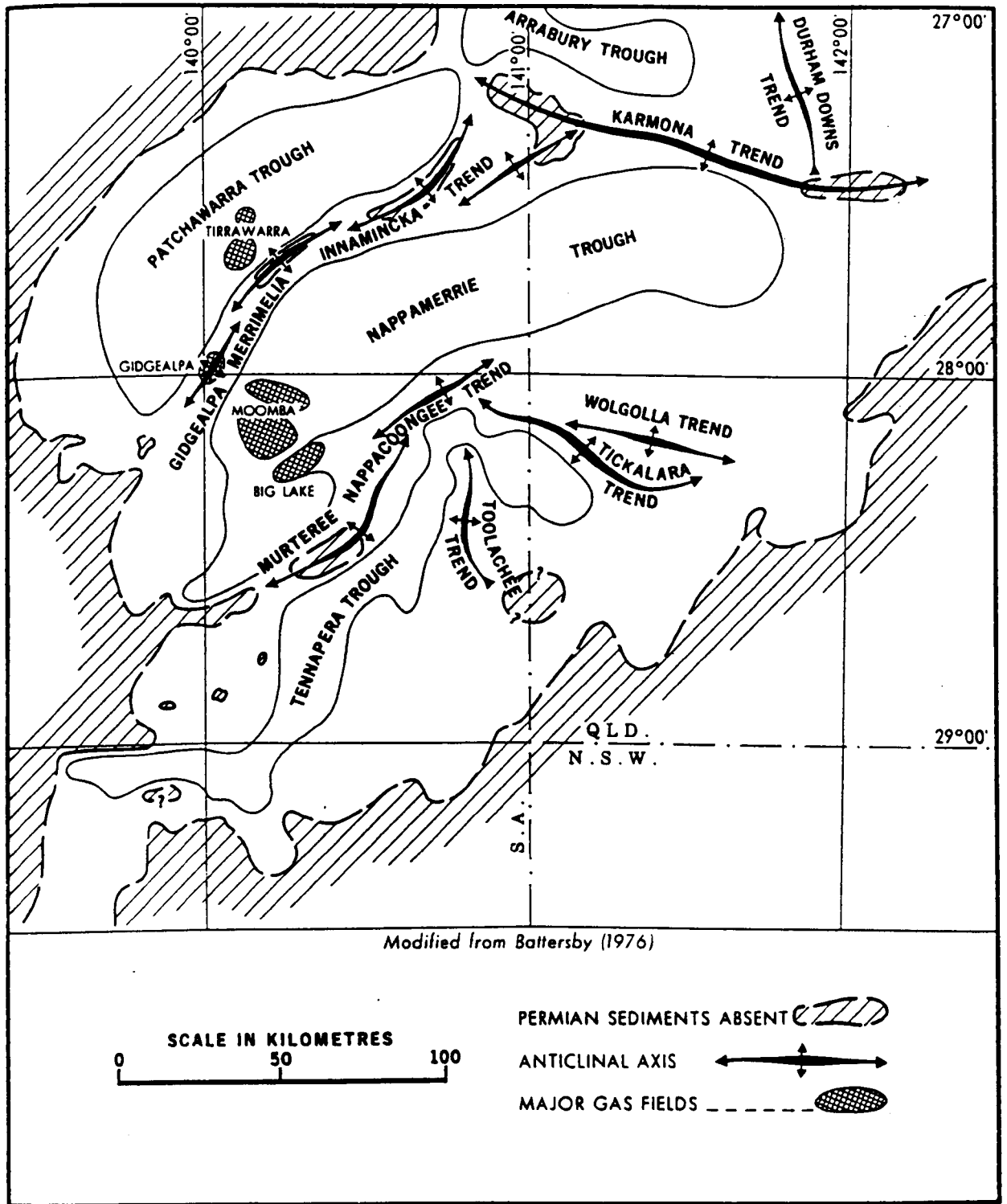


Figure 2.4 Major structural elements in the Cooper Basin (after Thornton, 1979).

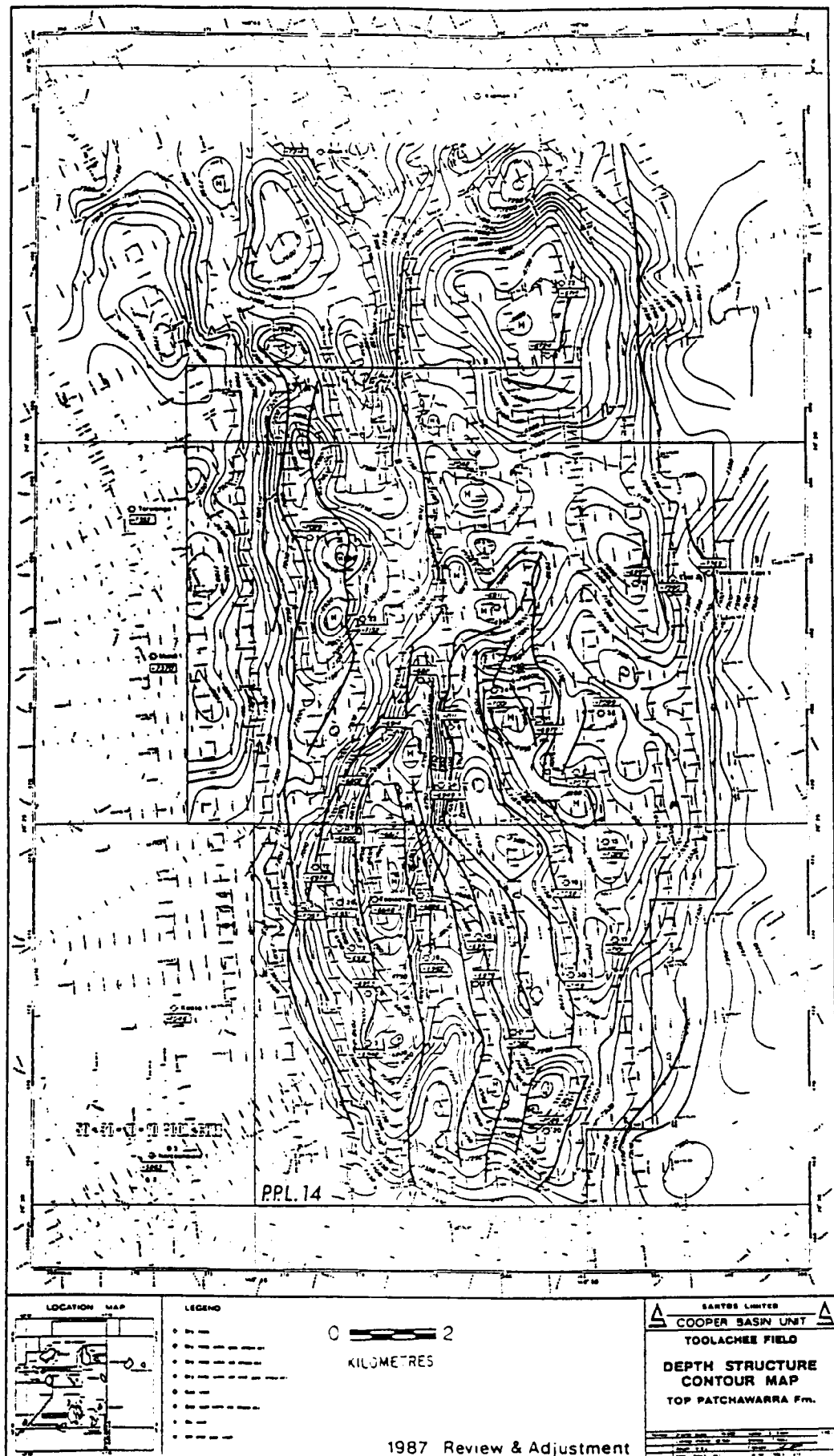


Figure 2.5 Depth-structure map of the Toolachee Field (from Santos Ltd. 1993).

Minor post Patchawarra Formation faulting also occurred, with some faulting continuing through deposition of the Epsilon Formation (Battersby (1976), Devine and Gatehouse (1977), Morton (1983)).

2.4 EXPLORATION HISTORY

Systematic exploration in the Cooper Basin commenced in 1958 and has continued more or less strongly to the present time. The first exploration well, Innamincka 1, was drilled in 1959 and the first commercial gas discovery, Gidgealpa 2, was made in 1963.

Following the large gas discovery at Moomba, two long pipelines were constructed to provide natural gas for industrial and domestic use in South Australia and New South Wales. Since then the Cooper Basin has become the major source of gas supplies in South Australia. In recent years natural gas from the basin has supplied over 30 per cent of the state's total energy needs (MESA, 1991).

The discovery of oil at Tirrawarra in 1970 was a major boost to exploration in the Cooper Basin. However, despite further oil and condensate discoveries at Moorari and Fly Lake, natural gas is still the main product from the Cooper Basin (Hollingsworth, 1989). To date 790 wells have been drilled and 71000 km seismic have been acquired (MESA, 1993).

The first exploration well in the Toolachee Field, Toolachee-1, was drilled in 1969 and flowed at rates of up to 7.0 MMCFD on drill stem tests over the Patchawarra Formation.

The field began producing in 1984. To date 50 wells (Figure 2.6) have been drilled in the field of which 36 are producing. The estimated initial gas in place is 828.9 BCF and approximately two-thirds of the recoverable raw gas has been produced (Domato and Male , 1992) (Table 2.2).

2.5 RESERVOIRS

Multi-zone fluvial sandstones in the Tirrawarra, Patchawarra and Toolachee formations provide the main reservoir rocks within the Cooper Basin. The Tirrawarra sandstone in the Tirrawarra Field holds 95 per cent of oil reserves while the Toolachee-Daralingie and Patchawarra Formations hold 40 and 30 per cent of the gas reserves in the Cooper Basin respectively (Heath, 1989).

Most of the commercial petroleum discoveries occur in channel and point bar sandstones (Stuart (1976), Battersby (1976)). The other important reservoirs are deltaic sequences comprising shoreline sandstones, and distributary and delta mouth bar deposits, which occur mainly within the Epsilon, the Daralingie and the upper part of the Patchawarra Formations (Stuart (1976), Stuart et al. (1992), MESA (1993)).

NUMBER OF WELLS DRILLED	50
<i>PRODUCING WELLS</i>	36
<i>NUMBER OF PRODUCING AND SHUT-IN WELLS WHICH PRODUCE WATER</i>	22
ORIGINAL GAS IN PLACE (BCF)	828.9
<i>PATCHAWARRA FORMATION</i>	800.6
<i>EPSILON FORMATION</i>	27.2
<i>TOOLACHEE FORMATION</i>	1.1
RECOVERABLE GAS IN PLACE (BCF)	585
<i>CUMULATIVE PRODUCTION AS AT 31/12/91 (BCF)</i>	368
<i>REMAINING RESERVES AS AT 31/12/91 (BCF)</i>	217
CURRENT PRODUCTION RATE	
<i>RAW GAS (MMSCF/D)</i>	75
<i>SALES GAS (MMSCF/D)</i>	52
<i>LPG (BBL/D)</i>	1960
<i>CONDENSATE (BBL/D)</i>	1720

Table 2.2 Toolachee field key statistics (from Domato and Male, 1992).

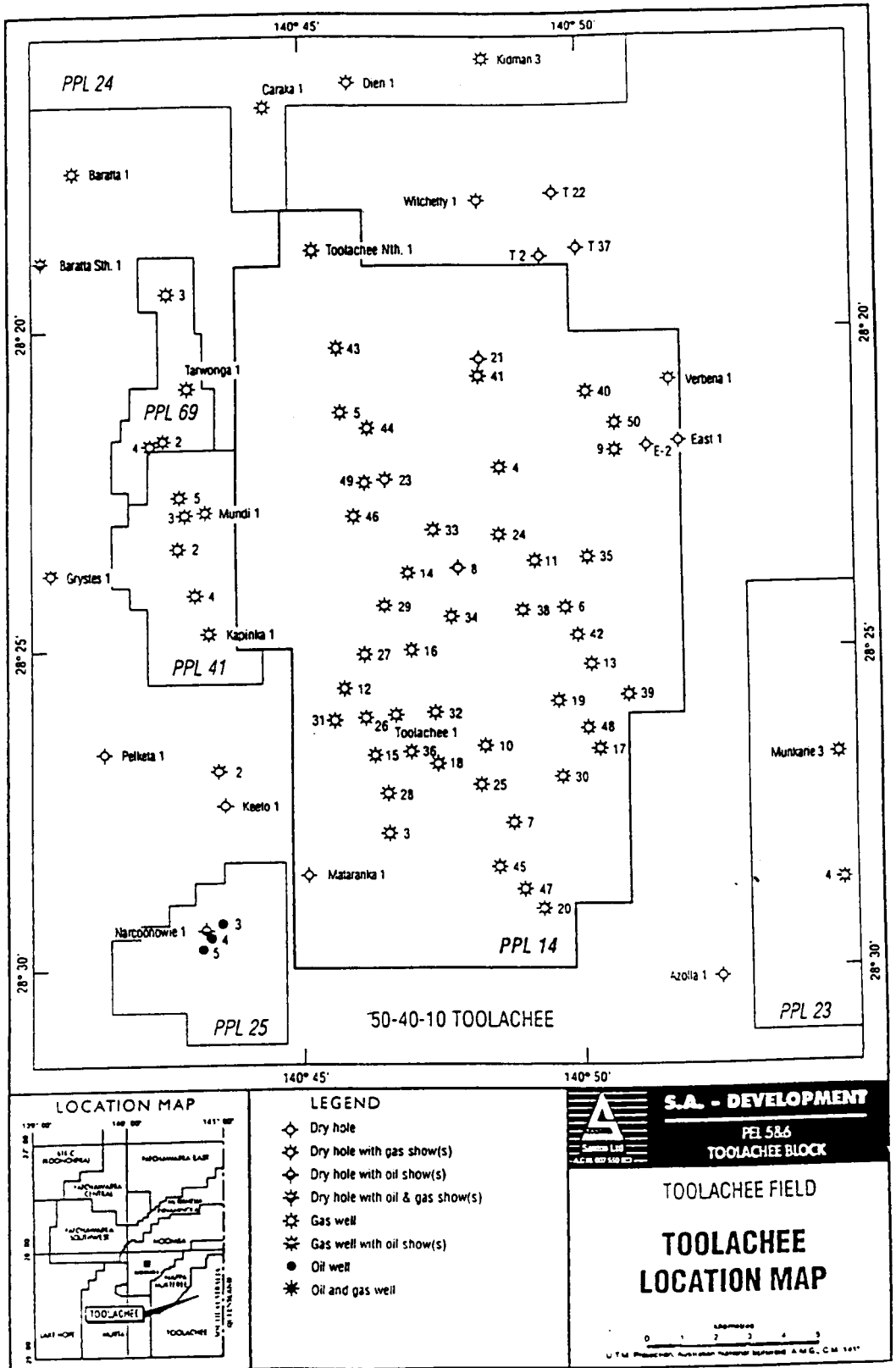


Figure 2.6 Well location map of the Toolachee Field (from Santos Ltd., 1993).

Reservoir properties in the Cooper Basin are controlled by the complex interaction of sedimentary factors, diagenesis and structural development (Stuart et al. , 1992). Primary (original intergranular) porosity, dissolution porosity and microporosity are recognised in the sandstone reservoir rocks of the Cooper Basin. Microporosity within clay minerals (dickite, kaolinite) in the reservoir rocks can provide significant storage space for gas (Schulz-Rojahn, 1991).

Reservoirs in the Cooper Basin are dominantly low-porosity, low-permeability sandstones. Ambient core porosity averages 10.7 per cent and permeability 30 md, with over 75 per cent of sandstones having permeabilities of less than 5 md. Despite its overall poor reservoir characteristics, the Cooper Basin is one of Australia's most important petroleum provinces (Stuart et al. , 1992).

In the Toolachee Field, the main reservoirs occur in sandstones of the Patchawarra Formation. Ten reservoirs are recognised. These are, from the top, the 73-0, 73-5, 74-4, 74-5, 74-6, 75-5, 75-6, 76-4, 76-5 and 81-6 reservoirs. Table 2.3 summarises the reservoir characteristic of these sandstones within the Patchawarra Formation in the study area.

<i>RESERVOIR</i>	<i>TOTAL PAY (ft)</i>	<i>AVERAGE POROSITY (percent)</i>	<i>AVERAGE WATER SATURATION (percent)</i>
73-0	229	12.7	25.2
73-5	409	12.2	19.0
74-4	437	13.3	15.7
74-5	18	12.8	17.4
74-6	704	13.5	18.1
75-5	48	10.7	18.9
75-6	347	12.6	24.4
76-4	435	11.7	30.8
76-5	2	8.6	39.7
81-6	7	12.6	30.8

Table 2.3 Summary of the parameters of the ten sandstone reservoirs within the Patchawarra Formation in the study area (from Santos .Ltd. , 1993).

2.6 SOURCE ROCKS

Hydrocarbons in the Cooper Basin are generally thought to have originated from the abundant dispersed organic matter in intraformational fluvial and deltaic shales and also possibly from the coals of the Toolachee and Patchawarra formations (Hunt et al. , 1989). The amount of total organic carbon, TOC, varies between 1 and 5 per cent (Jenkins,

1989) and the kerogens are mainly of type III (Hunt et al. , 1989). Volumetrically significant generation of oil from this organic matter type occurs over a maturity range indicated by vitrinite reflectances of 0.7 and 1.0 per cent (Jenkins, 1989). Geochemical and geological studies show that both the crude oil in the Tirrawarra Formation and the gas reservoired in the Patchawarra Formation are likely to have been derived from the Patchawarra Formation (Battersby (1976), Hunt et al. (1989)).

2.7 TRAPS AND SEALS

Anticlinal and faulted anticlinal traps form most of the hydrocarbon targets explored to date in the Cooper Basin, but potential remains high for discoveries in stratigraphic and subconformity traps (Stuart (1976), Heath (1989)), especially where the Permian sediments pinch out against the overlying Eromanga Basin succession (MESA, 1992).

Intraformational shales and coals form local seals in the major reservoir units (MESA, 1992). The Murteree and the Roseneath Shales and the Arrabury Formation in the Nappamerri Group form regional seals for the Patchawarra, Epsilon and Toolachee Formations respectively (Heath, 1989).

CHAPTER THREE

LOG-DERIVED LITHOLOGY INTERPRETATION IMPROVEMENT

3.1 INTRODUCTION

In quantitative log analysis, the lithology of a zone of interest is very important. Based on the lithology interpreted from the well logs, petrophysicists calculate the parameters required to quantify the amount of hydrocarbons in a reservoir, such as porosity, water saturation, moveable hydrocarbon etc. Misinterpreting a hydrocarbon-bearing zone as a non-reservoir interval and vice versa, may make a significant difference to estimated reserves. In fact, an accurate interpretation of lithology is the first step in a reliable formation evaluation.

In the Patchawarra Formation in the Toolachee Field the gross sandstone thickness indicated by conventional lithological interpretation of the well logs consistently underestimates the true thickness, as shown by cores, by up to 36 per cent. The

sandstone missed by the log interpretation occurs in thin beds which are at or below the resolution of the logging tools. Despite their thickness, there is evidence to suggest that at least some of these beds may act as effective reservoirs. If this is the case, then conventional lithological analysis of the logs will lead to a significant underestimation of reserves (Table 3.1).

<i>Well</i>	<i>Cored Interval (ft)</i>	<i>Gross Sandstone Thickness (ft)</i>		<i>Error</i>
		<i>Core</i>	<i>Log</i>	
<i>Toolachee-3 (389)</i>	267	147	112	24%
<i>Toolachee-5 (193)</i>	185	83	58	30%
<i>Toolachee-6 (362)</i>	307	148	95	36%

Table 3.1 Comparison between total sandstone thickness from conventional log analysis and core descriptions for representative wells in this study. Figures in bracket represent the thickness of the Patchawarra Formation (feet) in each well.

In order to improve log-derived lithology in the Patchawarra Formation in the Toolachee Field, a careful comparison was first made between the core lithology and the log-derived lithology obtained from the composite logs in wells with a relatively

long cored interval through the Patchawarra Formation. This comparison provided an overview of the ability of the conventional log-derived lithology to detect the sandstone beds in the study area.

The binary lithology method of Bateman (1990), which was developed for shaly sandstone sequences, was applied to a selected well. The results were encouraging, and the method was then applied to two other wells in which a substantial interval of the Patchawarra Formation had been cored. Comparison of log-derived lithology using this algorithm with core lithology provided guidelines for modification and calibration of the algorithm which will allow it to be used throughout the study area. The log analysis, programming and the other facilities available in the GEOLOG log analysis software package were widely used at this stage.

Application of the thin bed algorithm to detect thin beds shows that the method gives a more correct picture of reservoir rock distribution, and reveals more potential pay, than the conventional log analysis.

3.2 CONVENTIONAL LOG-DERIVED LITHOLOGY

The gamma ray and sonic logs are the two well logs commonly used in formation evaluation within the study area. The gamma ray log is used to determine lithology. A cut-off of 100 API units is commonly used to discriminate between sandstones and shales. On this basis, any gamma ray readings greater than 100 API are not identified as sandstone (Figure 3.1). This assumption provides a quick look approach for

lithology interpretation from the gamma ray, but is not adequate for detailed formation evaluation particularly in thinly bedded shaly sandstone sequences.

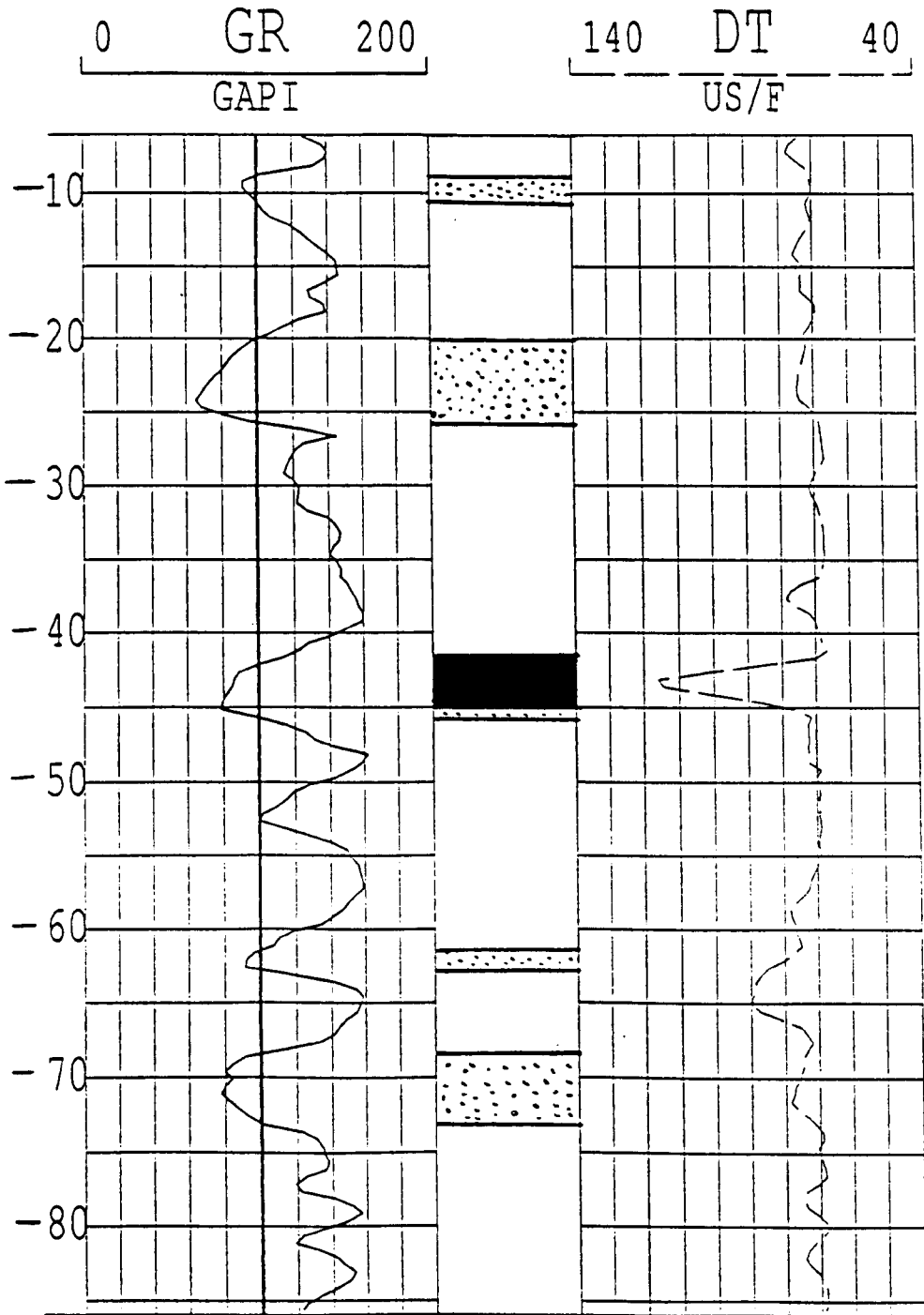


Figure 3.1 Conventional log-derived lithology using gamma ray and sonic logs in the Cooper Basin.

For instance, in a 50 feet thick interval from the upper part of the Patchawarra Formation in the gas producing well Toolachee-6, the log-derived lithology indicates a total of just 8 feet sandstone, whereas the core lithology shows 20 feet of sandstone (Figure 3.2).

Figure 3.2 shows that conventional wireline lithology analysis is unable to identify thin sandstone beds in interbedded shaly sandstone intervals where the thickness of the individual beds is less than 2 feet, resulting in an excessively pessimistic evaluation of sandstone percentage. Changing the gamma ray cut-off from 100 to 120 or 130 API units will detect some of the overlooked thin sandstone beds, but several shale intervals will then be misinterpreted as sandstone.

3.3 BED THICKNESS AND LOG RESPONSE

Conventional lithology interpretation from well log data becomes unreliable when the thickness of the target bed is below the vertical resolution limit of the logging tools. This limit is related to the dimensions of the zone contributing significantly to the measurement made at a point (Table 3.2). A bed which is thinner than this limit may still be identified but the value indicated on the log for this bed will be incorrect. The error depends on the contrast in the property being measured, the thickness of the thin bed and the adjacent formation properties, tool design, logging method and post logging signal processing (Bateman, 1990).

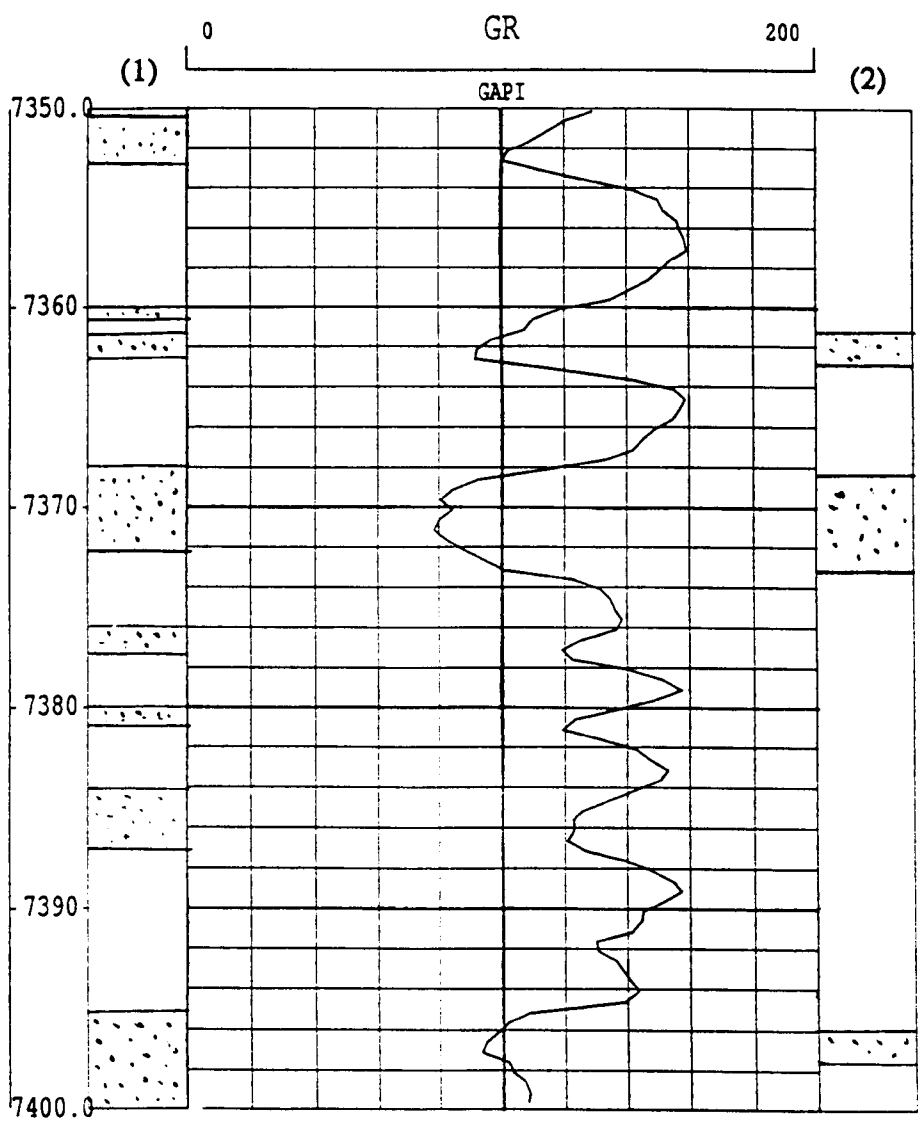


Figure 3.2 A comparison between core lithology and conventional log-derived lithology in the Patchawarra formation in Toolachee 6 from 7350 to 7400 ft (logger depth). (1) core lithology (from Alsop, 1990), (2) conventional log-derived lithology (from Toolachee 6 composite log profile).

<i>Tool</i>	<i>Emitter-Receiver Spacing (ft)</i>	<i>Minimum Vertical Resolution (ft)</i>
<i>Microlog</i>	0.1-0.2	0.5
<i>Sonic</i>	2	2
<i>Gamma ray</i>	-	2
<i>Density (FDC)</i>	1.5	2
<i>Neutron (CNL)</i>	1.6	2
<i>Laterolog D</i>	2.7	3.3
<i>Induction D</i>	3.3	6

Table 3.2 Minimum vertical resolution of some common logging tools under normal condition (modified from Hartman 1975, Rider 1986, Bateman 1990).

For instance, an induction tool (low vertical resolution) opposite a thin, resistive, sandstone bed in a shale sequence (Figure 3.3), shows a moderate to small deflection, whereas on a microlog (high vertical resolution) this becomes a fully developed peak (Rider, 1986).

Hence, where lithology varies rapidly and individual beds are thin, the log values become averaged, particularly those derived from long-spaced tools. The log will approximate the value of the dominant lithology (Hartman, 1975). Figure 3.4 shows an example of such averaging. Consider a 3 feet thick hydrocarbon-bearing sandstone of 20 Ω m resistivity sandwiched between shale shoulder beds of 1 Ω m.

Induction D tool theory shows that in this case about half the conducting contribution comes from the shale and about half from the sandstone (Anderson 1986).

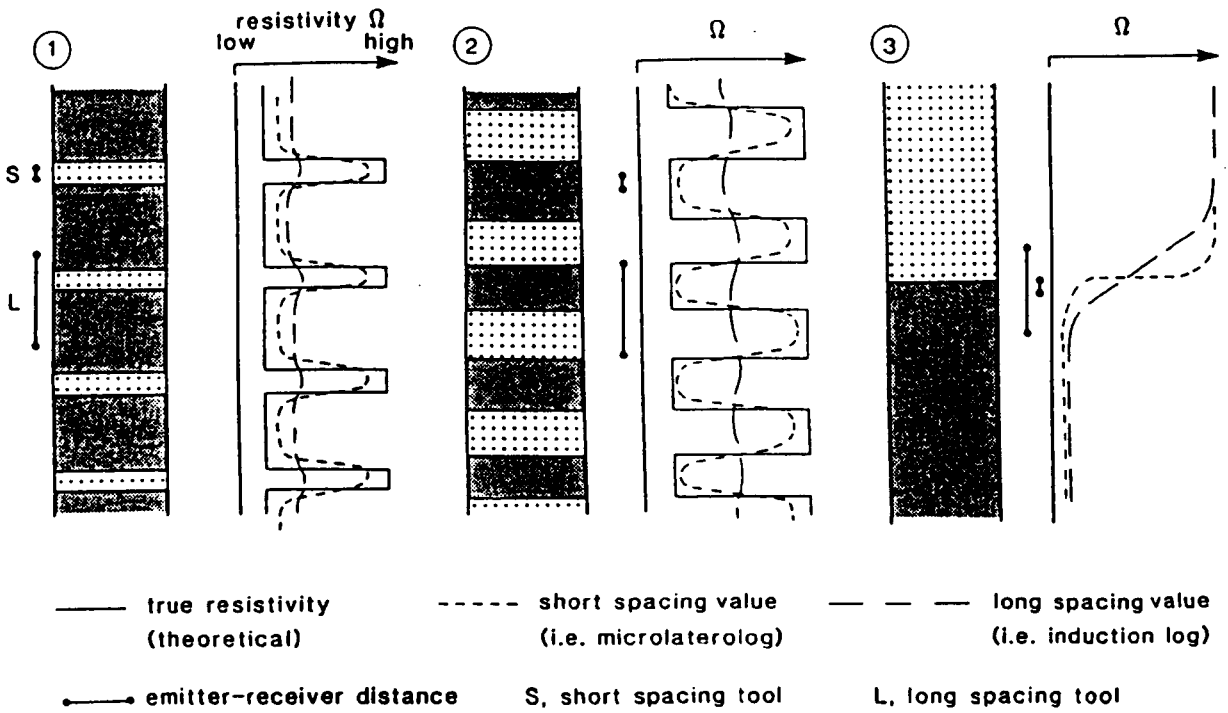


Figure 3.3 The effect of minimum resolution on logging-tool values for various scales of interbedding; (1) fine interbeds, (2) coarse interbedding, (3) single bed boundary (from Rider, 1986).

However, the experimental studies show that the induction tool response in the sandstone would be under $2 \Omega\text{m}$ (Bateman, 1990, Minette, 1990). The effect of the vertical averaging characteristics of conventional logging tools is to mask the presence of thin, potentially hydrocarbon-bearing reservoir rocks. Consequently, reserves may be overlooked, causing potentially economic wells to be abandoned. Even in cases

where thin hydrocarbon-bearing formations are correctly detected, reserve estimates are pessimistic (Fertl 1987, Bateman 1990).

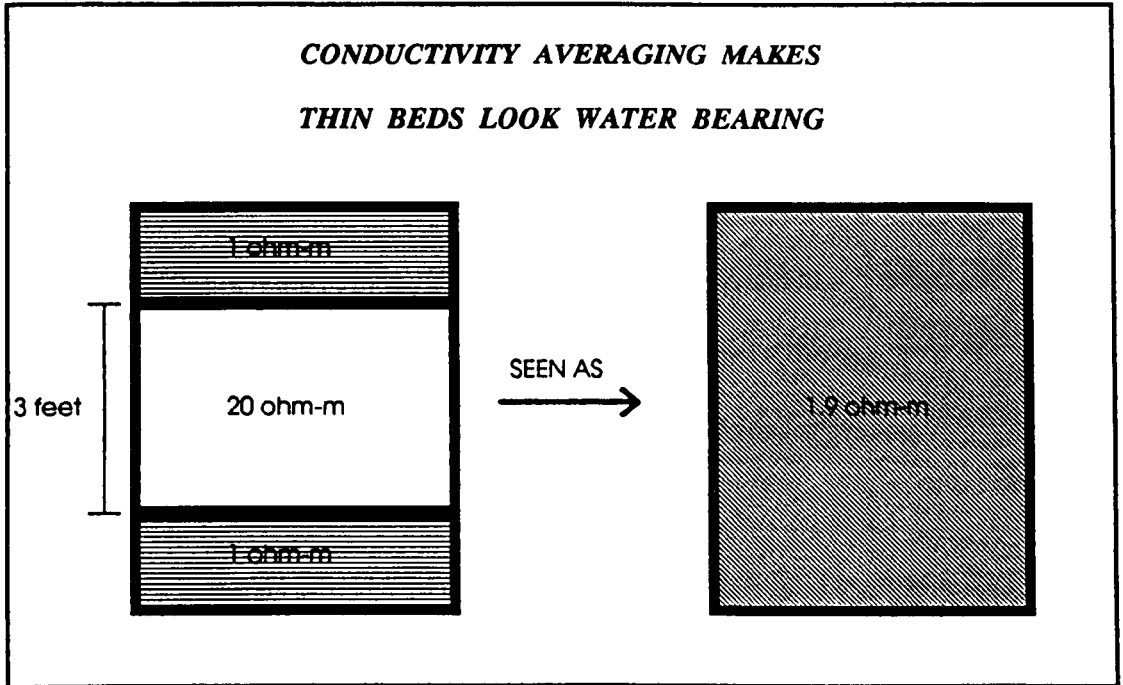


Figure 3.4 The effect of thin bed geometry on conductivity tool readings (Modified form Bateman, 1990).

Thin bed log analysis, therefore, has played an increasingly important role in formation evaluation over the past ten years. The ability to distinguish fairly homogeneous shaly sandstone from thinly-bedded layers of shale and sandstone is crucial if the log analyst wishes to accurately determine producible zones in a well (Minette, 1990). Hence, a variety of thin bed log analysis techniques have been developed (e.g. Suau 1984, Lyle

and Williams 1986, Flaum et al. 1987, Barber 1988, Minette 1990, Bateman 1990, Nelson and Mitchell 1990).

3.4 THE BINARY LITHOLOGY METHOD

Among the various published thin bed algorithms, the Binary Lithology Method (BLM) of Bateman (1990) is useful in laminated sandstone-shale sequences logged with conventional and limited logging suites. This represents the actual circumstances in the Toolachee Field. It assumes that the formation consists of alternating layers of clean sandstone and pure shale. This situation lies at one end of a continuous spectrum of shaly sandstone models. The other end point of this spectrum is represented by a homogenous fully dispersed shaly sandstone sequence.

The starting point for the binary sandstone/shale analysis is the assumption that conventional methods of shaly sandstone analysis produce shale volume curves which are valid at the resolution of the tools used to produce them. Generally, conventional neutron, density and gamma ray logs are used to compute shale content at a vertical resolution of about 2 feet. Thinner beds will show identifiable deflection on the logs, but the measured values will be incorrect. The BLM considers that the shale volume curve calculated from a conventional shaly sandstone routine contains more information than is usually used. By using simple signal processing routines, the BLM magnifies the small deflections on the original curve to give better bed resolution than the logs conventionally used to compute shale volume.

In order to resolve a given sandstone-shale sequence to its constituent binary layers, the following steps are required:

- I. Computation of shale volume (Vsh) using conventional techniques.
- II. Filtering of the Vsh curve with a short running average filter.
- III. Filtering of the Vsh curve with a long running average filter.
- IV. Generation of a ΔVsh curve by subtracting the short filtered version from the long filtered version.
- V. Plotting of the Vsh and ΔVsh curves, appropriately scaled, and definition of laminae boundaries at the cross overs between the curves.

Figure 3.5 shows this process graphically. In the first track from the left of the example log, a conventional Vsh curve is shown. In the second track, both long and short filtered versions of Vsh are shown. In the third track, ΔVsh , the difference between the long and short filtered versions, is overlaid on the original Vsh curve. Where the short filtered version reads less than long filtered, sandstone coding is used to highlight sandstone beds and vice versa for shales beds. Bed boundaries are picked where the ΔVsh and the conventional Vsh curves cross.

In signal processing filters are generally designed to reduce the variance in data by smoothing the data sequence. Since the data set consists of two components, a long-term signal or meaningful part, and superimposed random short-term noise. The

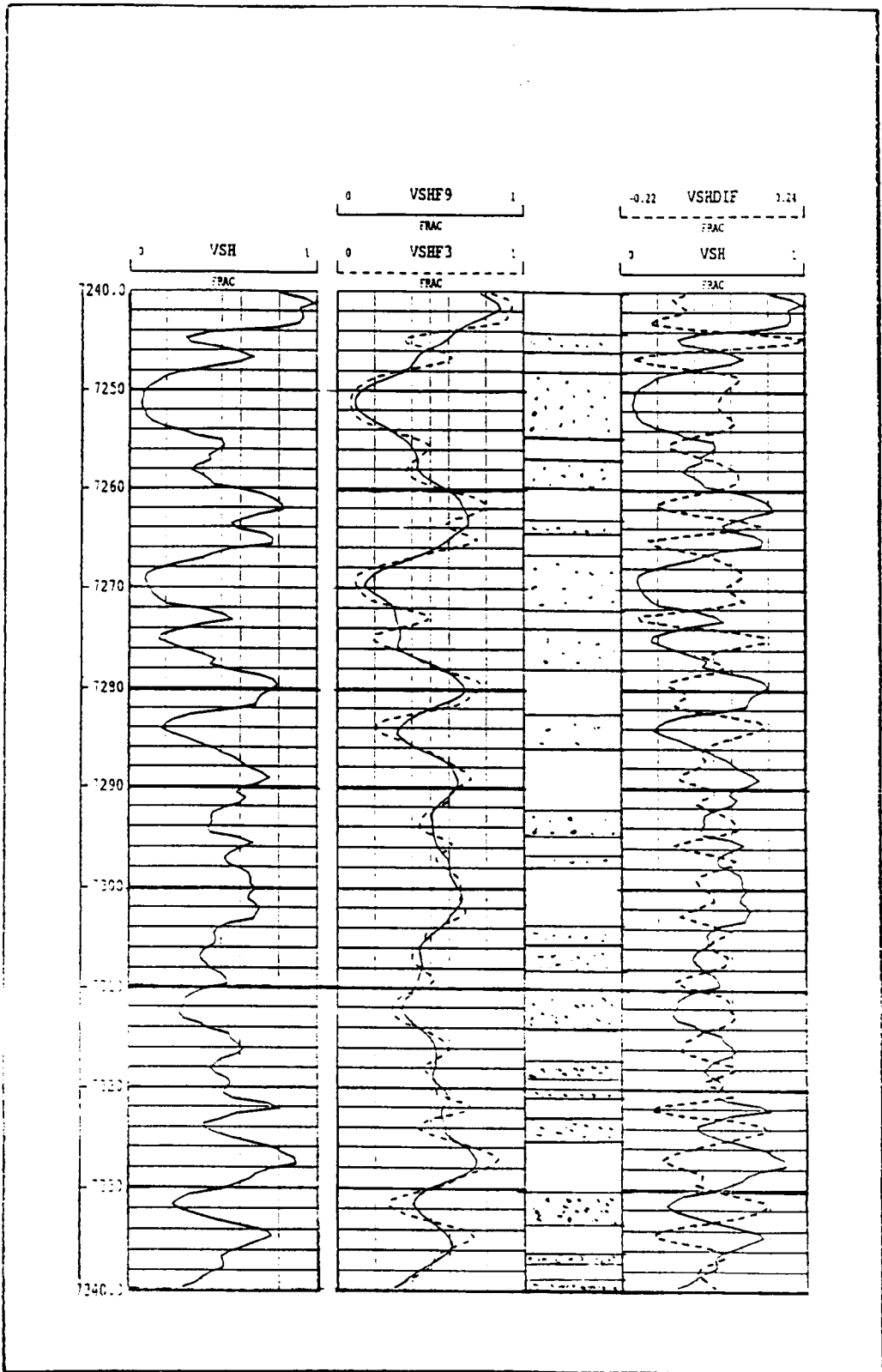


Figure 3.5 Deconvolution process used to derive binary sandstone/shale layers from conventional Vsh curve.

justification for such a filtering process is to reduce or eliminate the presence of noise. In contrast, in the thin bed algorithm the main purpose of the filtering operations, which can be as simple as equally weighted running averages, is to emphasise the small deflections on the Vsh curve. Comparison of the original Vsh and ΔVsh curves provides a new criterion for the log analyst in deciding which deflections on the original Vsh curve should be interpreted as a change in lithology from shale to sandstone or vice versa. This criterion is superior to the conventional gamma ray cut-off for lithology coding currently used in the log analysis routine in the study area.

Work by Bateman (1990), and the results of the present study, suggest that individual beds as thin as 6 inches can be resolved in this manner. Comparison with core data confirms the reliability of the BLM. A disadvantage of the method is its reliance on a deconvolution process which is subject to error in the presence of noise. This disadvantage is partially compensated by the wide applicability of the method to old or limited well log data.

3.5 APPLICATION OF THE BLM IN STUDY AREA

3.5.1 PROCESS

3.5.1.1 VSH AND FILTERING

To apply the BLM to available well log data over the Patchawarra Formation in the Toolachee Field, it was necessary to choose a conventional method for shale volume calculation. Although, there are some problems with using the gamma ray log as a shale indicator (Janson and Linke 1982, Rider 1986, Cant 1992, Stuart et al. 1992), it

is the only relatively reliable and commonly available log for lithology determination and shale volume calculation in Cooper Basin wells.

The gamma ray index, IGR, is a measure of shaliness and is computed from the equation:

$$IGR = (GR_{log} - GR_{min}) / (GR_{max} - GR_{min}) \quad (E 3.1)$$

where GR_{max} is the maximum gamma ray reading (180 API in the Cooper Basin), GR_{min} is the minimum gamma ray reading (20 API in the Cooper Basin), and GR_{log} is the measured gamma ray value.

This equation assumes a linear relationship between the gamma ray response and shaliness. Conventional formation evaluation in the Cooper Basin (e.g. Porter 1972, Overton and Hamilton 1986, Morton 1989) accepts this concept and simply assumes that:

$$V_{sh} = IGR \quad (E 3.2)$$

However, numerous authors have suggested that this relationship is not linear (Janson and Linke 1982, Asquith 1983, Asquith 1989, Cant 1992). According to Cant (1992) an IGR of 0.5 corresponds to a V_{sh} of about 0.3. Fertl and Frost (1979), Asquith (1983), Rider (1986), Fertl (1987), Asquith (1989) and Cant (1992) give the following non-linear equation for V_{sh} calculation in a consolidated sandstone from the gamma ray log response:

$$V_{sh} = 0.33 (2 (2 \times IGR) - 1.0) \quad (E 3.3)$$

This non-linear equation was used to compute the original or conventional Vsh in the first step of the BLM.

The second and third steps of the algorithm require smoothing of the original Vsh curve by filters of different lengths. Simple averaging was chosen as the filtering function. In order to decrease the noise effect on the Vsh curve since the actual sampling rate in the study area is 2 samples per foot, smoothing on three points was selected as the short filter. Different filters were tested to find the best possible long filter. Lithology coding obtained from the both seven and nine point averaging, as the long filters, and the short filter showed good agreement with core data in Toolachee 6. Work by Bateman (1990) also shows that the length of the long filter can be three times longer than the length of short filter. On this basis, the nine point running average was chosen as the long filter.

In addition to sandstone, siltstone and shale, the Patchawarra Formation contains coal seams which must be excluded from the binary lithology algorithm. Generally, the coal seams show sonic log readings greater than 90 microseconds per foot, and in most cases, very low gamma ray values as well as over gauge hole. Since sonic log values for both sandstones and shales are mostly less than 80 microseconds per foot, recognition of coal seams is not difficult. During lithology coding the sonic and caliper logs were checked and intervals with transit times and/or hole diameters exceeding appropriate cut-off values were interpreted as coal seam, regardless of the Vsh value.

3.5.1.2 SCALING OF ΔV_{sh} CURVE

In the final step, the V_{sh} and ΔV_{sh} curves are superimposed and bed boundaries are marked wherever the two curves cross over. Intervals in which ΔV_{sh} plots to the left of V_{sh} are classified as sandstones. The original V_{sh} curve is plotted between zero and one. The degree of bedding and the thickness of individual beds are highly controlled by the scaling factor selected for plotting the ΔV_{sh} curve. Hence, choosing an appropriate scale for ΔV_{sh} is a crucial issue. An incorrect scale for ΔV_{sh} produces more shale or more sandstone and mislocates the bed boundaries.

Bateman (1990) suggested that running some simple statistical measures of the distribution of values in the ΔV_{sh} curve can be useful as guide to the analyst to find the optimum scale for the ΔV_{sh} curve, but he did not explain how. As the ultimate arbiter, he assumed that if the ΔV_{sh} curve has been scaled correctly then the integration of the conventional V_{sh} curve with respect to depth will produce the same number of feet of shale as the thin bed algorithm. Bateman defined the monitor log as the difference between the cumulative thickness of shale given by the BLM, and the integral of V_{sh} with respect to depth.

$$\text{Monitor} = \int \text{shale bed from the BLM} - \int \text{conventional } V_{sh} \quad (\text{E } 3.4)$$

For optimal scaling the monitor should be close to zero throughout the whole interval of analysis. A program was written to find the best scale for the ΔV_{sh} curve. The program assumes that the optimum scaled version of ΔV_{sh} is linear function of ΔV_{sh} :

$$\text{Scaled } \Delta V_{sh} = a (\Delta V_{sh}) + b \quad (\text{E 3.5})$$

where

a and b are the linear scaling and shifting factors, respectively.

The program outputs for the cored interval through the Patchawarra Formation in Toolachee 6 indicated that there is no unique pair of values of a and b which minimises the monitor (Figure 3.6). However, all scaled ΔV_{sh} curves from a and b pairs which produce zero or close to zero monitor values (Figure 3.7), showed approximately the same gross sandstone thickness with good agreement of bed boundaries and thicknesses compared with the core data.

Despite the promising results, the use of integration of Vsh curves in the scaling of ΔV_{sh} is a time-consuming process which has not an exclusive output. Two other approaches were made to find the optimum scale for ΔV_{sh} in the representative well Toolachee 6. The results were compared with the core description for each approach.

A. Using The Maximum And Minimum Values

For the first trial, the maximum and minimum values of ΔV_{sh} were used as the track limits for plotting the ΔV_{sh} curve. This approach resulted in detection of beds as thin as 6 inches and the bed boundaries agreed well with the core data. Although the thicknesses of thin beds were exaggerated, resulting in an overestimation of the gross

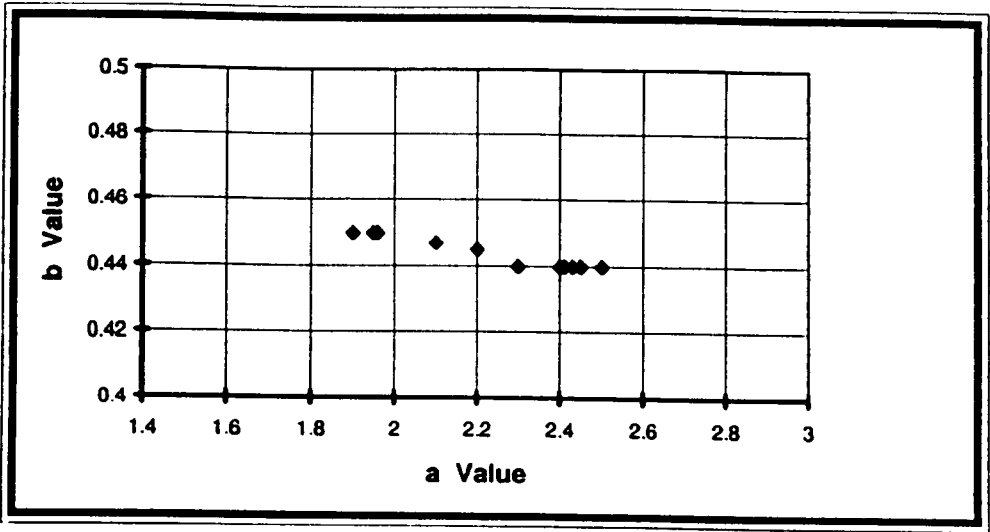


Figure 3.6 A number of a and b pairs which produce zero monitor over cored interval in Toolachee 6.

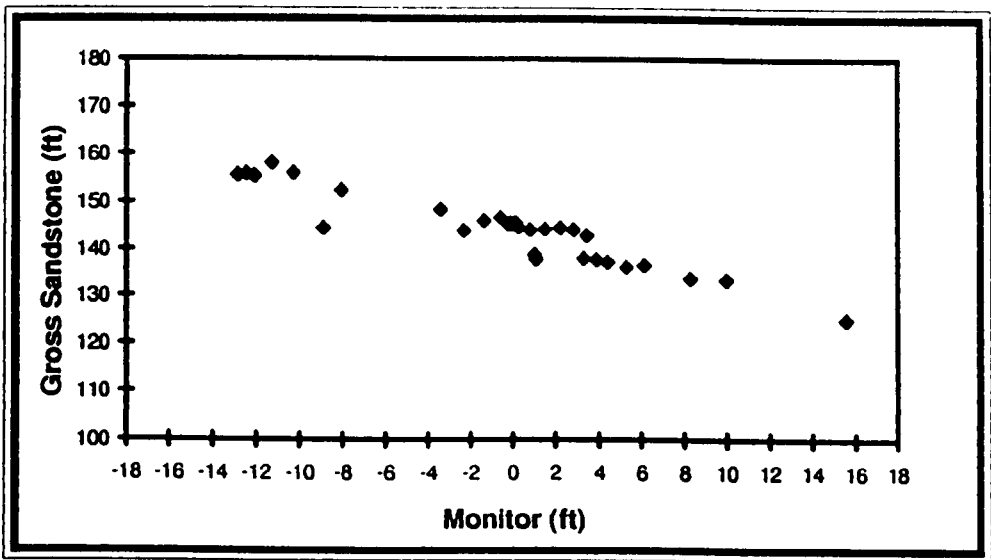


Figure 3.7 Variation of calculated gross sandstone as the monitor changes over cored interval in Toolachee 6.

sandstone by up to 10 percent, this simple approach provided a quick look method for lithology coding in thin bed algorithm.

B. Shifting The Maximum - Minimum Scale

To eliminate the exaggeration of thickness the left limit of the scale was altered from the value used in the previous approach. Various shifted scales were tested to optimise the plotting limits. Finally, to keep the method as uniform as possible, the minimum value of ΔV_{sh} plus the standard deviation of ΔV_{sh} over the cored interval, and the maximum value, were selected as the left and right limits of ΔV_{sh} curve respectively. The picked boundaries and the thickness of thin beds obtained from the shifting approach agree well with the core data to within about 5 per cent.

3.5.2 RESULTS

The BLM was run on the 3 wells listed in Table 3.1. The available core data enabled the accuracy of the algorithm to be checked. The result are presented in Table 3.3. Comparison of the BLM interpretation with core lithology shows that the BLM identifies all thin sandstone beds as thin as 6 inches. Although there is no unique scaling factor for ΔV_{sh} and there are small discrepancies in the gross sandstone derived from the differently scaled ΔV_{sh} curves in each well, in all cases the BLM gives a significantly more accurate result than the conventional method. Furthermore, the variation in gross sandstone thickness between the different methods is of little practical concern.

Returning to the Toolachee-6 example in which the core indicates 20 feet of sandstone (Figure 3.2), the BLM interprets 19 feet of sandstone in the same interval, while the conventional log-derived lithology distinguishes just 8 feet (Figure 3.8). According to the core data, the 307 feet cored interval through the Patchawarra Formation in Toolachee-6 contains 148 feet of gross sandstone, while the BLM gives 140 feet, a 5 per cent underestimation, and the conventional method gives 95 feet, a 35 per cent underestimation. Similar results were obtained in the other two wells with long cored interval. Enclosures 1, 2 and 3 show lithology interpretation using the BLM and the conventional methods over the cored interval in the Patchawarra Formation in wells listed in Table 3.1.

These results show that the BLM can increase the gross sandstone thickness interpreted from the normal suite of logs, relative to the conventional method, in the Patchawarra Formation in the Toolachee Field. The binary algorithm recognises most sandstone beds thicker than 6 inches within the formation. In contrast, the conventional log-derived lithology overlooks most of the thin sandstone beds and underestimates the gross sandstone by up to 35 per cent. Such underestimation may result in a significant reduction in the in-place reserve estimation for each well.

Another advantage of the BLM is its application in depth matching logs to core. Complex lithology with rapid variations, inadequate well log suites, and in many cases caved hole, can make the matching of logs to core a difficult task in the Patchawarra Formation in the Toolachee Field. Combination of the two gamma ray-derived curves, ΔV_{sh} and V_{sh} , creates an indicator which is very sensitive to rapid lithology variations

TOOLACHEE# 6

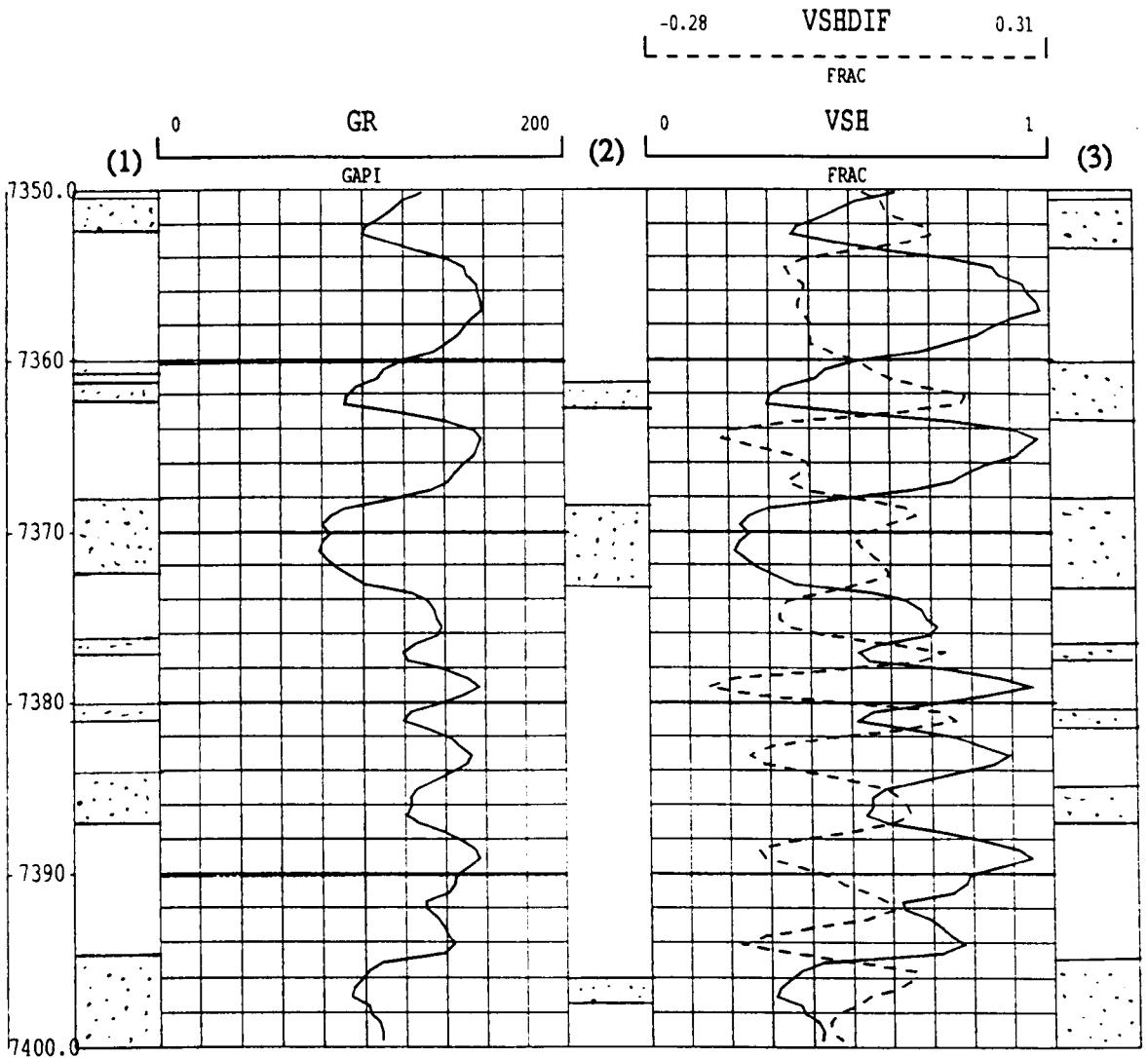


Figure 3.8 Comparison of lithology interpretation using binary lithology and conventional methods with core lithology in the Patchawarra Formation in Toolachee 6 from 7350 to 7400 ft (logger depth). (1) core lithology (from Alsop 1990), (2) conventional log-derived lithology (from Toolachee 6 composite log profile), (3) binary lithology interpretation method (this study).

in shale-sandstone sequences. The picked boundaries for thin beds obtained from the BLM match very well with core lithology. Hence, the thin bed algorithm has potential for log to core depth matching, particularly where the micro resistivity readings are not reliable due to over-gauge hole.

<i>Well</i>	<i>Cored Interval</i>	<i>Core</i>	<i>Conventional Method</i>	<i>Thin Bed Method I</i>	<i>Thin Bed Method II</i>	<i>Thin Bed Method III</i>
<i>Toolachee-3</i>	276	147	112	150	145	145
<i>Toolachee-5</i>	185	83	58	85	76	87
<i>Toolachee-6</i>	307	148	95	153	140	144

Table 3.3 Comparison of gross sandstone thickness interpreted by conventional method and thin bed algorithm with core data for representative wells in the study area. Figures are in feet. I, II and III refer to different scales for the ΔV_{sh} curve, the maximum-minimum, the shifted maximum-minimum, and the integrated shale beds scaling method respectively.

3.6 RESERVOIR POTENTIAL AND INDUSTRIAL APPLICATION OF THIN BEDS

Recognition of the laminated reservoir character is important and has implications for well completion, reservoir engineering and production behaviour (Fertl, 1987). Core lithology and the results of the BLM confirm that, in the Patchawarra Formation in the Toolachee Field, most of the thin sandstone beds occur in unit 1 (Apak, 1994), in the

upper part of the formation, and comprise up to 30 per cent of total gross sandstone within the Patchawarra Formation in many wells. This percentage shows the potential contribution of thin sandstone beds to the reservoir rocks in the study area.

The upper part of the Patchawarra Formation in the Toolachee Field is a proven economic gas-bearing zone. It contains at least two separate gas reservoirs, the 73-0 and 73-5 sandstones, which have been intersected in widely distributed wells in the study area. The 73-0 and 73-5 reservoirs are not often both developed in the same well (Marcus, 1987). The promising point is that thin sandstone beds commonly occur adjacent to these recognised reservoirs, but because of their thicknesses they have generally been overlooked by conventional log analysis.

Of 50 wells drilled to date in the Toolachee Field, only 16 have core data in the Patchawarra Formation and just 5 wells are cored over a considerable thickness of the formation. In the other partially cored well, there is little core data from thin sandstone beds. Hence, for a field-wide assessment of thin bed reservoir potential the available core data is not representative.

Ambient core porosity in thin sandstones is typically greater than 8 per cent, the porosity cut-off used in conventional formation evaluation in the Patchawarra Formation (Marcus, 1987). Porosity calculations using the modified time average equation of Overton (1986) for the Cooper Basin, also give porosity values from 9 to 10.5 per cent for thin beds. This shows that porosity values in thin sandstones are

above the economic cut-off used in the Cooper Basin. Ambient core permeability values, on the other hand, are commonly less than 0.5 millidarcies.

Despite the few core data, log character and drill stem test results imply the presence of gas-bearing zones in some intervals consisting of thin sandstone beds. For instance, in Toolachee-15, separation between shallow and deep resistivity logs over thin sandstone beds may indicate the presence of relatively permeable zones, and drill stem test results also show the presence of a gas-bearing zone from 7110 to 7185 feet depth, which flowed at 4.24 MMCFD (Figure 3.9).

Sediments within the upper part of the Patchawarra Formation in the Toolachee Field are interpreted to have been deposited in distributaries, distributary mouth bars and shoreline environments (Alsop 1990, Apak 1994). Ripple cross laminated sandstone (Sr) and interlaminated sandstone with siltstone (Sw/Fw), with very fine to fine grain size and moderate to good sorting, are the dominant lithofacies within the thin sandstone beds in the study area (Alsop, 1990). Ripple cross laminated sandstones, lithofacies Sr, were a product of the lower flow regime and were deposited under waning channel flow conditions (Galloway and Hobday, 1983). These sandstones are often interlaminated with fine siltstones and muds, and may be interpreted as bioturbated sandstones of the Sw/Fw lithofacies (Alsop 1990, Schulz-Rojahn 1991).

Petrographic studies on the reservoir rocks in the Cooper Basin confirm that where illite contents are high, porosity and permeability are typically low. Conversely, permeability and porosity are higher in samples which contain more kaolin (Schulz-

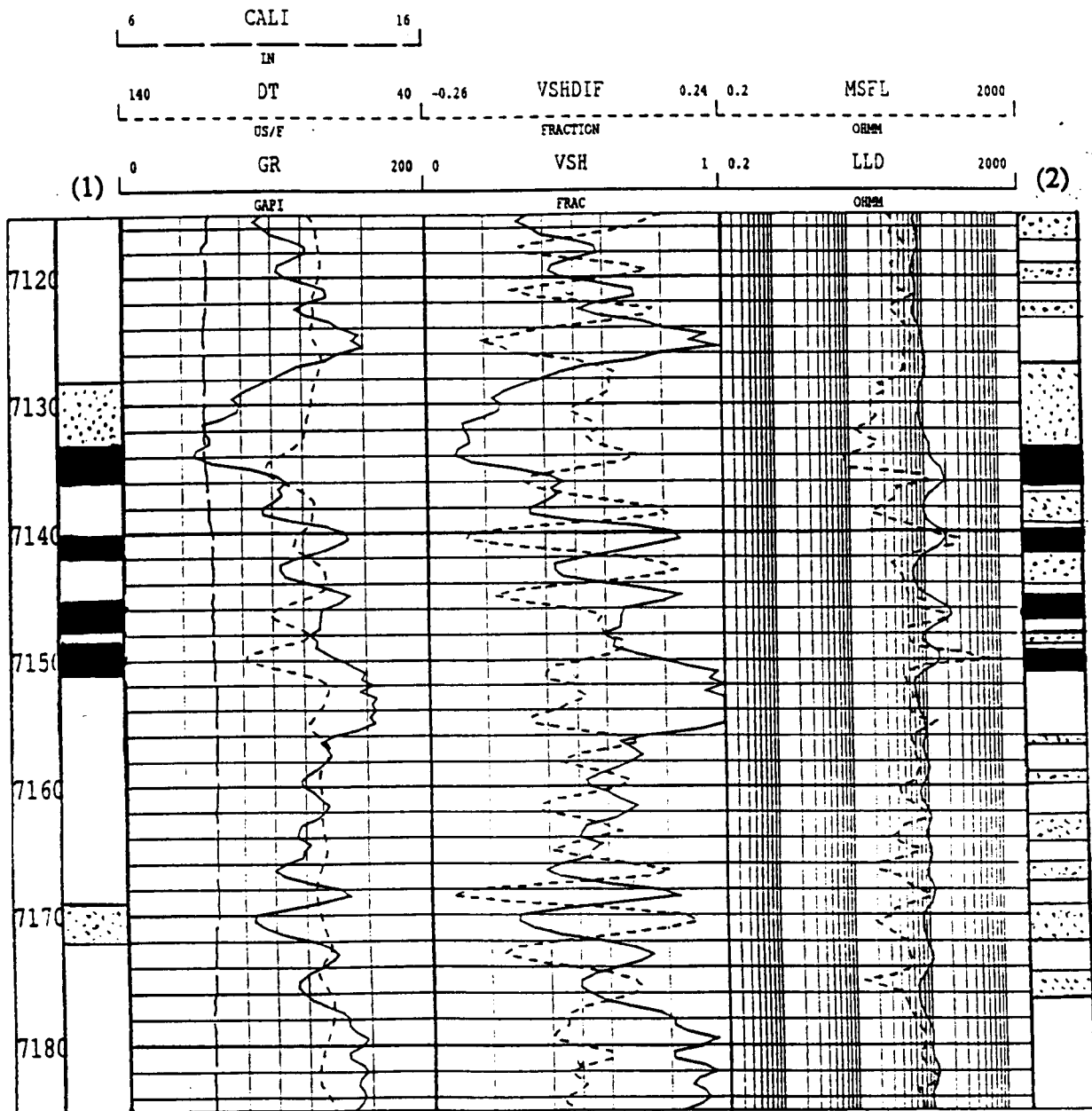


Figure 3.9 Separation between shallow and deep resistivity logs over thin sandstone intervals may indicate relatively permeable zones. Drill stem test results also show the presence of a gas-bearing zone from 7110 to 7185 ft (logger depth) with 4 MMCFD. (1) conventional log-derived lithology (from Toolachee 15 composite log profile) (2) binary lithology interpretation method (this study).

Rojahn and Phillips 1989, Stuart et al. 1992). Due to the high degree of sorting and their stratigraphic occurrence, there is a general lack of detrital clay (illite) in the distributary mouth bar/shoreline sandstones and interdistributary channel fills. The resulting well developed fine to very fine grain sandstones represent high-quality reservoirs with considerable economic significance for exploration and development in the Cooper Basin (Table 3.4). At Dirkala-2 in the Big Lake area, a hydrocarbon flow of 6.9 MMCFD and 287 BCPD was recorded from a very fine to fine proximal distributary mouth bar/shoreline sandstone in the basal Epsilon Formation. Also, at the top of the Patchawarra Formation in Moomba-6, a thin shoreline sandstone interval flowed in excess of 6 MMCFD (Stuart et al. 1992).

	<i>Number of Data</i>	<i>Average Porosity (per cent)</i>	<i>Average Permeability (md)</i>
<i>Distributary channel, Proximal mouth bar /Shoreline Sandstones</i>	34	17.30	112.7
<i>Distal mouth bars</i>	12	8.70	0.54
<i>Mouth bars (undifferentiated)</i>	61	11.00	16.0
<i>Pro-delta shales & Delta plain deposits</i>	4	5.75	0.045

Table 3.4. Ambient core porosity and permeability for sandstone reservoirs in delta/shoreline facies in the Cooper Basin (Stuart et al. , 1992, from Thomas 1990, Alsop 1990)

Conventionally, in the Cooper Basin, intervals with very low permeability (less than 0.5 millidarcies) are categorised as very poor to tight reservoirs or non reservoirs (Stuart et al. (1992), Tingate and Luo, (1992)). However, tight gas reservoirs in low permeability, gas-bearing formations are present in many gas producing basins throughout the world (Spencer and Mast, 1986). For instance, the Medina tight gas sandstone reservoirs in Pennsylvania, USA, have an average in place permeability of less than 0.1 millidarcies. These reservoirs can produce up to 1000 MCFD after stimulation (Laughers and Harper 1986). Similarly in the Cooper Basin, in recent years, hydraulic fracture stimulation has been successfully applied to reservoir sandstones of the Patchawarra Formation in the Big Lake area (Stanley and Halliday, 1984) and in the Toolachee Field (Domato and Male, 1992).

By analogy, the low permeability thin beds of Patchawarra Formation reservoirs in the Toolachee Field may also be a development target, even though they may require stimulation before economic levels of production can be obtained. Since perforating unaccessed gas reserves is recommended in the development plan for the Toolachee Field (Domato and Male, 1992), reanalysing the existing well log database in order to recognise potential gas pay in thin sandstone beds should be considered. The BLM would allow this to be done cheaply using the current log database. A detailed study of the geological, petrophysical and engineering aspects would be necessary to determine the productivity of thin sandstone beds in the study area.

CHAPTER FOUR

POROSITY AND PRESSURE DEPLETION

4.1 INTRODUCTION

Among the wells which have been drilled in recent years in the Cooper Basin, there are a number in which reservoirs appear to have anomalously low porosity (as calculated from the sonic log) and yet exhibit a high level of depletion. The Tirrawarra sandstone in Bookabourdie-11, unit C of the Toolachee Formation in Big Lake-52, and the 73-0 reservoir in the Patchawarra formation in Toolachee-48 are examples of this phenomenon (Table 4-1).

Clearly, reliable determination of porosity and its variation within the reservoir rocks is essential to accurate reserve estimate and field production management. However, the shortage of information due to limited well log suites and the lack of conventional and sidewall core data means that there is no alternative but to use the sonic log for porosity calculation in most of the depleted reservoirs of the Cooper Basin.

<i>Sandstone Reservoir</i>	<i>Well Name</i>	<i>Depth (ft)</i>	<i>Sonic Porosity (%)</i>	<i>Average Porosity in Field (%)</i>	<i>Formation Pressure (RFT) (psi)</i>	<i>Estimated Initial Pressure (psi)</i>
73-0	<i>Toolachee-48</i>	7277	7.3	12.6	1060	3258
74-4	<i>Toolachee-35</i>	7453	7.4	13.3	919	3274
75-6	<i>Toolachee-35</i>	7586	8.4	12.6	2003	3286
75-6	<i>Toolachee-39</i>	7827	5.9	12.6	2007	3300

Table 4.1 Examples of anomalously low log-derived porosities in depleted sandstone reservoirs of the Patchawarra Formation in the Toolachee Field, Cooper Basin (from Santos Ltd. , 1993).

To investigate the relationship between low porosity and pressure depletion in sandstone reservoirs of the Patchawarra Formation in the Toolachee Field, a review of the existing petrophysical data in the study area was performed. A series of cross plots were produced and the possible reasons for the observed correlation in the cross plots were investigated. Combination of previous works in the study area with published experimental studies, yielded a possible explanation for the association of low sonic porosities with low pore pressures in the Toolachee Field.

The results of this study suggest that the anomalously low log-derived porosity values observed in pressure depleted reservoirs are caused by the effect of reduced pore

pressure on compressional wave velocity. The conventional method of porosity calculation from sonic log data in the Cooper Basin does not account for the variation of compressional wave velocity due to pore pressure changes between depleted and non-depleted reservoirs, and underestimates the porosity of depleted reservoirs.

An empirical equation for the correction of the sonic tool response for the pressure conditions in the study area was derived from the available information. A detailed laboratory study is recommended for more accurate calibration.

In this chapter an overview of the petrophysical data and the observed relationship between sonic porosity and repeat formation tester (RFT) pressure data is presented. In the following chapter four possible explanations for the observed relationship are discussed in detail.

4.2 DEFINITIONS

Before proceeding any further, it will be useful to introduce a variety of pressure terms which will be referred to constantly in the following sections.

The *Overburden Pressure*, P_c , at any point in the formation is usually defined as the vertical stress caused by the total weight of the overlying formations (Exlog, 1981).

This is expressed as:

$$P_c(z) = 0.433 \int \rho(z) dz \quad (\text{E 4.1})$$

where

P_c = Overburden pressure (psi),

z = Depth (ft) and

ρ = Bulk density (g/cm^3).

The overburden pressure gradient is therefore proportional to the average density to the depth of interest. Since the average density of a thick sedimentary sequence is approximately 2.3 g/cm^3 , a value of 1 psi per foot is usually assumed for the total overburden pressure gradient (Gretener, 1981):

$$dP_c/dz \simeq 1 \text{ psi/ft} \quad (\text{E 4.2})$$

The term *Confining Pressure* refers to an isotropic pressure. In the crust of the earth the confining pressure is the lithostatic or geostatic pressure resulting from the load of overlying rocks, and is equal to overburden pressure. In experimental work, the confining pressure is usually a hydrostatic pressure, produced by liquids, which is used to simulate overburden pressures in the laboratory.

In any porous system an applied load will be carried jointly by the matrix framework and the pressure in the pore fluid (Gretener, 1981). The *Formation Pressure* or *Pore Pressure*, P_p , is usually defined as the pressure exerted by a column of free formation fluid which would be in equilibrium with the formation (Gregory, 1977). This leads to a typical pore pressure gradient (dP_p/dz) of about 0.45 psi/ft:

$$dP_p/dz \simeq 0.45 \text{ psi/ft} \quad (\text{E 4.3})$$

Pore pressure is described as being normal, or above or below normal. Normal pressure at a point in the geological section is the hydrostatic pressure due to the average density and vertical depth of the column of fluids above the point (Exlog, 1981). Pore pressures leading to an overall pressure gradient in the range of 0.43 to 0.48 psi/ft have been termed normal (Gretener, 1981). The term geopressure applies specifically to fluid pressures that are in excess of the normal hydrostatic pressure (Exlog, 1981).

The *Differential Pressure* or *Net Overburden Pressure*, P_d , on a point is defined as the difference between the total overburden pressure P_c and the pore pressure P_p (Gretener, 1981). Hence any increase or decrease of the pore pressure under constant overburden pressure results in a change in the differential pressure. The difference between the total overburden and the pore pressure gradients under normal pressure condition results in a differential pressure gradient of 0.55 psi/ft:

$$dP_d/dz \simeq 0.55 \text{ psi/ft} \quad (\text{E 4.4})$$

The term *Effective Pressure*, P_e , refers to the interplay of overburden and pore pressure on the physical properties or processes. The different influences of P_c and P_p on a given physical property can be considered by using the concept of effective pressure (Christensen and Wang, 1985). For cases where P_p does not cancel P_c exactly, an empirical factor, n , can be introduced to define the effective pressure

$$P_e = P_c - nP_p \quad (E 4.5)$$

Theoretically, n is given by

$$n = 1 - (\beta_s / \beta) \quad (E 4.6)$$

where β_s is the compressibility of the solid grains (matrix) and β is the compressibility of the bulk material (Biot and Wills, 1957). Because the bulk compressibility decreases with decreasing differential pressure, so does n (Gregory 1976, Christensen and Wang, 1985). The value of n is different for different rocks (Gregory 1976, Nur and Wang 1989) and can be determined experimentally. A value of n less than 1 implies that the effect on a given rock property of a given pore pressure increment does not entirely cancel the effect of an equal confining pressure increment (Christensen and Wang, 1985).

4.3 PRESSURE CONDITIONS IN THE TOOLACHEE FIELD

In the Toolachee Field the Patchawarra Formation has been intersected at KB depths ranging from 6822 to 8200 ft. The observed thickness of the Patchawarra Formation ranges from 106 to 702 ft with an average of 355 ft. Since the overlying formations are all sedimentary rocks, the resulting total overburden pressure gradient of 1 psi/ft leads to an overburden pressure (in psi) approximately equal to the depth (in feet) at

any point within the Patchawarra Formation. On this basis, the overburden pressure over the study area should range from 6822 to 8200 psi.

The available pressure data in the Toolachee Field, including drill stem tests in early wells, indicate that the pore pressure within the Patchawarra reservoir rocks is slightly higher than normal pressure. Table 4.2 shows that 0.51 psi/ft is a reasonable estimate of the initial pore pressure gradient in the study area. Based on this assumption, the initial pore pressure within the Patchawarra Formation in the Toolachee Field ranges from approximately 3480 to 4180 psi.

In another approach, Santos Ltd. uses the following equation to determine the initial pore pressure:

$$P(Z) = P(Z_o) - G (Z_o - Z) \quad (E 4.7)$$

where

$P(Z)$ is the initial pore pressure (psi) at subsea depth Z (ft),

$P(Z_o)$ is the initial pore pressure (psi) at datum, 3262 psi in the study area,

G is the gas pressure gradient (psi/ft), 0.073 psi/ft in the study area, and

Z_o is the datum depth (feet), 7075 ft in the study area

This equation gives initial pore pressures ranging from 3243 to 3446 psi for the reservoir rocks in the study area. In contrast, the DST results in early wells and the RFT data in recently drilled wells indicate pore pressures up to 3886 and 3615 psi

respectively. Since the DST and RFT pressures are the in-situ measurements, in present study the average initial pore pressure over the Patchawarra Formation is assumed to be 3700 psi.

<i>Well Name</i>	<i>DST Number</i>	<i>From (ft)</i>	<i>To (ft)</i>	<i>Pressure (psi)</i>	<i>Pore Pressure Gradient (psi/ft)</i>
<i>Toolachee-1</i>	5	6834	6898	3566	0.51
<i>Toolachee-2</i>	4	6960	7080	3717	0.52
<i>Toolachee-3</i>	4	7162	7260	3717	0.52
<i>Toolachee-4</i>	3	7104	7294	3726	0.52
<i>Toolachee-5</i>	7	7225	7353	3738	0.51

Table 4.2 DST-derived formation pressures in early wells in the Toolachee Field. Depth intervals are from kelly bushing (From Well Completion Reports and Domato and Male, (1992)).

4.4 DATA AVAILABILITY AND LIMITATION

To study the relationship between apparent porosity decrease and formation pressure depletion the key information, in the absence of core data, is log-derived porosities and formation pressure. The caving which occurs in many wells and a large gas effect cause density and neutron tool readings to be unreliable in the Cooper Basin.

Therefore, the only generally available and relatively reliable porosity tool is the sonic tool. Sonic log data are available for all wells in the Toolachee Field.

The RFT and DST are two methods by which direct pore pressure measurements are obtained in the Cooper Basin. DST-derived pore pressures are average values of pore pressure within the testing interval. This interval is generally between 50 and 100 feet within the Toolachee Field. Due to rapid lithology variation in the Patchawarra Formation, a 50 feet interval may contain two or more sandstone reservoirs with different levels of depletion and therefore different pore pressures. Hence, DST-derived pore pressures may not represent the pore pressure of individual sandstone reservoirs within the test interval. In contrast, the RFT tool with vertical resolution of a few millimetres (Bateman, 1985) gives a reliable estimation of pore pressure for individual beds. Unfortunately, RFT data in the Toolachee Field are not as complete as one would like, both with respect to the number of wells surveyed, and the information available for individual reservoir sandstones.

Unfortunately, no cores have been cut in intervals for which pore pressures are available. Absence of such core data meant that petrographic studies could not be performed, which would otherwise have provided control on the interpretation of the relationship between log-derived porosity and pressure depletion in the Patchawarra Formation reservoir rocks.

However, a total of 198 RFT values from 22 wells in the Toolachee Field were available for the present study (Table 4.3). These data were obtained from the Santos

Ltd. database. For each RFT value, the sonic log value, the log-derived porosity, the estimated shale volume and the water saturation were obtained from the Santos Ltd. database and the composite logs in well completion reports. The wells from which these data were collected are widely distributed over the field and have been drilled in both crestal and flanking positions (Figures 2.5 and 2.6).

1- Toolachee-1	(1)	9- Toolachee-34	(6)	17- Toolachee-45	(14)
2- Toolachee-10	(7)	10- Toolachee-35	(10)	18- Toolachee-46	(2)
3- Toolachee-11	(12)	11- Toolachee-36	(5)	19- Toolachee-47	(18)
4- Toolachee-12	(6)	12- Toolachee-38	(9)	20- Toolachee-48	(9)
5- Toolachee-14	(2)	13- Toolachee-39	(19)	21- Toolachee-49	(6)
6- Toolachee-15	(4)	14- Toolachee-41	(12)	22- Toolachee-50	(14)
7- Toolachee-18	(12)	15- Toolachee-42	(13)	Total Number of RFT Data: 198	
8- Toolachee-32	(9)	16- Toolachee-43	(8)		

Table 4.3 List of Toolachee Field wells used in this study. Refer to Figure 2.6 for well locations. Values in brackets represent number of RFT measurements in the Patchawarra Formation for each well.

4.5 GENERAL OBSERVATIONS

Porosities calculated from the sonic log in intervals for which RFT measurements are available range from 4.4 to 21.2 per cent, with an average of 12.8 per cent . Pore pressure values range up to 3641 psi with a minimum value of 919 psi (Table 4.4 and Figure 4.1 and 4.2). Most of the RFT values were obtained immediately after drilling the wells and in the main show pressure conditions in virgin or undepleted reservoirs. Pore pressures greater than 3000 psi indicate undepleted reservoirs, whereas those less than 2000 psi represent highly depleted reservoirs in the study area (Chamalaun, Santos Ltd. personal communication, 1994).

<i>Data</i>	<i>Units</i>	<i>Minimum</i>	<i>Maximum</i>	<i>Mean</i>	<i>Standard Deviation</i>
<i>Formation Pressure</i>	psi	919	3641	2768	608
<i>Sonic Travel Time</i>	µs/ft	63.00	92.00	77.52	5.45
<i>Log-Derived Porosity</i>	%	4.40	21.20	12.82	3.16
<i>Estimated Clay Content</i>	Fraction	0.00	0.40	0.11	0.09
<i>Estimated Water Saturation</i>	%	3.6	100	25	21.4

Table 4.3 Statistics of the database for the Patchawarra Formation in the Toolachee Field.

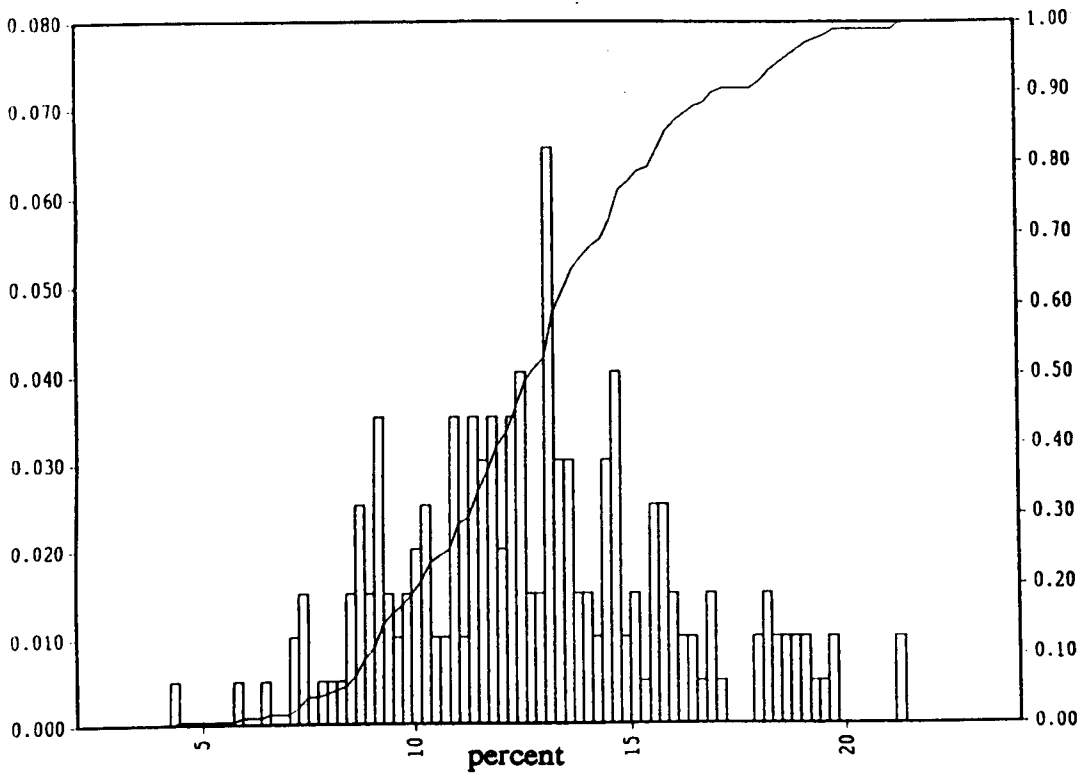


Figure 4.1 Histogram of log-derived porosities used in current study.

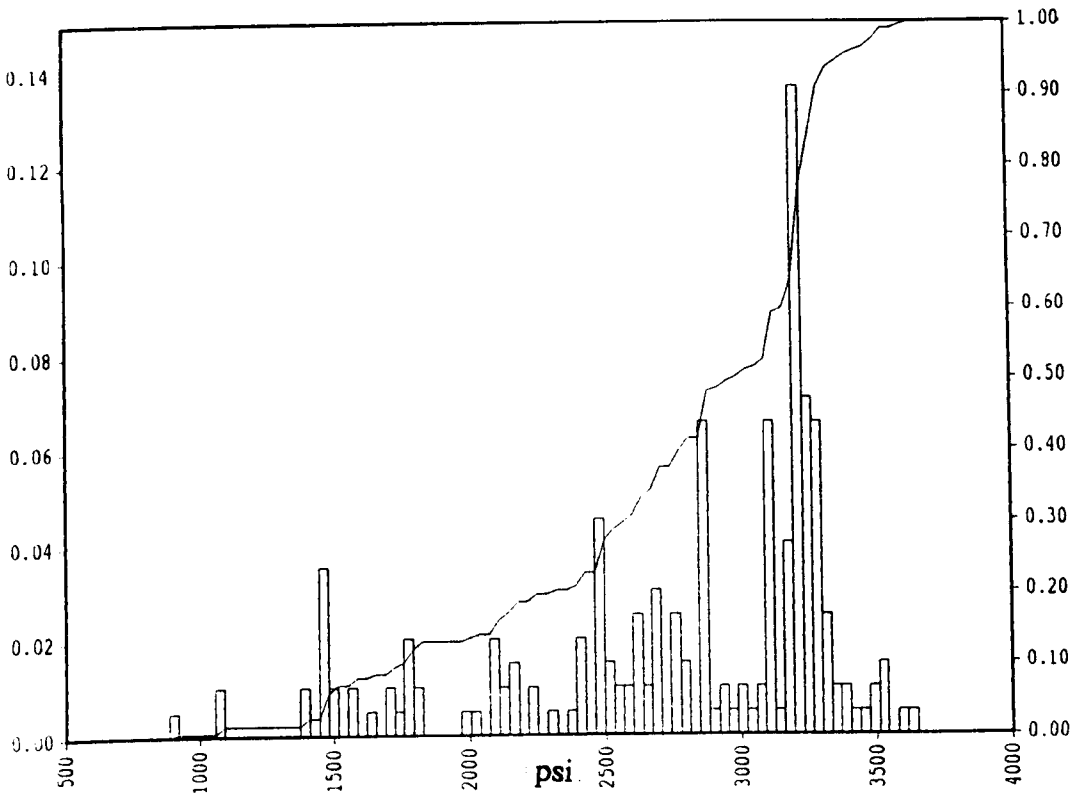


Figure 4.2 Histogram of RFT derived pore pressure data used in current study.

A cross plot of sonic-derived porosities versus pore pressure shows a positive correlation between these two reservoir parameters (Figure 4.3). There is significant scatter, which can be at least partly accounted for as follows:

I. The data come from different reservoirs in wells which are scattered throughout the Toolachee Field. According to previous sedimentological studies on the Patchawarra Formation in the Toolachee Field (Faridi and Hunt 1985, Alsop 1990, Apak 1994), different sandstone reservoirs can be classified in different chronostratigraphic units. Consequently, structure, depositional facies, stratigraphy and diagenetic history may vary from well to well and between different reservoirs within the Patchawarra formation in the same well.

II. The present pore pressure in the gas-producing reservoirs of the study area is controlled by both the pore pressure gradient across the region and the production history of the reservoirs. On the other hand, porosity in the Cooper Basin is the result of a complex interaction between sedimentary facies, basin structure development and diagenetic history. Therefore, even within a particular reservoir in a particular well, rocks with different porosities may have similar pore pressure. This fact may increase the scatter of RFT values in the cross plot.

III. There are some uncertainties in the conventional porosity calculation from the sonic log (Wyllie equation) in gas-bearing shaly sandstone rocks (see Raymer et al.

(1980), Rider (1985) and Han et al. (1988)), which may expand the scatter of porosity values in the cross plot.

Based on the RFT data, the sandstone reservoirs of the Patchawarra Formation can be subdivided into three groups. These groups are:

I. Undepleted reservoirs with pore pressures greater than 3000 psi, an average log-derived porosity of 13.7 per cent, and a maximum porosity of 21 per cent.

II. Moderately depleted reservoirs with the pore pressure between 2000 and 3000 psi, an average log-derived porosity of 12.1 per cent and maximum porosity of 19.4 per cent.

III. Highly depleted reservoirs with the pore pressures less than 2000 psi, an average log-derived porosity of 11.7 per cent and a maximum porosity of 14.5 per cent.

The association of low sonic porosity values with low pore pressures can be seen for the entire data set and also within the groups of data from the moderately and highly depleted reservoirs. When the sonic porosities are averaged over 500 psi intervals the association becomes more apparent (Figure 4.4)

For individual reservoirs also, the general trend of sonic porosity reduction with decreasing formation pressure is recognisable in most cases, as shown in Figures 4.5 to

4.10 most of the RFT data with pressures less than 2000 psi correspond to sonic porosities of less than 15 per cent.

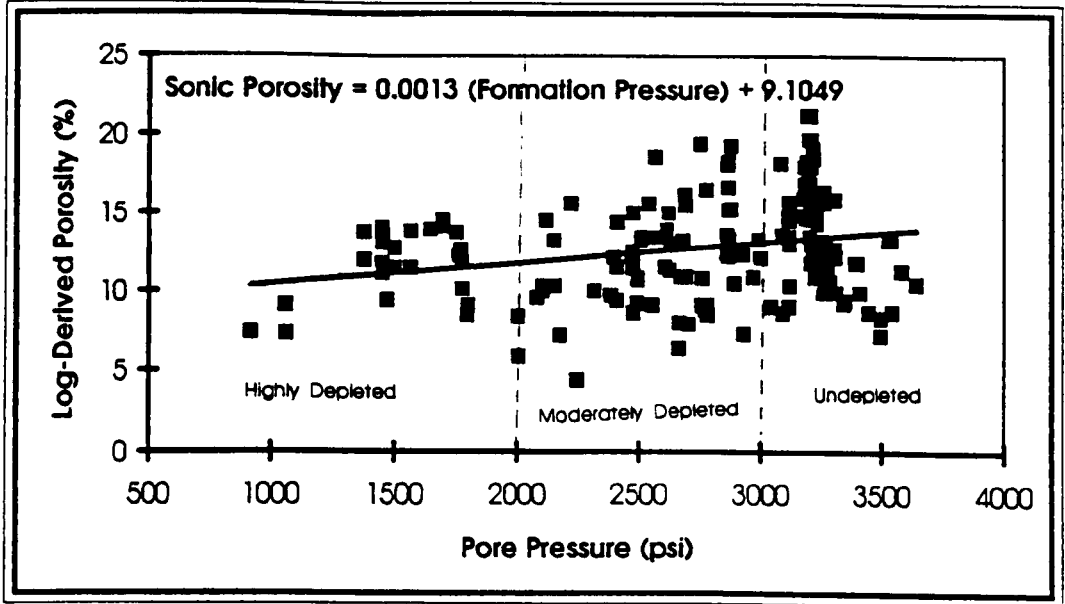


Figure 4.3 Cross plot of sonic porosity (per cent) versus pore pressure (psi).

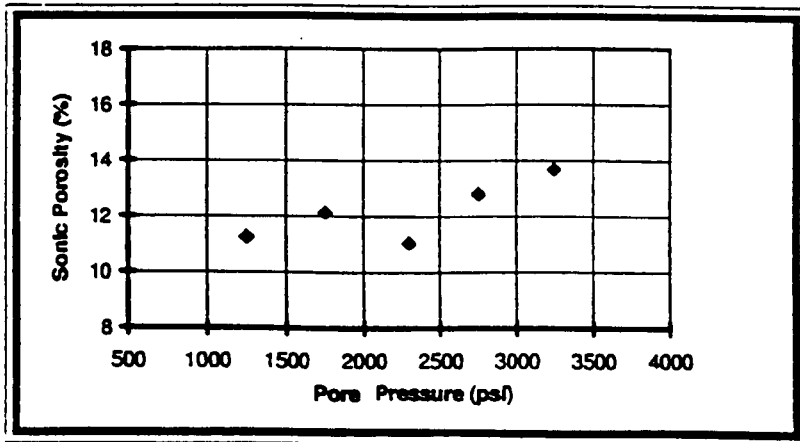


Figure 4.4 Cross plot averaged sonic porosity over 500 psi intervals versus pore pressure.

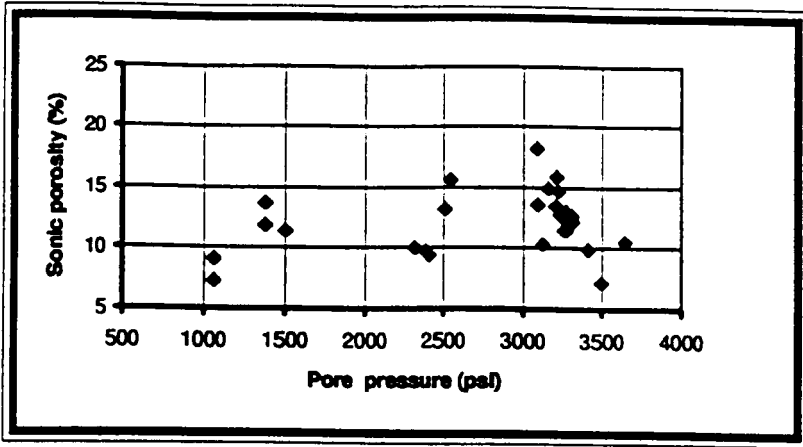


Figure 4.5 Cross plot of sonic porosity versus pore pressure for the 73-0 reservoir.

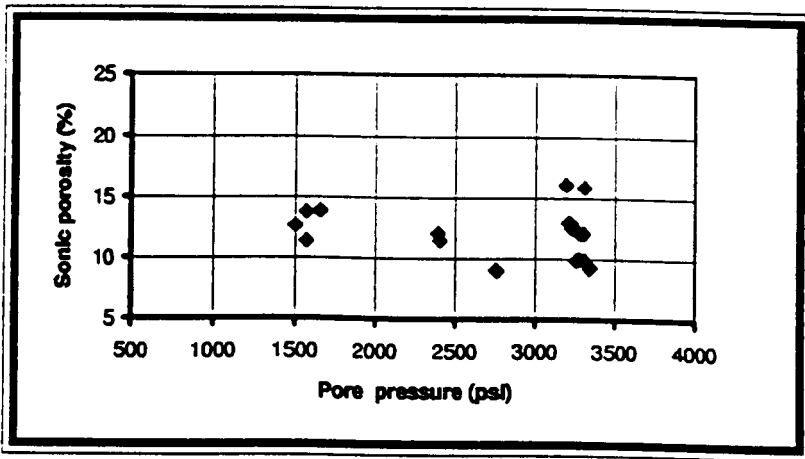


Figure 4.6 Cross plot of sonic porosity versus pore pressure for the 73-5 reservoir.

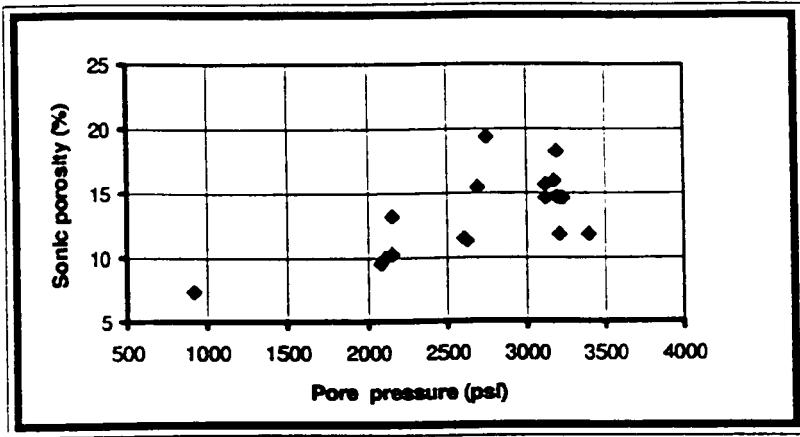


Figure 4.7 Cross plot of sonic porosity versus pore pressure for the 74-4 reservoir.

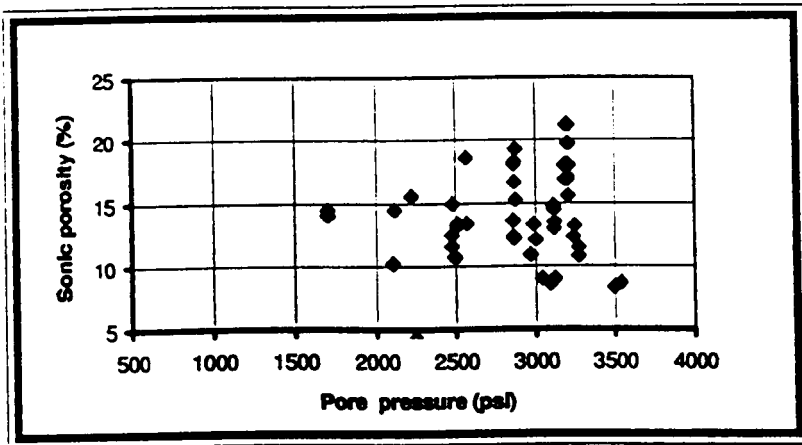


Figure 4.8 Cross plot of sonic porosity versus pore pressure for the 74-6 reservoir.

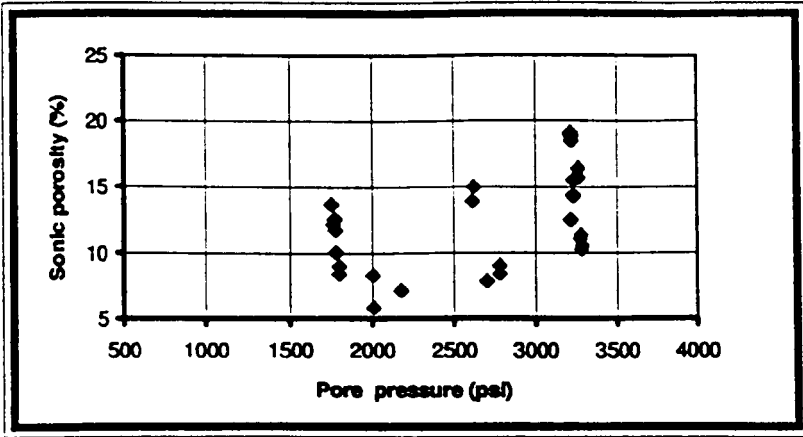


Figure 4.9 Cross plot of sonic porosity versus pore pressure for the 75-5 and 75-6 reservoirs.

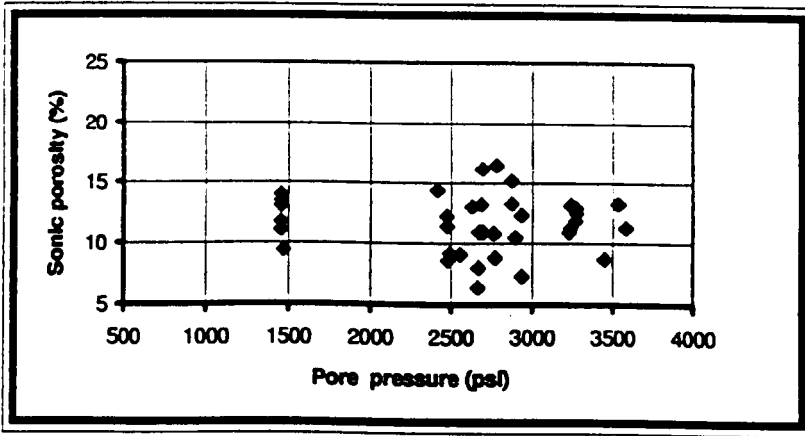


Figure 4.10 Cross plot of sonic porosity versus pore pressure for the 76-4 reservoir.

CHAPTER FIVE

AN INVESTIGATION OF THE RELATIONSHIP BETWEEN APPARENT POROSITY DECREASE AND PRESSURE DEPLETION

5.1 INTRODUCTION

The cross plots between the sonic porosities and the RFT data presented in the previous chapter, despite the large amount of scatter, indicate the association of low formation pressures with the low sonic porosities in the Patchawarra Formation in the Toolachee Field. Four possible reasons for this relationship are:

The apparent porosity decrease is real, and results from:

- I. Additional compaction caused by increasing effective stress as pore pressure decreases.

II. Formation damage caused by production.

The apparent porosity decrease is not real, but results from:

III. The effect of reduced pore pressure on the compressional wave velocity measured by the sonic log.

IV. The effect of increased water saturation on the compressional wave velocity measured by the sonic log.

The following section discusses these mechanisms and their merits and implications in study area.

5.2 POROSITY REDUCTION BY ADDITIONAL COMPACTION

5.2.1 MECHANICAL COMPACTION

One of the most obvious changes that occurs during diagenesis is the volume reduction, and consequently porosity reduction, caused by mechanical compaction.

The reduction in porosity of sediments is dominantly induced by the continuing accumulation of sediment increasing the vertical stress (Jones and Addis, 1985). The rate of compaction in sedimentary rocks decreases as the depth of burial increases.

Lithology and diagenetic events such as cementation are other factors controlling compaction caused by burial (Jones and Addis (1985), Houseknecht (1987)).

Schulz-Rojahn (1991) and Stuart et al. (1992) investigated the factors affecting porosity and permeability in the Permian sandstone reservoirs of the southern Cooper Basin. These studies indicate that the main effect in the reduction of porosity and permeability in these rocks is mechanical compaction. This factor is stronger in finer grained rocks such as shales and poorly sorted sandstones with detrital clay. However, in many moderately to well sorted sandstones, compactional effects are minimal, due to the occurrence of early silicification.

5.2.2 PRODUCTION AND ADDITIONAL COMPACTION

The depletion of a shallow hydrocarbon reservoir or the excessive production of ground water from a shallow aquifer create abnormally low pore pressure. This results in an increase in net overburden pressure in the reservoir. Such conditions can cause additional compaction and often surficial subsidence (Gretener, 1981). Poland (1972) listed a number of cases of land subsidence caused by fluid withdrawal from oil and gas fields (Table 5.1).

The bulk compressibility of the sediments is a basic parameter required to evaluate the degree of compaction resulting from a given increase in effective stress. The bulk compressibility of sediments is known to decrease substantially as the effective overburden load increases. Laboratory measurements of the mechanical characteristics of reservoir rocks can be used to construct stress-strain curves, from which the compressibility of the reservoir can be determined. For instance, experiments show that, at effective stresses of 1500-3000 psi, some sands may be as compressible as clays or shales (Poland, 1972).

<i>Location</i>	<i>Age</i>	<i>Depth Range of Compacting Beds (ft)</i>	<i>Maximum Subsidence (ft)</i>	<i>Time of Occurrence</i>
<i>Italy (Po Delta)</i>	<i>Quaternary</i>	<i>300-1300</i>	<i>6-10</i>	<i>1950-61</i>
<i>Japan (Niigata)</i>	<i>late Cenozoic</i>	<i>300-3000</i>	<i>8</i>	<i>1956-69</i>
<i>Venezuela (Lake Maracaibo)</i>	<i>Miocene</i>	<i>2000-4500</i>	<i>13 (?)</i>	<i>1930-60</i>
<i>California (Wilmington)</i>	<i>Miocene- Pliocene</i>	<i>2000-4000</i>	<i>29</i>	<i>1938-65</i>

Table 5.1 Examples of major land subsidence due to fluid withdrawal from oil and gas fields. (Summarised from Poland, (1972)).

5.2.3 ROCK COMPRESSIBILITY IN THE COOPER BASIN

Porosity measurements made on core under overburden pressure are the only available information on the mechanical properties of the sandstone reservoirs in the Cooper Basin(Schlichting, Santos Ltd. personal communication, 1994). Core porosities measured under pressures of up to 5000 psi show very little porosity reduction compared to ambient (403 psi) core porosities. Based on these measurements Overton (1986) derived an equation relating fractional core porosities measured at ambient and overburden pressures for the Cooper Basin :

$$\text{Porosity}_{\text{Overburden}} = 0.947 \times \text{Porosity}_{\text{Ambient}} + 0.0022 \quad (\text{E } 5.1)$$

Work by Morton (1990) also showed that for the sandstones of the Cooper Basin the difference between core porosity measured at ambient and overburden pressures (2900 to 5800 psi) is only 0.5 porosity unit. He suggested the following equation for converting the ambient core porosities to in-situ porosities in the Cooper Basin:

$$\text{Porosity}_{\text{Overburden}} = 0.95 \times \text{Porosity}_{\text{Ambient}} \quad (\text{E } 5.2)$$

These studies imply that, due to low compressibility, the bulk volume of the reservoir rocks in the study area does not change significantly under increasing effective pressure caused by production.

5.2.4 DEPLETION AND ADDITIONAL COMPACTION IN THE STUDY AREA

As Table 5.1 shows, most of the subsidence phenomena caused by fluid withdrawal in oil and gas fields have occurred in shallow, young sediments. For instance, the principle oil zones in the Wilmington oil field in California occurred in Miocene and Pliocene sandstones at depths of 2000 to 4000 ft. The effective pressures after depletion in the 1950s were 1500 to 3000 psi. Axial loading tests showed the reservoir sandstones to be as compactable, or more so, than the siltstones at the field's effective stresses. Above the 4000 ft, the sandstones are uncemented and loose (Poland, 1972).

In contrast, the sandstones in the Patchawarra Formation in the Toolachee Field occur at depths between 6800 and 8200 ft, and have been well compacted both mechanically and by process during several phases of diagenesis.

Based on the existing information on mechanical properties, previous petrographic studies on the reservoir rocks in study area, and analogy, it can be concluded that there is no significant additional compaction in depleted reservoirs in the Toolachee field. Hence, production is unlikely to affect reservoir porosity significantly.

5.3 POROSITY REDUCTION CAUSED BY FORMATION DAMAGE

5.3.1 FORMATION DAMAGE

The majority of reservoir rocks in the subsurface exist in a metastable diagenetic equilibrium with little potential for further changes in petrophysical properties. Field development including drilling and hydrocarbon production will upset the equilibrium that exists in a reservoir between formation and its pore fluid. Kantorowicz, et al. (1986) used the term rock-fluid interaction to describe the changes in reservoir characteristics such as porosity and permeability which occur as a consequence of production operations in reservoir rocks.

The type and mode of occurrence of clay minerals in sandstones play important roles in this rock-fluid interaction. Authigenic clays, because they commonly occur within pores, will readily contact any introduced fluids. As little as 1 to 2 percent clay as coatings on the grains of a sandstone could cause formation damage (Pitman and Thomas, 1979). Loose or loosely attached clay minerals or other fine particles in

sandstone may mechanically move with fluids during flow. These particles may eventually reach an obstruction, usually a pore throat, plug flow channels and reduce both permeability and porosity (Gregory (1977), Pittman and Thomas (1979), Pittman and King (1986), Harper and Buller (1986) and King (1992)). Among the clay minerals, kaolinite appears to be particularly susceptible to movement through the formation (Pittman and Thomas, 1979).

Formation damage caused by migration of fines increases with the hydrocarbon flow rate and may be characterised by a critical velocity. At velocities greater than the critical velocity, fines will move in sufficient quantities to alter porosity and permeability. The effect of velocity is most apparent where flow is totally radial and velocity increases as the fluid converges near the well bore (King, 1992).

5.3.2 CLAY MINERALS, PORE TEXTURE AND FORMATION DAMAGE IN THE STUDY AREA

Dickite and kaolinite form part of the kaolin sub-group of clay minerals, and are the most abundant clay minerals present in the study area. Under the scanning electron microscope these minerals are evident as subhedral to euhedral booklets which infill pores (Alsop (1990) and Stuart et al. (1992)).

Kaolin occurs in two forms within the sandstones. One form is patchy, and the second form is intergranular fillings or authigenic matrix. Patches in relatively clean sandstones with dissolution are loosely framed with relatively high porosity, whereas kaolin matrix fillings usually are tighter (Stuart et al. (1992), Tingate and Luo (1992)).

Pore structure and microporosity associated with clay minerals in the reservoir sandstones of the study area increase the tortuosity of the pore network, making clay particles prone to dislocation by fluid flow during production. The mechanical damage from migrating fines is considered to be a moderate to major problem for commercial gas production from the Patchawarra Formation reservoirs in other areas of the Cooper Basin such as the Big Lake Field (Stanley and Halliday, 1984).

However, the data used in the current study represent pre-production conditions within the wells from which they were obtained. Hence, formation damage caused by fine migration due to fluid flow toward the well bore could not affect the porosity of reservoir rocks adjacent to the well bore. In contrast, the pressure differential between the mud and the partially depleted formation will create a relatively deep invasion of mud fluid into the formation. Since drilling mud particles are sized to stop at the formation face, the high differential pressure between mud and the reservoir may cause a high flow rate from the well bore into the formation. This might dislodge loose fine grains from the invaded zone into the undisturbed formation, perhaps resulting in both permeability and porosity increases in the invaded zone near the well bore.

Since log-derived porosity usually measures the porosity of the invaded zone, it can be concluded that formation damage is unlikely to cause the apparent sonic porosity reduction in pressure depleted reservoirs in the Toolachee Field. It follows that the low sonic porosities measured in depleted reservoirs are not reflecting actual porosity accurately.

5.4 POROSITY UNDERESTIMATION BY THE SONIC LOG

5.4.1 EFFECT OF VARIOUS FACTORS ON WAVE VELOCITY

A knowledge of the elastic wave velocities in sedimentary rocks is of considerable interest in the fields of geological engineering, geophysics and petroleum engineering (King, 1966). It is well known that the acoustic velocities of sedimentary rocks are controlled by mineralogy, pore fluid, porosity, pore geometry, degree of consolidation, cementation, confining pressure, pore pressure, temperature and other factors (Nur and Wang, 1988). As Figure 5.1 shows porosity, gas saturation and pressure have significant effects on wave velocity for a rock of given mineralogy. Wyllie et al. (1956 and 1958) experimentally investigated the factors affecting compressional wave velocities. The time-average equation of Wyllie et al. (1956) shows that velocity is determined primarily by porosity, mineral composition and pore fluid:

$$1 / V_p = (\phi / V_f) + ((1-\phi) / V_m) \quad (E 5.3)$$

where

V_p is the compressional velocity of a liquid-saturated rock, ϕ is the fractional porosity, V_f is the velocity of the pore fluid and V_m is the velocity of the rock matrix.

This simple equation is adequate to first order for clean sandstone in the middle range of porosity, $10\% < \phi < 25\%$, (Han et al. , 1986). Wyllie et al. (1958) also

demonstrated that for water-saturated oil-wet Berea Sandstone, of Mississippian age from the Appalachian Basin, USA, under hydrostatic conditions, the effect of an increase in confining pressure (P_c) on wave velocities is cancelled by the effect of an equal increase in pore pressure (P_p). Conversely, for a given confining pressure, the velocity of compressional waves changes as the pore pressure changes. Hence, velocity is constant for a given differential pressure $P_d (= P_c - P_p)$.

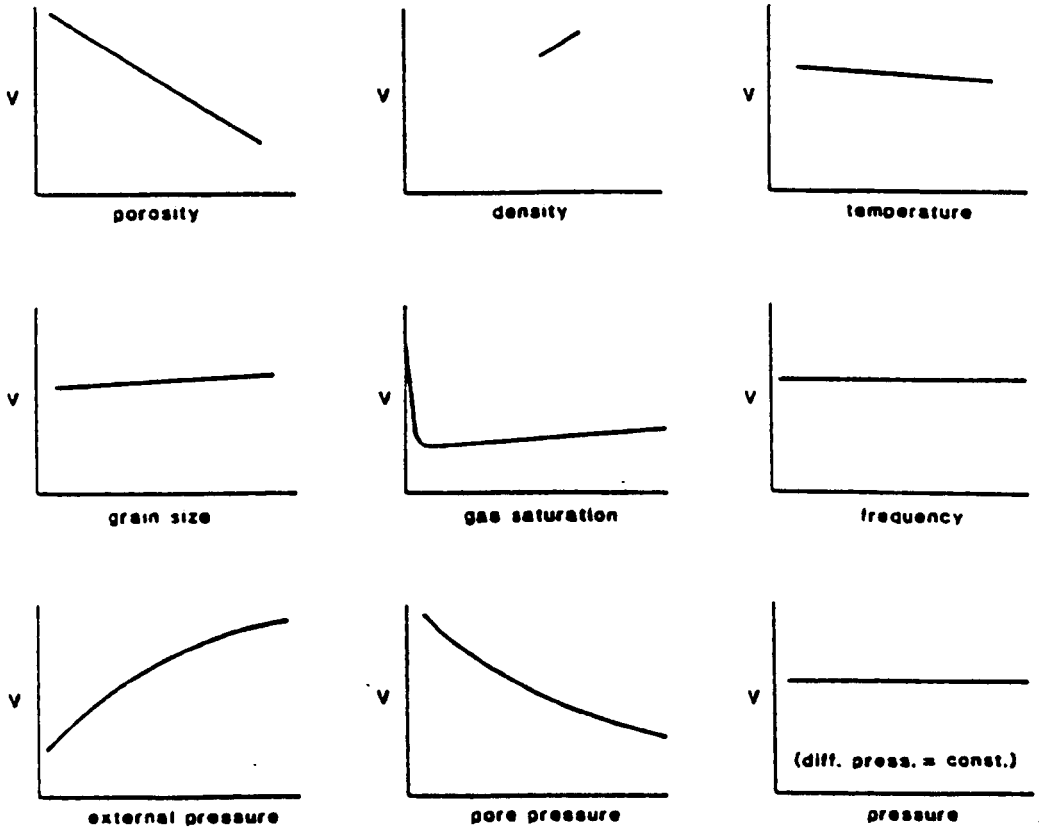


Figure 5.1 Various factors which affect rock velocity (from Rider (1986) after Hilterman (1977)).

The sensitivity of the acoustic velocity to pore pressure can be used to identify overpressure from the sonic log. Other things remaining constant, an increase in pore pressure is indicated by an increase in the sonic transit time (Rider, 1985). It is possible to calculate the amount of overpressure from the deviation of the sonic travel time from the normal compaction trend (Hottman and Johnson, 1965), when the shale transit time is plotted on a logarithmic scale versus the burial depth (Figure 5.2).

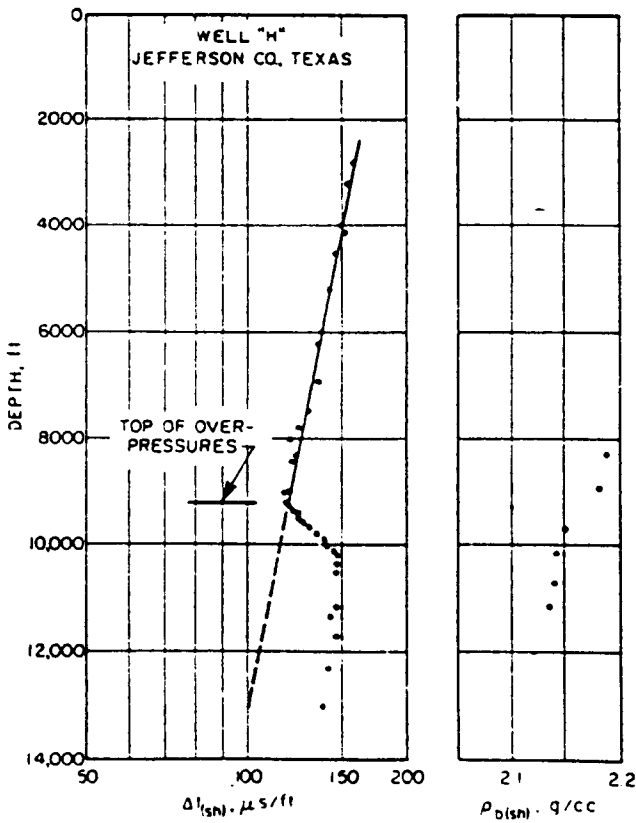


Figure 5.2 Application of the sonic log to the estimation of overpressuring (from Hottman and Johnson, 1965).

Experimental work by Gregory (1976) showed that the difference between the velocity of a fully water saturated rock ($S_w = 100\%$) and the velocity of the same rock when fully gas saturated ($S_w = 0\%$) varies with the porosity of the rock. In rocks with porosity less than 10% the coupling between the fluid and the solid is the important factor affecting velocity, while in high porosity rocks (porosity greater than 25%) the dominant factor influencing velocity is the compressibility of the pore fluids (Figure 5.3). For rocks with a moderate porosity (10% to 25%) a small amount of gas added to the pore fluid will cause the velocity to decrease to a minimum value from which it does not show a marked change as the amount of gas increases (Figures 5.1 and 5.3).

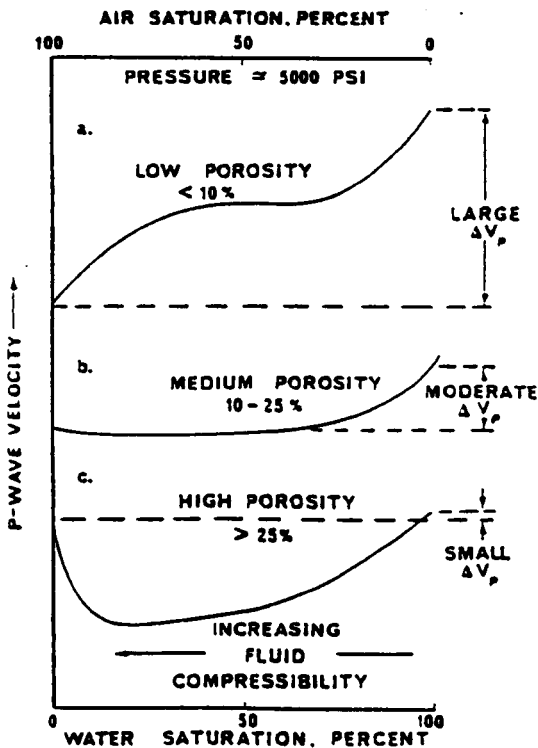


Figure 5.3 Effect of gas saturation on rock velocity (from Gregory, 1976).

5.4.2 DIFFERENTIAL PRESSURE AND VELOCITY

Following on from the work of Wyllie et al. (1958), the effect of differential pressure on the velocity of elastic waves has been studied by numerous investigators. King (1966), Todd and Simmons (1972), Christensen and Wang (1985), Yu et al. (1991) and many others have experimentally demonstrated the effect of differential pressure on wave velocity for different rocks.

Experiments indicate that confining and pore pressures have roughly equal, but opposite, effects on P wave velocity. If the differential pressure increases, the velocity increases. This effect can be interpreted to mean that: (1) the velocity of pore fluid increases because the pressure on the pore fluid increases, (2) the acoustic coupling between pore fluid and matrix increases when pore pressure increases or (3) both of these factors are operating (Gregory 1976). Following is a summary of the results of these laboratory measurements for four different rock types.

5.4.2.1 CLEAN SANDSTONE

The high porosity, permeability and uniformity of the Berea Sandstone of Mississippian age has led to it being selected by several workers as an ideal clean sandstone on which to measure the compressional wave velocities (V_p) under different confining and pore pressures (Wyllie et al. (1958), King (1966), Christensen and Wang (1985)). Their results show the high dependence of V_p on differential pressure (Figure 5.4 to 5.6). For instance, as Christensen and Wang (1985) demonstrated, for a confining pressure of 4350 psi, reducing pore pressure to 3350, 2350 and 350 psi increases V_p by 10.6, 17.9 and 19.7 per cent respectively, relative to V_p at hydrostatic conditions.

In terms of sonic transit time (Δt) values, Δt decreases from 88.75 to 75.27 $\mu\text{s}/\text{ft}$ as pore pressure decreases from 4350 to 2350 psi under a constant confining pressure of 4350 psi. Table 5.2 summarises the results of the three experiments on the Berea sandstone by the authors mentioned above.

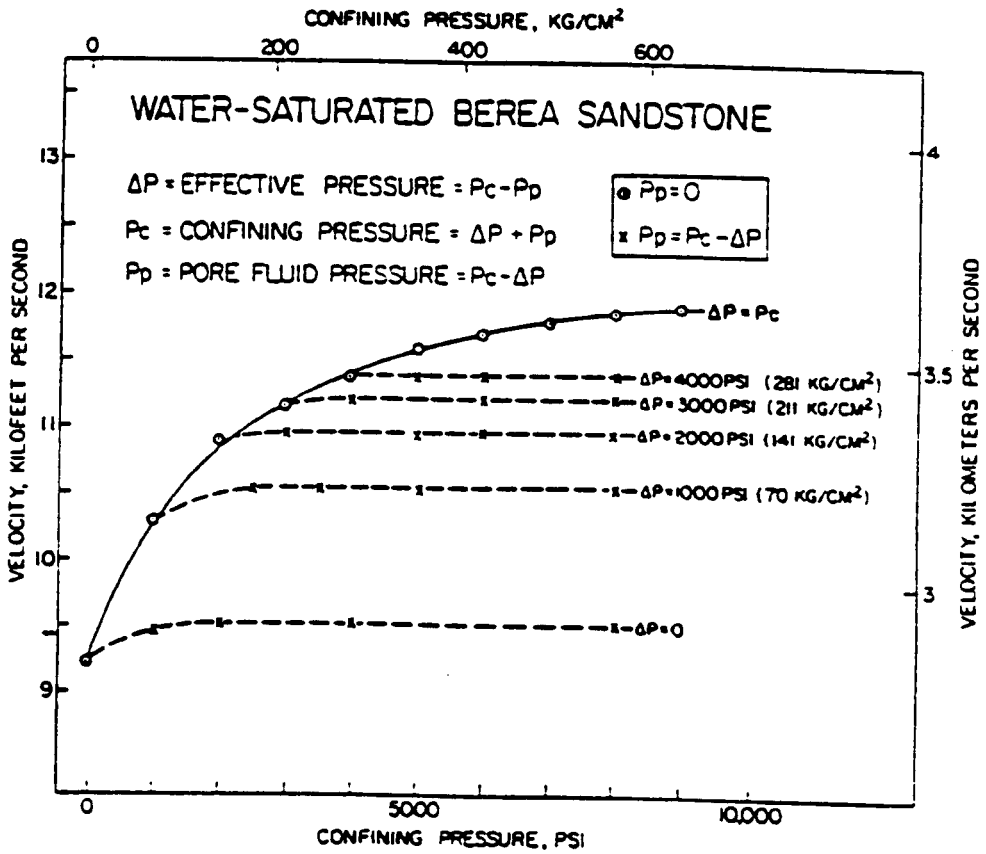


Figure 5.4 Compressional wave velocity as a function of confining and differential pressures in the Berea sandstone (from Wyllie et al. , 1958).

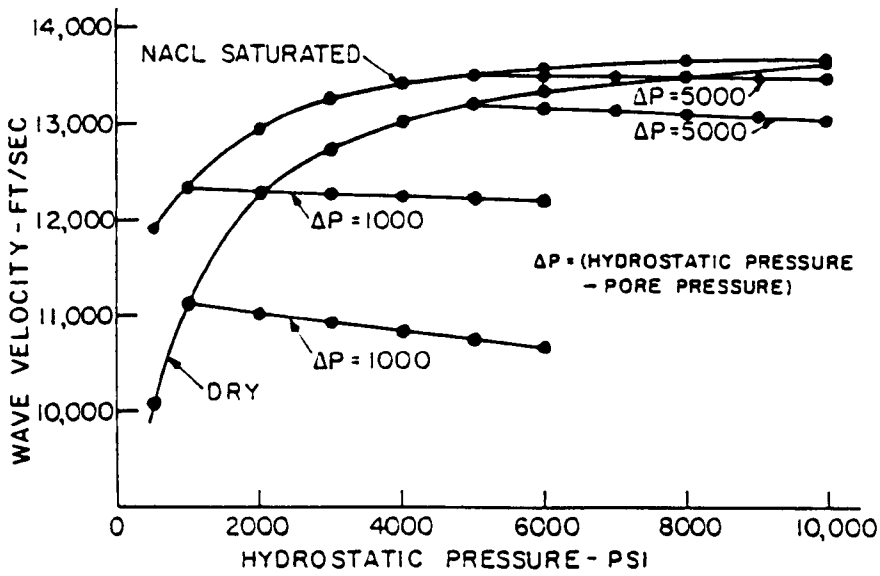


Figure 5.5 Compressional wave velocity as a function of confining and differential pressures in the Berea Sandstone (from King, 1966).

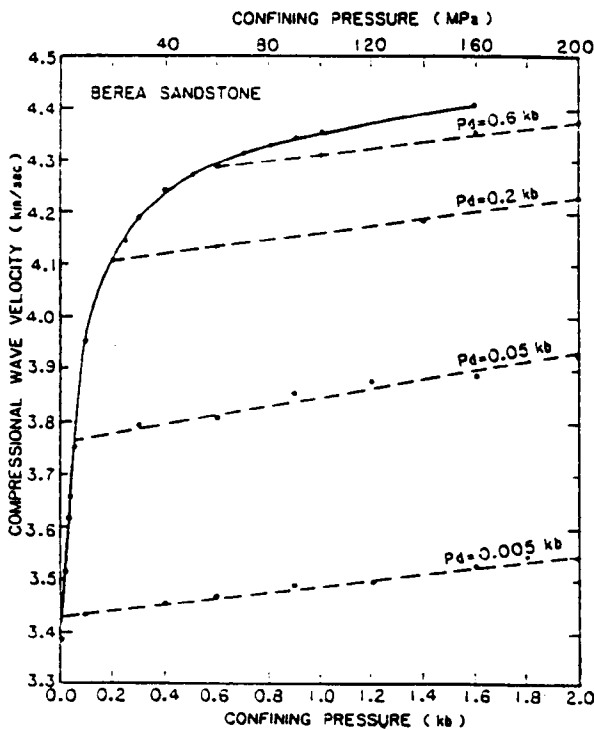


Figure 5.6 Compressional wave velocity as a function of confining and differential pressures in the Berea Sandstone (from Christensen and Wang, 1985).

Confining Pressure (psi)	Differential Pressure (psi)	V _p (km/s)		
		Wyllie et al (I)	King (II)	Christensen & Wang (I)
1450	0	2.896	3.048	3.430
1450	1000	3.223	3.375	3.790
2900	1000	3.223	3.388	3.795
2900	2000	3.352	3.698	3.950
4350	1000	3.223	3.297	3.800
4350	2000	3.352	3.673	4.050
4350	4000	3.419	3.841	4.110
7250	1000	3.223	3.225	3.817
7250	2000	3.352	3.581	3.862
7250	3000	3.419	3.739	4.129
7250	6000	3.569	4.051	4.200

Table 5.2 Compressional wave velocities as a function of differential pressure for the Berea Sandstone. (I) Water saturated, (II) Nitrogen saturated. Data for the Berea Sandstone: Porosity 19-21 per cent, Permeability 250 md, Bulk density 2.14 g/cm³, Petrographic analysis: Quartz 70 per cent, Clay minerals 10 per cent, Lithic fragments; Feldspars and opaques 20 per cent, Carbonate and Quartz are the cementation materials. Summarised from Wyllie et al. (1958), King (1966) and Christensen and Wang (1985). Tabulated values interpolated from Figures 5.4 to 5.6 for comparison.

5.4.2.2 LOW POROSITY ROCKS

Todd and Simmons(1972) investigated the effect of differential pressure on wave velocities in the Chelmsford granite from New England in the USA, and the Trigg limestone from Texas. These are examples of low porosity rocks ($\phi = 0.5\%$).

Although the variation of V_p with differential pressure for low porosity rocks is not as great as that in the Berea Sandstone, the results of these experiments also show that, for a constant confining pressure, the higher the differential pressure, the higher the wave velocity (Figure 5.7 and Table 5.3).

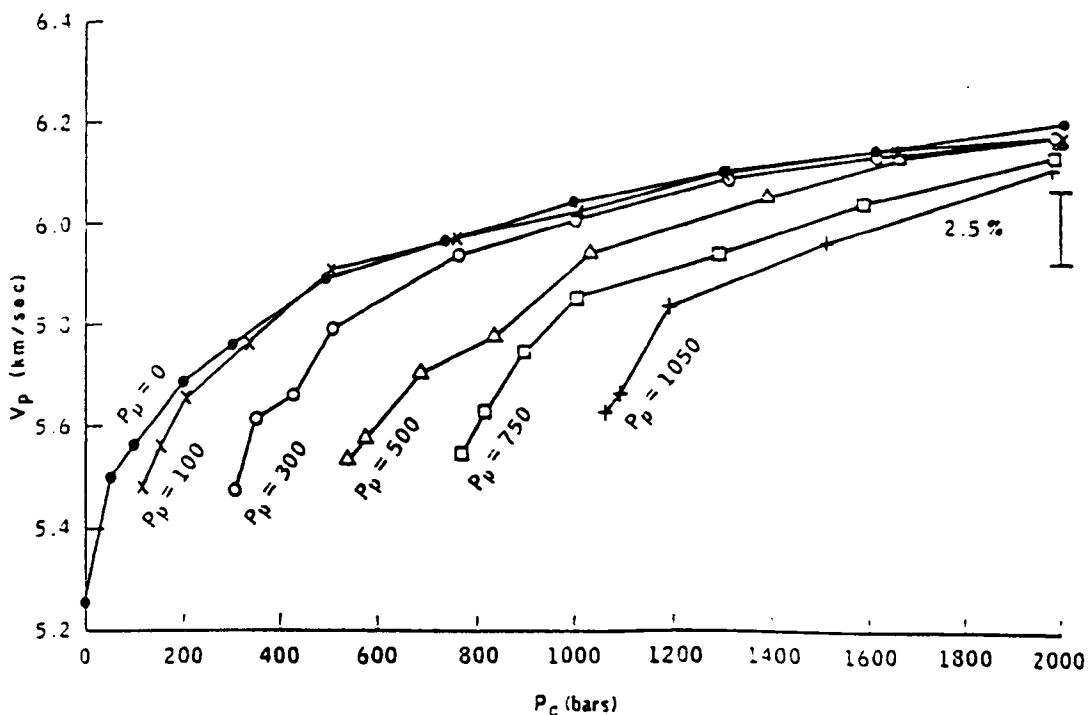


Figure 5.7 Compressional wave velocity as function of confining and differential pressures in Chelmsford granite (from Todd and Simmons, 1972).

<i>Confining Pressure (psi)</i>	<i>Differential Pressure (psi)</i>	<i>V_p (km/s)</i>	
		<i>Granite</i>	<i>Limestone</i>
1450	0	5.450	5.388
1450	1450	5.563	5.596
2900	1450	5.659	5.598
2900	2900	5.689	5.688
4350	0	5.463	5.420
4350	2900	5.732	5.769
4350	4350	5.758	5.777
7250	2900	5.780	5.495
7250	5800	5.909	5.810
7250	7250	5.893	5.983

Table 5.3 Compressional wave velocities as a function of differential pressure for Chelmsford granite and Trigg limestone.

Data for Chelmsford granite: Porosity 0.5 per cent, Bulk density 2.619 g/cm³, Petrographic analysis; Quartz 31 per cent, Microcline 31 per cent, Oligoclase 31 per cent, Mica 5 per cent and Chlorite 2 per cent.

Data for Trigg limestone: Porosity 0.5 per cent, Density 2.767 g/cm³, Petrographic analysis; Carbonate 95 per cent, Quartz 5 per cent.

Summarised from Todd and Simmons (1972).

5.4.2.3 COAL

Yu, Vozoff and Durney (1991) studied the effect of pore pressure on V_p in coal sampled from the Permian black coal seams in New South Wales, Australia. The results of this study show that V_p in coal decreases with increasing pore pressure at constant confining pressure. They also observed that the effect of confining pressure increase was not exactly cancelled by an equal increase in pore pressure. Instead there was a gradual increase in V_p with simultaneous increase in both confining and pore pressure (Figure 5.8)

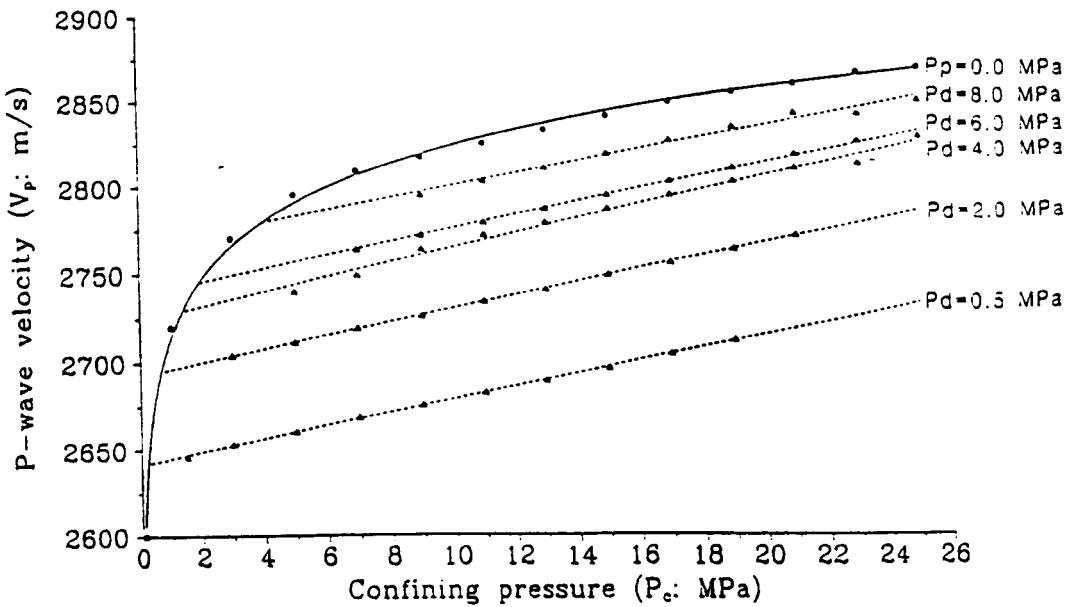


Figure 5.8 Compressional wave velocities as a function of differential pressure for black coal (Yu, Vozoff and Durney, 1991)

5.4.3 SONIC POROSITY AND DEPLETION

5.4.3.1 LOG-DERIVED POROSITY

As mentioned previously the sonic log is the only available porosity log in the study area. However, the sonic log does not directly measure porosity. Instead, it measures the time required for a sound wave to traverse a given distance in a formation. This measured transit time must then be converted into porosity.

Various equations have been proposed to accomplish this. They have been based on theoretical developments, experimental data, or a combination of the two (Raymer et al, 1980).

The Overton equation (1986) is the empirical method currently used by Santos Ltd. for porosity calculations in the Cooper Basin. This equation is based on the time-average formula of Wyllie et al (1958)

$$\phi = (\Delta T - \Delta T_{\text{m}}) / (\Delta T_{\text{f}} - \Delta T_{\text{m}}) \quad (\text{E } 5.4)$$

where

ϕ is the sonic porosity (fraction)

ΔT is the sonic transit time ($\mu\text{s}/\text{ft}$),

ΔT_{m} the transit time of the matrix, 55.5 $\mu\text{s}/\text{ft}$ in the Cooper Basin,

ΔT_{f} is the sonic transit time of the pore fluid, which for the Patchawarra Formation in the Toolachee Field, is obtained from Table 5.4.

Gamma Ray Reading (API)	ΔT_n ($\mu\text{s}/\text{ft}$)
20	230
30	225
50	225
50-80	$0.51\text{GR} + 199.3$
80	240.4

Table 5.4 The empirical values of ΔT_n ($\mu\text{s}/\text{ft}$) used in the Overton equation for the Patchawarra Formation in the Toolachee Field (Overton and Hamilton, 1986).

5.4.3.2 ΔT AND RFT DATA

Figure 5.9 shows the relation of the sonic log readings and the sonic porosities used in the present study. Although there is some scatter in this figure, for example 6 different porosity values ranging from 10 to 15 per cent for a sonic reading of 74 $\mu\text{s}/\text{ft}$, the plot shows an excellent correlation between ΔT and sonic porosities. As a result, the cross plot of the RFT versus the sonic data (Figure 5.10) is very similar to the cross plot of the RFT and sonic porosities in Figure 4.3.

5.4.3.3 ΔT AND WATER SATURATION

Figure 5.11 shows the relationship between the calculated water saturation and the sonic log readings in this study. Despite some scatter, the plot mainly shows as the water saturation decreases (the gas saturation increases) the sonic log value increases. However, the cross plot of the pore pressures versus water saturations (Figure 5.12) indicates that as pore pressure decreases water saturation does not

change significantly. On this basis, it can be included the pressure depleted reservoirs in the study area are still gas saturated.

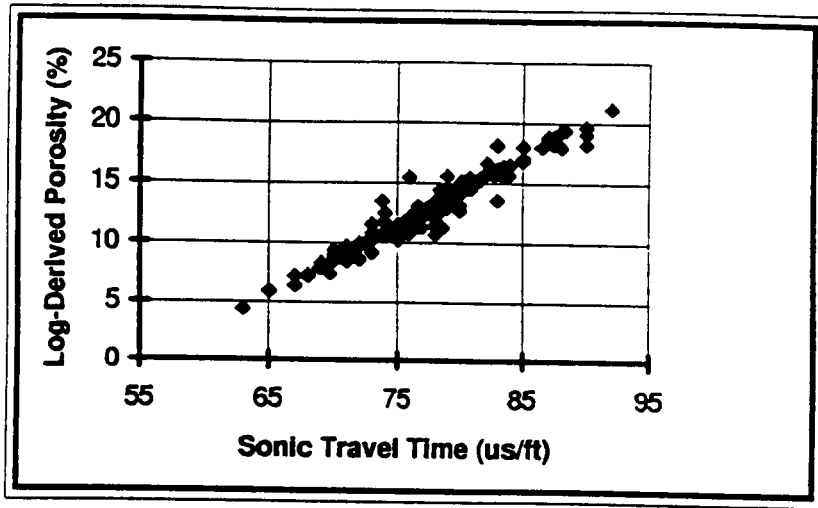


Figure 5.9 Cross plot of sonic porosity versus sonic transit time in the study area.

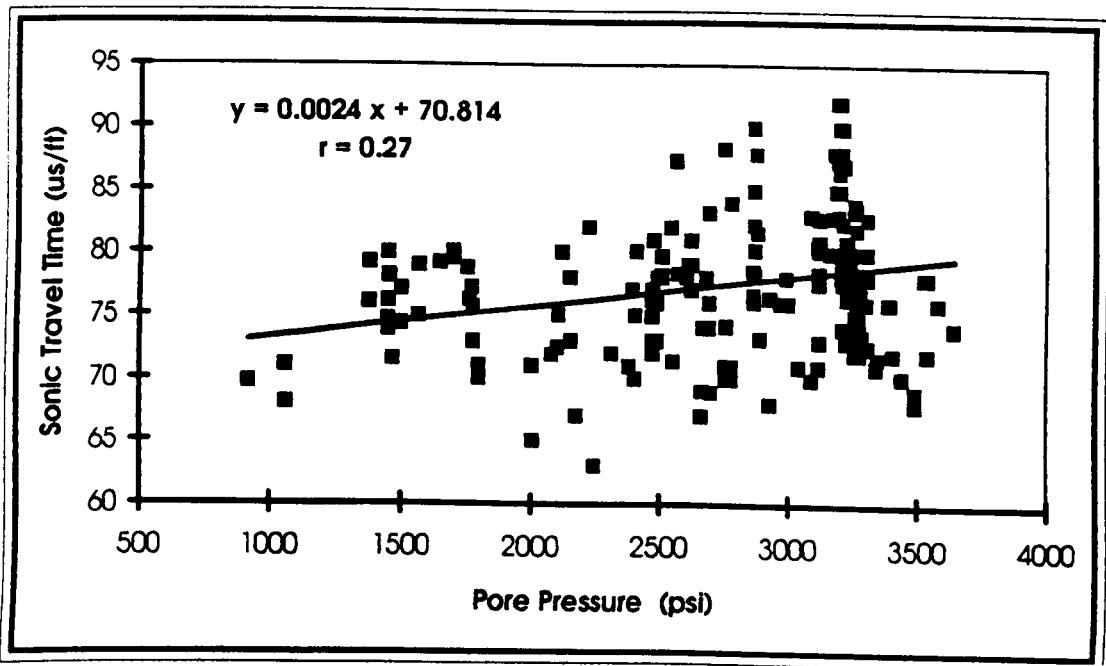


Figure 5.10 Cross plot of sonic transit time versus pore pressure in the study area.

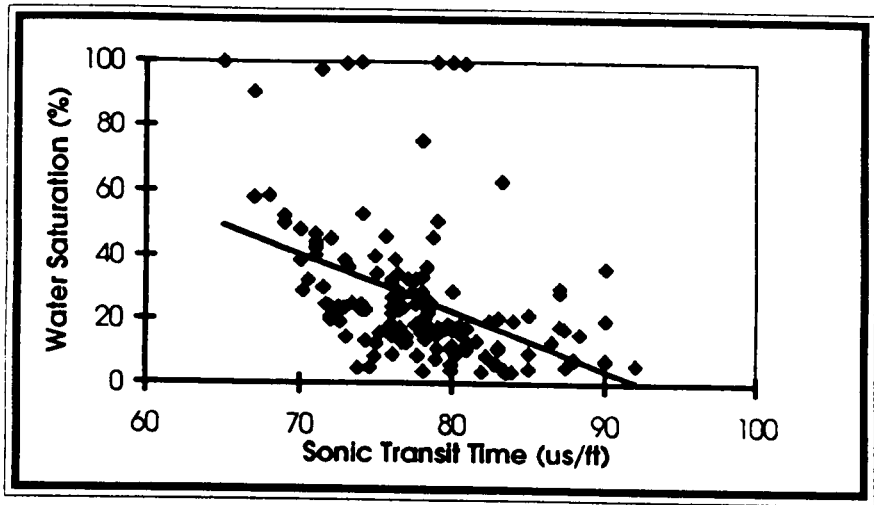


Figure 5.11 Cross plot of calculated water saturation versus sonic transit time.

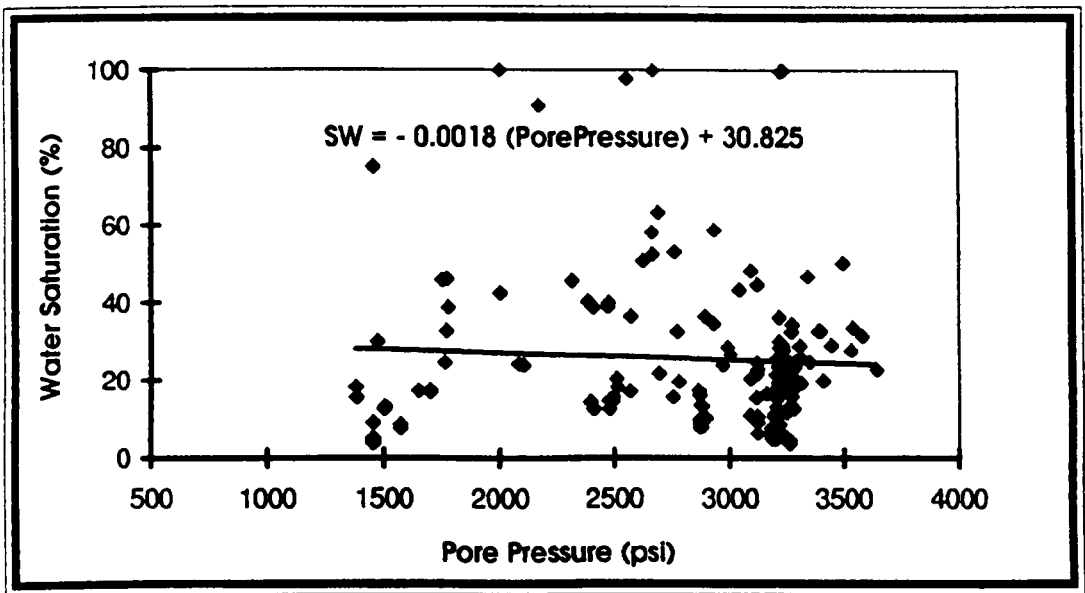


Figure 5.12 Cross plot of calculated water saturation versus pore pressure.

5.5 DISCUSSION

5.5.1 GENERAL

The formation environment may be disturbed irrecoverably by the withdrawal of fluid from reservoir rocks (Rider 1986). The gas saturation and pore pressure, two major factors affecting V_p , are reduced by production from a gas-bearing reservoir. This may cause the sonic log to be influenced by the changing formation environment.

Conventional log analysis indicates that there is no marked decrease in calculated gas saturation values in depleted reservoirs in the Toolachee Field. Therefore, the minimal gas saturation reduction is unlikely to affect the wave velocity significantly. Hence, it seems reasonable to reject the hypothesis that the observed porosity underestimation by the sonic log is due to increasing water saturation with production.

The available RFT data, however, show a significant decrease in pore pressure within the depleted reservoirs in the study area. Reduction of pore pressure, caused by production, at constant overburden pressure, results in greater differential pressure in depleted reservoirs, by up to 2600 psi compared with the differential pressure in virgin reservoirs.

Integration of existing information with the concept of the effect of pore pressure on wave velocity, provides valuable clues to explain the association of the low sonic porosities with low pore pressures in the Toolachee Field. Considering that the sonic and RFT tools are being affected by the same formation environment near the well bore, other things remaining constant, a decrease in pore pressure would be expected

to cause a reduction in the sonic transit times. Hence, for a reservoir sandstone with a given porosity, the sonic log will indicate decreasing porosity as the pore pressure of the reservoir decreases.

5.5.2 COMPARISON WITH THE BEREA SANDSTONE

Unfortunately, no measurements of velocity as a function of confining and differential pressures exist for Patchawarra Formation sandstones. Hence there are no direct measurements available to verify the mechanism believed to be responsible for the low transit times seen in depleted reservoirs. However, comparing the observed transit time changes with those measured under similar pressure conditions on the Berea Sandstone provides at least some control on the plausibility of the mechanism being invoked, despite differences in porosity, clay content, etc. between the Berea Sandstone and the Patchawarra Formation reservoirs. At the average overburden pressure in study area, 7200 psi, Figures 5.4 to 5.6 indicate that ΔT in the Berea Sandstone decreases by up to 6 per cent as the pore pressure decreases from 3700 to 700 psi. A plot of ΔT averaged over 700 psi intervals versus the pore pressure for the Patchawarra data, shows a very similar trend to King's experimental data (1966) for the Berea Sandstone (Figure 5.13).

The variation in ΔT over the same range of pore pressures was somewhat lower for the other two sets of experimental data (Wyllie et al.(1958) and Christensen and Wang (1985)). It may be significant that the pore fluid in King's experiments was nitrogen, which has a compressibility much closer to the natural gas in the Patchawarra

reservoirs, than the water used as the pore fluid in the other two sets of measurements on the Berea Sandstone.

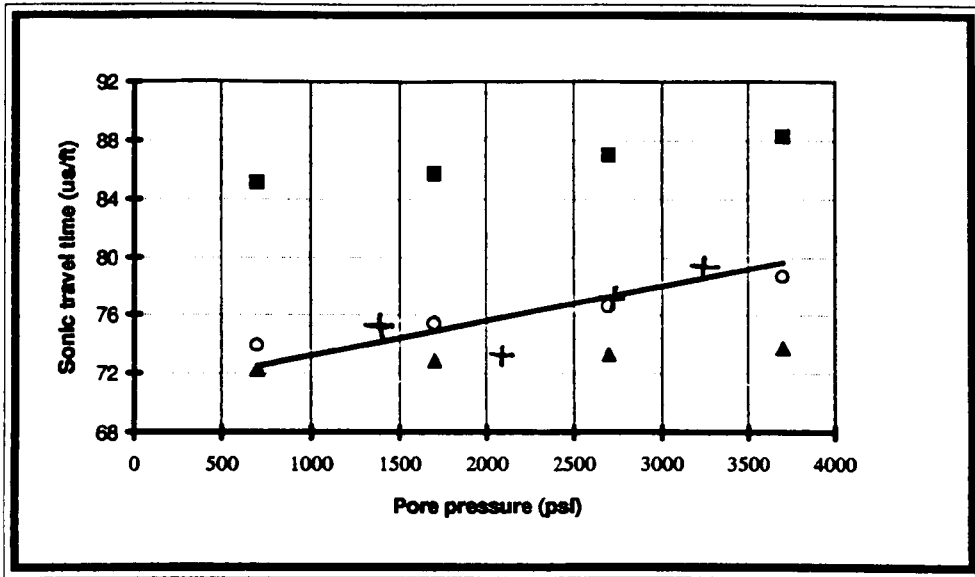


Figure 5.13 Comparison of effect of pore pressure variation on sonic transit times for the Berea Sandstone, and the Patchawarra Formation in the Toolachee Field (see text).

■ Wyllie et al. (1958), ○ King (1966), ▲ Christensen and Wang (1985), + averaged ΔT over 700 psi intervals in the Toolachee Field, and regression line from Figure 5.10. Overburden pressure 7200 psi in all cases.

Assuming that the Berea Sandstone analogy is valid, Table 5.5 shows the range in ΔT and consequently the sonic porosity decrease caused by pressure depletion for four porosities. The following assumptions were made to fix the values in Table 5.5 .

- I The overburden pressure is 7200 psi,
- II The initial pore pressure is 3700 psi,

- III The gamma ray reading is constant for the four cases and,
- IV The Overton equation gives reliable porosity calculations in the Patchawarra Formation in the Toolachee Field.

According to Table 5.5, porosity underestimation by the sonic log due to 1000 and 3000 psi reductions in pore pressure for actual porosities of 17.4 and 8.5 per cent, ranges from 1.3 to 3.0 porosity units (7.4% to 17.4%) and from 1.0 to 2.5 porosity units (11.7% to 29.4%), respectively.

Comparison of the values in Tables 5.5 and 4.1 suggests that the ΔT decrease caused by depletion in the study area might be somewhat greater than that in King's experiments on the Berea Sandstone. Since the average porosity within the reservoir sandstones of the Patchawarra Formation in the Toolachee Field is 12.7 per cent and the porosity cut-off currently used in reserve estimation is 8 per cent, even the inexact range of reduction in ΔT due to pore pressure decrease indicated by Table 5.5 may result in significant underestimates of gas reserves in depleted reservoirs. This is likely to be a continuing and increasing problem in development wells. The underestimation will come about through two effects. Firstly, low porosity reservoir intervals (in the range 8% to 11%) may have sonic porosities below the 8% cut-off, and so not be counted as net reservoir. Secondly, the porosity assigned to all depleted reservoirs may be up to 3% too low, resulting in an underestimate of hydrocarbon pore volume.

Hence, if the sonic log is to remain the only porosity log run in the study area, then calibration of the sonic tool response for the pressure conditions of the reservoir will be crucial to accurate reserve estimate.

Pore Pressure (psi)	Case 1		Case 2		Case 3		Case 4	
	ΔT ($\mu s/ft$)	ϕ_{Sonic} (%)	ΔT ($\mu s/ft$)	ϕ_{Sonic} (%)	ΔT ($\mu s/ft$)	ϕ_{Sonic} (%)	ΔT ($\mu s/ft$)	ϕ_{Sonic} (%)
3700	85.00	17.4	80.00	14.5	75.00	10.3	70.00	8.5
2700	82.76	16.1	77.89	13.2	73.02	10.3	68.16	7.5
1700	81.44	15.3	76.65	12.5	71.86	9.6	67.07	6.8
700	79.86	14.4	75.17	11.6	70.47	8.8	65.77	6.0

Table 5.5 The approximate range of reduction in ΔT and the sonic porosity caused by pore pressure decrease in the Toolachee Field, assuming King's data for the Berea Sandstone holds for the Patchawarra Formation. Overburden pressure is 7200 psi (see text).

5.6 CALIBRATION OF THE SONIC LOG FOR PORE PRESSURE

5.6.1 GENERAL

The experimental studies suggest that at a constant confining pressure the velocity of compressional waves in a rock is strongly dependent on the pore pressure. The stress-dependent nature of V_p leads to the concept that, in a producing field, when the sonic

log is used to determine porosity, the pressure conditions in the reservoir will need to be taken into account.

It is often necessary to make corrections to log data prior to using them for petrophysical evaluation. For many logging tools there are correction charts to remove environmental effects, such as mud type, temperature, salinity of the formation water and so on. However, there is no published correction chart for porosity calculation from the sonic log at different pressure conditions.

Hence, in order to calibrate the sonic tool response to the pressure variation in the study area, the existing field data is the only source of information. The following analysis provides an empirical correction for the ΔT values for use in porosity calculation in low formation pressure reservoirs of the Patchawarra Formation in the Toolachee Field.

5.6.2 ΔT -PORE PRESSURE CALIBRATION

The data scatter in the plot of transit time versus pore pressure (Figure 5.10) suggests that there is little point in using anything more complicated than a linear function to calibrate transit time for pore pressure. The experimental data on the Berea Sandstone (Figure 5.13) also suggests that a straight line will adequately represent the calibration function.

Least square linear regression of ΔT on the pore pressures (Figure 5.10) results in the equation:

$$\Delta T = 0.0024 (\text{Pore Pressure}) + 70.8138, \quad (\text{E } 5.5)$$

with a correlation coefficient of $r = 0.27$.

Although the correlation coefficient of the regression line is low, equation 1 has strong statistical significance because of the relatively large sample size ($n = 198$). A t-test was used to examine the correlation coefficient.

$$t = [r (n - 2)^{0.5}] / (1 - r^2)^{0.5} \quad (\text{E } 5.6)$$

where

r is the correlation coefficient (here $r = 0.27$),

n is the number of data (here $n = 198$), and

t is the t-test value of sample correlation.

The t-test value of equation 1 is 3.926, which is greater than 2.576, the critical value of t for a sample size of 198, and 1.0 per cent level of significance. In other words, the correlation between the sonic transit time and the pore pressure in the study area shown by equation 1 is real with a probability of 99%.

As a result, equation 1 can be used to calculate an empirical calibration of the sonic log readings for the pore pressure variation within the study area. This correction is:

* Tables and statistical formulae in Davis (1986) were used in statistical analysis throughout this chapter.

$$\Delta T_{\text{corr}} = 0.0024 (\Delta Pp) \quad (\text{E } 5.7)$$

where

ΔT_{corr} is expressed in $\mu\text{s}/\text{ft}$, and

ΔPp is the pressure depletion in psi.

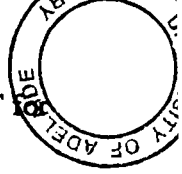
Equation 3 provides an approximate correction for the sonic log readings in depleted reservoirs in the study area. For a ΔPp reduction (from the initial pressure) in pore pressure, ΔT_{corr} should be added to the sonic log reading prior to using it to calculate porosity.

$$\Delta T = \Delta T_{\text{log}} + \Delta T_{\text{corr}} \quad (\text{E } 5.8)$$

Application of equations 3 and 4 in conventional log analysis may reduce or eliminate the porosity underestimation by the sonic log in low pressure gas reservoirs in the study area.

5.6.3 NOTATION

The proposed calibration of ΔT for the pressure decline in the Toolachee Field is only based on the available information. Absence of core data and other porosity logs in the present study mean that a comparison between corrected sonic porosity and porosities obtained from the other sources can not be presented. Such independent



data clearly would have provided control and modification on the calibration of ΔT pore pressure. However, comparison of the sonic porosities in Table 4.1 with the porosities calculated from corrected ΔT values suggests that the proposed calibration yields reasonable sonic porosities (closer to the average porosity in field) compared to the average porosity in the field (Table 5.6).

It is worth noting that the calibration presented here does not make any assumptions about the mechanism causing the observed correlation between transit time and pore pressure. The correction is simply an empirical one based on measured data.

Although a mechanism to explain the observed correlation has been suggested, the calibration does not require that this mechanism be the cause of the correlation.

<i>Sandstone Reservoir</i>	<i>Well Name</i>	<i>Sonic Porosity (%)</i>	<i>Corrected Sonic Porosity (%)</i>	<i>Average Porosity in Field (%)</i>	<i>Pore Pressure (RFT) (psi)</i>	<i>Estimated Initial Pressure (psi)</i>
73-0	<i>Toolachee-48</i>	7.3	10.4	12.6	1060	3258
74-4	<i>Toolachee-35</i>	7.4	10.7	13.3	919	3274
75-6	<i>Toolachee-35</i>	8.4	10.2	12.6	2003	3286
75-6	<i>Toolachee-39</i>	5.9	7.7	12.6	2007	3300

Table 5.6 Comparison of the conventional and the corrected sonic porosities in low pressure reservoirs in the Patchawarra Formation in the Toolachee Field. The initial pressures were obtained from Santos Ltd. (1993).

CHAPTER SIX

CONCLUSIONS AND RECOMMENDATIONS

6.1 CONCLUSIONS

6.1.1 LOG-DERIVED LITHOLOGY INTERPRETATION IMPROVEMENT

Conventional log-derived lithology overlooks most of the thin sandstone beds. This leads to an underestimation of gross sandstone in the Patchawarra Formation in each well in the study area by up to 35 per cent.

Log character and flow test results imply the presence of gas-bearing zones within thin sandstone beds. Overlooking thin reservoir beds may influence reserve estimates markedly.

Without the need for high resolution devices, the thin bed log analysis method, using the concept of binary lithology and an adaptive filtering technique applied to conventional logging suites, is able to resolve beds as thin as 6 inches.

Application of thin bed log analysis to lithology interpretation in the Patchawarra Formation gives gross sandstone thicknesses which agree with core data to within 5%. The method gives a more correct picture of reservoir rock distribution, and reveals more potential gas pay than the conventional log analysis.

6.1.2 SONIC POROSITY AND DEPLETION

Existing information in the Toolachee Field within the Patchawarra Formation shows that there is an association between low sonic porosities and low pore pressures.

Previous studies on the effect of overburden pressure on porosity in the Cooper Basin indicate that there is very little porosity reduction when core plugs are subjected to confining pressures of up to 5000 psi. Thus, the effect of high overburden pressure on porosity in the study area is unlikely to be significant. In contrast, pore pressures may decrease in depleted reservoirs by up to 70 per cent of the initial value, resulting in higher differential pressures.

The combination of published experimental studies on the effect of pore pressure on the compressional wave velocity and data in the study area suggest that the anomalously low sonic porosities may be due to the effect of differential pressure on the sonic tool response in depleted reservoirs.

Conventional porosity calculations from the sonic log may lead to underestimation of the actual porosity of the reservoir rocks in a depleted reservoir. The range of such

underestimation depends on differential pressure and the ΔT value at initial formation pressure.

The proposed equation for the calibration of the sonic log readings for the pore pressure variation provides an approximate correction for the sonic porosities in pressure depleted reservoirs in the study area. A detailed multidisciplinary study is required to verify the mechanism and to derive a more accurate correction.

6.2 RECOMMENDATIONS

6.2.1 THIN BED LOG ANALYSIS

Since the applied thin bed log analysis method does not require the use of any high resolution logging devices, there is the possibility of re-evaluating existing well log data in order to identify thin sandstone beds in the study area.

Further studies may be focused on the petrophysical characteristics and hydrocarbon productivity of thin bedded sandstone reservoirs in the Patchawarra Formation. The results of such studies may also be useful in formation evaluation in similar hydrocarbon reservoirs in the Cooper Basin and elsewhere.

6.2.2 PRESSURE DEPLETION AND FORMATION EVALUATION

6.2.2.1 LITHOLOGY AND FIELD CONTROL

The interpretation of the observed association of low pore pressures with low sonic porosities is only based on the available well log and RFT data. Absence of core data means that there is no petrographic control on this interpretation. Depleted reservoirs

now exist within a number of fields in the Cooper Basin. It is recommended that an investigation be carried out on the relationship between sonic transit time and pore pressure within the areas in which core data and other porosity logs are available. If such data does not exist, another approach would be to program a full suite of porosity logs (density, neutron and sonic), conventional and/or sidewall cores in a production well which is expected to drill a reservoir sandstone likely to be depleted.

Obviously, comparison of porosity tools responses and core porosity combined with a petrographic study will examine the effect of pore pressure on wave velocity in the well bore environment. The outcome may modify the proposed calibration of the sonic transit time for the pore pressure in the Toolachee Field and yield more accurate calibration in the other fields within the Cooper Basin.

Another way of investigating the effect of pressure depletion on the sonic log would be to record a second logging suite in cased hole, after the well has been on production for a while, and it becomes necessary to pull the production string. This logging suite could consist of a cement bond log (CBL), variable density log (VDL), casing collar locator (CCL) and gamma ray tool string, which is the standard cement bond log tool string. In addition, if the full waveforms are recorded, it will be possible to compute ΔT behind casing. This would not involve any cost in rigtime and a minimal incremental cost of logging. Comparison of the cement bond log-derived porosity with the open hole sonic porosity would give more information about the relationship between pressure depletion and sonic transit time.

6.2.2 ΔT CALIBRATION

A detailed laboratory study is recommended to precisely determine the V_p variation due to change in differential pressure in the sandstone reservoirs of the Patchawarra Formation in the Toolachee Field as well as other reservoirs in the Cooper Basin.

The wave velocity measurements should be made at different pore pressures for constant confining pressures on selected samples saturated with different fluids and different petrographic characters.

These experiments will provide data for the calibration of the sonic tool response to the pore pressure changes caused by production. Another output will be the empirical determination of the effective pressure factor n . Knowing the effective pressure factor is useful for determination of the in-situ stress state within a reservoir, and prediction of the variation of some stress-dependent reservoir properties such as permeability and deformation.

During the proposed experiments consideration might also be given to an investigation on the effect of gas and clay content versus porosity on the acoustic velocity, using a number of samples covering a wide range of porosities and clay contents, for the reservoir rocks of the study area. Although this investigation was not within the main objectives of the project, the outcome might modify the current methods of porosity calculation from the sonic log in the Cooper Basin.

REFERENCES

- Addis, MA and M.E. Jones, 1985, Volume change during diagenesis. *Marine Petrol. Geol.* Vol. 2, 241-45.
- Alsop, D. , 1990, The effect of diagenesis and facies distribution on reservoir quality in the Permian sandstones in the Toolachee Field. M.Sc Thesis, University of Adelaide, Australia, 83p.
- Anderson, B. , 1986, Analysis of some unresolved induction interpretation problems using computer modelling. *The Log Analyst* Vol. 27, 60-73.
- Apak, S.N. , W.J. Stuart and N.M. Lemon, 1993, Structural-stratigraphic development of the Gidgealpa-Merrimellia-Innaminka trend with implications for petroleum trap styles, Cooper Basin Australia. *Aust. Petrol. Explor. Assoc. J.* Vol. 33(1), 94-104.
- Apak, S.N, 1994, Structural development and control on stratigraphy and sedimentation the Cooper Basin northeastern South Australia and southwestern Queensland. PhD Thesis, University of Adelaide, Australia.
- Asquith, G. , 1982, Basic well log analysis for geologist. *Am. Assoc. Petrol. Geol. , Methods in Exploration Series No. 3*, 91-95.
- Asquith, G. , 1989, Log evaluation of shaly sandstone reservoirs: a practical guide. *Am. Assoc. Petrol. Geol. , Methods in Exploration Series No. 31*, p 15-16.
- Barber, T.D. , 1988, Induction vertical resolution enhancement - physics and limitation. SPWLA 29th Annual Logging Symposium, paper O.

- Bateman, R.M. , 1985, Open-hole log analysis and formation evaluation. D. Reidel Publishing Company, Boston USA, 647p.
- Bateman, R.M. , 1990, Thinbed analysis with conventional log suites. SPWLA 31st Annual Logging Symposium, paper II.
- Battersby, D.G. , 1976, Cooper Basin oil and gas fields. In Leslie, R.B. , H.J. Evans and C.L. Knight (eds.) Economical geology of Australia and New Guinea, 3. Petroleum Australia, Inst. Min. Metal. Monogr. 7, 321-70.
- Biot, M.A. and D.G. Willis, 1957, The elastic coefficient of theory of consolidation. J. Appl. Mech. Vol. 24, 594-601.
- Cant, D. , 1992, Subsurface facies analysis. In Walker, R.G. and N.P. James (eds.) Facies model response to sea level change, Geological Association of Canada, 27-45.
- Christensen, N.I. and H.F. Wang, 1985, The influence of pore pressure and confining pressure on dynamic elastic properties of Berea sandstone. Geophysics Vol. 50, 207-13.
- Davine, S.B. and C.G. Gatehouse, 1977, Sandstone reservoir geometry of non-marine sediments in the Toolachee Gas Field. Aust. Petrol. Explor. Assoc. J. Vol. 17(1), 50-57.
- Davis, J.C. , 1986, Statistics and data analysis in geology. John Wiley and Sons New York, 635p.
- Domato, B.W. and P.T. Male, 1992, Toolachee Field development plan. Santos Ltd. internal report, 73p.
- Exlog, 1981, Theory and evaluation of formation pressures, the pressure log reference manual. 186p.

- Falum, C. , 1987, Enhanced vertical resolution processing of dual detector gamma-gamma density logs. SPWLA 28th Annual Logging Symposium, paper Q.
- Faridi, H. and J.W. Hunt, 1987, Sedimentology facies analysis and hydrocarbon prospectivity of the Patchawarra Formation in the Nappaconage-Murteree and Toolachee Blocks. Delhi Ltd. internal report, 25-27.
- Fertl, W.H. , 1987, Log derived evaluation of shaly clastic reservoir. J. Pet. Tech. Vol. 39, 178-193.
- Frost, J.R. and W.H. Fertl, 1979, Integrated core and log analysis concept in shaly clastic reservoirs. The Log Analyst Vol. 22, 3-16.
- Gatehouse, C.G. , 1972, Formations of Gidgealpa Group in the Cooper Basin. Australian Oil and Gas Review 18:12, 10-15.
- Gregory, A.R. , 1976, Fluid saturation effects on dynamic elastic properties of sedimentary rocks. Geophysics Vol. 41, 895-921.
- Gregory, A.R. , 1977, Aspects of rock physics from laboratory and log data that are important to seismic interpretation. In Payton, C.E. (ed.), Seismic stratigraphy, application to hydrocarbon exploration, Am. Assoc. Petrol. Geol. Memoir 26, 15-46.
- Gretener, P.E. , 1981, Pore pressure: fundamental, general, ramifications and implication for structural geology (revised). Am. Assoc. Petrol. Geol. , Education Course Note Series No. 4, 131p.
- Han, De-hua, A. Nur, and D. Morgent, 1986, Effect of porosity and clay content on wave velocities in sandstones. Geophysics Vol. 51, 2093-2107.
- Harper, T.R. and D.C. Buller, 1986, Formation damage and remedial stimulation. Clay Minerals, Vol. 21, 735-51.

Hartman, D.J. , 1975, Effect of bed thickness and pore geometry on log response. SPWLA 16th Annual Logging Symposium, paper Y.

Heath, R. , 1989, Exploration in the Cooper Basin. Aust. Petrol. Explor. Assoc. J. Vol. 29(1), 366-378.

Hollingworth, R.J.S. , 1989, The exploration history and status of the Cooper and Eromanga Basins. In O'Neil, B.J. (ed.) the Cooper and Eromanga Basins, Australia. Proceedings of Petroleum Exploration Society of Australia, Society of Petroleum Engineers and Australian Society of Exploration Geophysics (SA Branches), Adelaide, 3-9.

Hottman, C.E. and R.K. Johnson, 1965, Estimation of formation pressure from log-derived shale properties. J. Pet. Tech. Vol. 17, 717-22.

Houseknecht, D.W. 1987, Assessing the relative importance of compaction processes and cementation to reduction of porosity in sandstones. Am. Assoc. Petrol. Geol. Bull. Vol. 71, 633-42.

Hunt, J.W. , R.S. Heath and P.E. Mckenzie, 1989, Thermal and maturity and other geological controls on the distribution and composition of Cooper Basin hydrocarbon. In O'Neil, B.J. (ed.) the Cooper and Eromanga Basins, Australia. Proceedings of Petroleum Exploration Society of Australia, Society of Petroleum Engineers and Australian Society of Exploration Geophysics (SA Branches), Adelaide, 509-23.

Jenkins, C.C. , 1989, Geochemical correlation of source rocks and crude oils from the Cooper and Eromanga Basins. In O'Neil, B.J. (ed.) the Cooper and Eromanga Basins, Australia. Proceedings of Petroleum Exploration Society of Australia, Society of Petroleum Engineers and Australian Society of Exploration Geophysics (SA Branches), Adelaide, 525-39.

- Johns, W.L. and B. Like, 1982, Some practical application to improve formation evaluation of sandstone in the Mackenzie Delta. SPWLA Shaly Sand Reprint Volume, chapter v, 47-79.
- Kantorowicz, L. , L. Lievarrt, J.G.R. Eylander and M.R. Eigner, 1986, The role of diagenetic studies in production operations. Clay Minerals Vol. 21, 769-80.
- Kappel, A.J. , 1966, The Cooper Creek Basin. Aust. Petrol. Explor. Assoc. J. Vol. 6(1), 71-5.
- King, M.S. , 1966, Wave velocities in rocks as a function of changes in overburden pressure and pore fluid saturation. Geophysics Vol. 31, 50-73.
- King, G.E., 1992, Formation clays: are they really a problem in production? In Houseknecht, D.W. and E.D. Pittman (eds.), Original, diagenesis and petrophysics of clay minerals in sandstones, SEPM Special Publication No. 47, 265-72.
- Laughrey, C.D. and J. Harper, 1986, Comparison of Devonian and Lower Silurian tight formation in Pennsylvania- geological and engineering. In Spencer G.W. and R.F. Mast (eds.), Geology of Tight Gas Reservoir, Am. Assoc. Petrol. Geol. Studies in geology No. 24, 9-43.
- Laws, R. A. , 1989, Preface. In O'Neil, B.J. (ed.) the Cooper and Eromanga Basins, Australia. Proceedings of Petroleum Exploration Society of Australia, Society of Petroleum Engineers and Australian Society of Exploration Geophysics (SA Branches), Adelaide, v-vi.
- Layle W.D. and D.M. William, 1986, Deconvolution of well log data: an innovative approach. SPWLA 29th Annual Logging Symposium, paper QQ.
- Marcus, G. , 1987, Toolachee Field: proved and probable gas in place. Santos Ltd. internal report, 22p.

MESA, 1991, South Australian energy resources. Fact sheets 4,5 and 6.

MESA, 1992, Petroleum exploration and development in South Australia. 8th edition, 96-101.

MESA, 1993, Petroleum exploration and development in South Australia. 9th edition, 84-7.

Minette, D. , 1990, Thin bed resolution enhancement: potential and pitfalls, SPWLA 31st Annual Logging Symposium, paper GG.

Morton, J.J. , 1983, The geology and reserves of the Toolachee Field Cooper Basin South Australia. South Australian Department of Mine and Energy, 3.

Morton, J.J. , 1989, Petrophysics of Cooper Basin South Australia. In O'Neil, B.J. (ed.) the Cooper and Eromanga Basins, Australia. Proceedings of Petroleum Exploration Society of Australia, Society of Petroleum Engineers and Australian Society of Exploration Geophysics (SA Branches), Adelaide, 153-171.

Morton, J.J. , 1990, Cooper Basin core and d log analysis for gas reserves assessment. NERDDP project No. 1033, 64p.

Nelson, R.J. and W.K. Mitchell, 1990, Improved vertical resolution of well logs by resolution matching. SPWLA 31st Annual Logging Symposium, paper JJ.

Northcott, I.W. and R.C.M. McDonough, 1989, TARDIS, a computer model to predict future gas supply. Aust. Petrol. Explor. Assoc. J. Vol. 29(1), 41-51.

Nur, A. and Z. H. Wang, 1988, Seismic and acoustic velocities in reservoir rocks experimental studies. Soc. Explor. Geophys. reprint series No. 10 Vol. 1, 1-9.

Overton, M. and N. Hamilton, 1986, A petrophysical review of unit fields, Cooper Basin South Australia. Santos Ltd. , internal report, 63p.

Pittman, E.D. and J.B. Thomas, 1979, Some application of scanning electron microscopy to the study of reservoir rock. J. Pet. Tech. Vol 31, 1375-80.

Pittman, E.D. and G.E. King, 1986, Petrology and formation damage control, Upper Cretaceous sandstone, offshore Gabon. Clay Minerals Vol. 21, 781-90.

Ploand, J.F. , 1972, Subsidence and its control. In Cook, T.D. (ed.) Underground waste management and environmental implication, Am. Assoc. Petrol. Geol. , Memoir 18, 50-71.

Porter, C.R. , 1972, Petrophysics of the Cooper Basin South Australia. Aust. Petrol. Explor. Assoc. J. Vol. 12, 23-27.

Raymer, L.L. , E.R. Hunt and J.S. Gardner, 1980, An improved sonic transit time -to-porosity transform. SPWLA 21st Annual Logging Symposium paper P.

Rider, M.H. , 1986, The geological interpretation of well logs. Blackie, Scotland, 175p.

Schulz-Rojahn, J.P. and S.E. Phillips, 1989, Diagenesis alteration of Permian Reservoir sandstones in the Nappamerri Through and adjacent areas, southern Cooper Basin. In O'Neil, B.J. (ed.) the Cooper and Eromanga Basins, Australia. Proceedings of Petroleum Exploration Society of Australia, Society of Petroleum Engineers and Australian Society of Exploration Geophysics (SA Branches), Adelaide. 629-45.

Schulz-Rojahn, J.P. , 1991, Origin, evolution and controls of Permian reservoir sandstones in the southern Cooper Basin, South Australia. PhD Thesis, University of Adelaide, Australia, 180p.

Spencer, G.W. and R.F. Mast, 1986, Geology of tight gas reservoirs. Am. Assoc. Petrol. Geol., Studies in geology No. 24, iv-vii.

Stanley, D.J. and G. Halliday, 1984, Massive hydraulic fracture simulation of Early Permian gas reservoirs Big Lake Field Cooper Basin. Aust. Petrol. Explor. Assoc. J. Vol. 24, 180-195.

Stuart, W.J. , 1976, The genesis of Permian and Lower Triassic reservoir sandstones during phases of southern Cooper Basin development. Aust. Petrol. Explor. Assoc. J. Vol. 16(1), 37-47.

Stuart, W.J. , B.B. Farrow, N.M. Lemon, P.R. Tingate, J.P. Schulz-Rojahn, S. Apak and P. Luo, 1992, Porosity and permeability in Permian sandstones southern Cooper Basin. ERDC Project No. 1407, Final Report, National Centre for Petroleum Geology and Geophysics, University of Adelaide, Australia, 200p.

Suau, T. , 1984, Interpretation of very thin gas sand in Italy, SPWLA 25th Annual Logging Symposium, paper A.

Thomas, A. , 1990, The diagenesis of Permian arenaceous and argillaceous units in the Moomba Gas Field, southern Cooper Basin. MSc. Thesis, University of Adelaide, Australia, 162 p.

Thornton, R.C.N. , 1979, Regional stratigraphic analysis of the Gidgealpa Group southern Cooper Basin Australia. Geol. Sur. S. Aust. Bul. 49, 140p.

Tingate, P.R. and P. Luo, 1992, Silica diagenesis and pore development in Permian sandstones southern Cooper Basin. Aust. Petrol. Explor. Assoc. J. Vol. 32(1), 325-337.

Todd, T. and G. Simmons, 1972, Effect of pore pressure on the velocity of compressional waves in low-porosity rocks,. J. Geophys. Res. Vol. 77, 3731-43.

Williams, B.P.J. , E.K. Wild and R.J. Suttill, 1985, Paraglacial aeolianites, potential new hydrocarbon reservoirs, Gidgealpa Group, Southern Cooper Basin. Aust. Petrol. Explor. Assoc. J. Vol. 25(1), 291-310

Wyllie, M.R. , A.R. Gregory and L.W. Gardner, 1956, Elastic wave velocities in heterogenous and porous media. Geophysics Vol. 21, 41-70.

Wyllie, M.R. , A.R. Gregory and L.W. Gardner, 1958, An experimental investigation of factors affecting elastic wave velocities in porous media. Geophysics Vol. 28, 459-93.

Yu, G. , K. Vozoff and D.W. Durney, 1991, Effect of pore pressure on compressional wave velocity in coals. Exploration Geophysics Vol. 22, 475-80.

APPENDIX A

SYMBOLS AND UNITS OF MEASUREMENTS

A1. SYMBOLS AND ABBREVIATIONS

ΔV_{sh}	Difference of Vsh Values
ρ	Bulk Density
β	Compressibility of Solid Grains
ϕ	Porosity
ΔP_p	Pressure Depletion
β_s	Compressibility of Bulk Material
$\mu s/ft$	Microsecond per Foot
ΔT	Sonic Transit Time
ΔT_{corr}	Corrected Sonic Transit Time
ΔT_f	Sonic Transit Time of Pore Fluid
ΔT_{log}	Sonic Log Value
ΔT_{ma}	Sonic Transit Time of Matrix
API	American Petroleum Institute Standard
BBL	Barrel
BBL/D	Barrel per Day
BCF	Billion(10^9) Cubic Feet
Cali	Caliper Log
CBL	Cement Bond Log

CCL	Casing Collar Locator
DST	Drill Stem Test
DT	Sonic Transit Time
Frac	Fraction
G	Gas Pressure Gradient
GAPI	API Gamma Ray Unit
GR	Gamma Ray Log
GR _{max}	Maximum Gamma Ray Log Value
GR _{min}	Minimum Gamma Ray Log Value
IGR	Gamma Ray Index
kb	Kilo (10 ³) Bar
KB	Kelly Bushing
LLD	Laterolog Deep
LPG	Liquid Petroleum Gas
MCFD	10 ³ Cubic Feet per Day
md	Millidarcy
MMCF/D	Million (10 ⁶) Cubic Feet per Day
MMSTB	Million (10 ⁶) Stock Tank Barrel
MPa	Mega (10 ⁶) Pascal
MSFL	Micro-Spherically Focused Log
<i>n</i>	Effective Pressure Factor
<i>n</i>	Sample Size
OHMM	Ohm Metre
P(z)	Initial Pore Pressure
P(z _o)	Pore pressure of Datum
P _c	Confining or Overburden Pressure
P _d	Differential Pressure
P _e	Effective Pressure
P _p	Pore Pressure

Prox	Proximity Log
psi	Pound Per Square Inches
r	Correlation Coefficient
RFT	Repeat Formation Test
SW	Water Saturation
t	t-Test Value
TCF	Trillion (10^{12}) Cubic Feet
VDL	Variable Density Log
V_f	Compressional Wave Velocity of Fluid
V_m	Compressional Wave Velocity of Matrix
V_p	Compressional Wave Velocity
Vsh	Volume of Shale
VSHDIF	Difference of the Filtered Shale Volume Curves
VSHF3	Short Filtered Shale Volume Curve
VSHF9	Long Filtered Shale Volume Curve

A2. SI METRIC CONVERSION FACTORS

$$\text{bar} = 10^5 \text{ Pa}$$

$$\text{bbl} = 1.59 \times 10^{-1} \text{ m}^3$$

$$\text{ft} = 3.048 \times 10^{-1} \text{ m}$$

$$\text{inch} = 2.54 \times 10^{-2} \text{ m}$$

$$\text{psi} = 6.896 \times 10^3 \text{ Pa}$$

APPENDIX B

LOG-CORE DEPTH MATCHING

All core logs used in this project have been recorded relative to driller's depth marked on the core boxes which show a depth discrepancy with wireline logs. To obtain the best possible matching of core and log data, a combination of all available wireline logs was used with core logs at a scale of 1 cm representing 1 foot. Sonic and gamma ray logs were used for lithology detection and shallow resistivity logs (MSFL or PROX) were used for bed boundary determination.

Using this method results in reliable depth matching compared with previous efforts, involving composite logs, Alsop (1990) and Morton (1990) where only gamma ray and sonic logs were used. The results of log-core depth matching for all cored wells in the Patchawarra Formation in the study area are included in Table B.1.

<i>WELL NAME</i>	<i>DRILLER'S DEPTH (ft)</i>	<i>DEPTH CORRECTION (ft)</i>
<i>TOOLACHEE-1</i>	6890-6907	+8
	6907-6958	+7
<i>TOOLACHEE-2</i>	6867-7077	+1
<i>TOOLACHEE-3</i>	7191-7251	+8
	7251-7311	+9
	7311-7369	+8
	7369-7467	+6
<i>TOOLACHEE-4</i>	7160-7296	+13
<i>TOOLACHEE-5</i>	7226-7424	+7
<i>TOOLACHEE-6</i>	7339-7556	+7
	7556-7586	+8
	7586-7646	+7
<i>TOOLACHEE-7</i>	7348-7403	-19
	7415-7528	-19
<i>TOOLACHEE-8</i>	7330-7390	-2
<i>TOOLACHEE-9</i>	7282-7341	+9
<i>TOOLACHEE-12</i>	7182-7213	+6
<i>TOOLACHEE-14</i>	7365-7347	+11
	7347-7395	+8
<i>TOOLACHEE-15</i>	7363-7393	+12
<i>TOOLACHEE-18</i>	7363-7345	+6
<i>TOOLACHEE-19</i>	7613-7643	+7
<i>TOOLACHEE-21</i>	7347-7356	+11
	7356-7377	+8

Table B.1 Driller's depth to logger's depth conversion in cored wells in the study area.

APPENDIX C

LIST OF DATA USED IN CHAPTERS FOUR AND FIVE

<i>Depth</i> (ft)	ΔT ($\mu s/ft$)	<i>Sonic</i> <i>Porosity</i> (%)	<i>Formation</i> <i>Pressure</i> (psi)	<i>Sandstone</i> <i>Reservoir</i>	<i>Clay</i> <i>Content</i> (fraction)	<i>KB</i> (ft)	<i>WELL Name</i>
6961.0	76.0	15.5	2693	74-4	0.1	194.38	TOOLACHEE-1
7218.0	83.0	16.1	3194	73-5	0.2	211.24	TOOLACHEE-10
7323.5	79.0	15.6	3204	74-6	0.1	211.24	TOOLACHEE-10
7413.0	79.9	14.3	3229	75-6	0.1	211.24	TOOLACHEE-10
7425.0	77.7	12.5	3216	75-6	0.0	211.24	TOOLACHEE-10
7459.0	70.2	8.7	3443	76-4	0.1	211.24	TOOLACHEE-10
7462.0	78.6	11.3	3235	76-4	0.1	211.24	TOOLACHEE-10
7464.0	76.7	13.1	3234	76-4	0.0	211.24	TOOLACHEE-10
7345.0	82.9	16.0	3175	74-4	0.1	224.15	TOOLACHEE-11
7376.0	75.2	11.5	3269	74-6	0.1	224.15	TOOLACHEE-11
7378.0	75.9	10.8	3270	74-6	0.3	224.15	TOOLACHEE-11
7389.5	80.0	13.2	3246	74-6	0.1	224.15	TOOLACHEE-11
7447.0	76.7	11.4	3278	75-6	0.2	224.15	TOOLACHEE-11
7460.0	83.9	15.7	3257	75-6	0.1	224.15	TOOLACHEE-11
7460.0	81.9	15.7	3262	75-6	0.1	224.15	TOOLACHEE-11
7464.0	83.5	16.4	3262	75-6	0.0	224.15	TOOLACHEE-11
7465.0	83.4	15.7	3260	75-6	0.0	224.15	TOOLACHEE-11
7505.0	78.3	12.5	3268	76-4	0.1	224.15	TOOLACHEE-11
7513.0	78.4	12.9	3269	76-4	0.1	224.15	TOOLACHEE-11

7521.0	76.7	11.9	3265	76-4	0.0	224.15	TOOLACHEE-11
7286.0	87.4	18.3	3192	74-4	0.0	180.06	TOOLACHEE-12
7294.0	80.0	14.7	3192	74-4	0.1	180.06	TOOLACHEE-12
7358.0	86.5	18.1	3200	74-6	0.1	180.06	TOOLACHEE-12
7365.0	85.0	17.1	3200	74-6	0.1	180.06	TOOLACHEE-12
7440.0	80.8	15.5	3229	75-6	0.0	180.06	TOOLACHEE-12
7444.0	80.0	14.4	3231	75-6	0.1	180.06	TOOLACHEE-12
7322.0	80.5	14.6	3229	74-4	0.2	235.66	TOOLACHEE-14
7325.0	79.0	14.6	3206	74-4	0.1	235.66	TOOLACHEE-14
7381.0	87.0	18.5	3219	75-6	0.1	200.04	TOOLACHEE-15
7387.0	90.0	19.1	3214	75-6	0.1	200.04	TOOLACHEE-15
7392.0	87.0	18.9	3217	75-6	0.1	200.04	TOOLACHEE-15
7395.0	87.0	18.9	3215	75-6	0.1	200.04	TOOLACHEE-15
7397.0	90.0	19.1	3215	75-6	0.1	200.04	TOOLACHEE-15
7204.0	78.0	13.5	3204	73-0	0.1	206.93	TOOLACHEE-18
7316.0	90.0	19.7	3202	74-6	0.0	206.93	TOOLACHEE-18
7316.0	90.0	19.7	3210	74-6	0.0	206.93	TOOLACHEE-18
7326.0	92.0	21.2	3194	74-6	0.0	206.93	TOOLACHEE-18
7326.0	92.0	21.2	3207	74-6	0.1	206.93	TOOLACHEE-18
7337.0	88.0	18.0	3181	74-6	0.1	206.93	TOOLACHEE-18
7337.0	88.0	18.0	3209	74-6	0.1	206.93	TOOLACHEE-18
7347.0	85.0	16.9	3184	74-6	0.0	206.93	TOOLACHEE-18
7347.0	85.0	16.9	3191	74-6	0.0	206.93	TOOLACHEE-18
7347.0	85.0	16.9	3203	74-6	0.0	206.93	TOOLACHEE-18
7478.0	79.0	13.2	3239	76-4	0.0	206.93	TOOLACHEE-18
7483.0	73.0	10.9	3224	76-4	0.1	206.93	TOOLACHEE-18
7092.0	72.0	9.9	3408	73-0	0.4	192.30	TOOLACHEE-32
7101.0	74.0	12.5	3258	73-0	0.3	192.30	TOOLACHEE-32
7126.0	72.0	10.0	3277	73-5	0.4	192.30	TOOLACHEE-32
7130.0	72.0	9.9	3258	73-5	0.3	192.30	TOOLACHEE-32
7193.0	74.0	11.8	3209	74-4	0.2	192.30	TOOLACHEE-32
7222.0	90.0	18.3	2867	74-6	0.0	192.30	TOOLACHEE-32

7234.0	82.2	16.7	2866	74-6	0.1	192.30	TOOLACHEE-32
7248.0	85.0	18.1	2865	74-6	0.1	192.30	TOOLACHEE-32
7175.0	80.0	14.9	3159	73-0	0.2	200.55	TOOLACHEE-34
7199.0	74.0	10.5	3641	73-0	0.3	200.55	TOOLACHEE-34
7229.0	78.0	12.1	3276	73-5	0.3	200.55	TOOLACHEE-34
7338.0	76.0	10.9	2968	74-6	0.3	200.55	TOOLACHEE-34
7347.0	87.9	19.3	2877	74-6	0.1	200.55	TOOLACHEE-34
7361.0	81.6	15.3	2878	74-6	0.1	200.55	TOOLACHEE-34
7360.0	68.0	7.2	3493	73-0	0.4	224.25	TOOLACHEE-35
7453.0	69.7	7.4	919	74-4	0.3	224.25	TOOLACHEE-35
7463.0	71.9	9.6	2081	74-4	0.0	224.25	TOOLACHEE-35
7465.0	72.5	10.0	2103	74-4	0.2	224.25	TOOLACHEE-35
7508.0	76.0	12.1	3000	74-6	0.0	224.25	TOOLACHEE-35
7516.0	78.0	13.3	2990	74-6	0.1	224.25	TOOLACHEE-35
7579.0	68.9	7.9	2702	75-6	0.2	224.25	TOOLACHEE-35
7586.0	71.0	8.4	2003	75-6	0.0	224.25	TOOLACHEE-35
7620.0	71.4	9.1	2555	76-4	0.0	224.25	TOOLACHEE-35
7655.0	74.0	10.9	2671	76-4	0.0	224.25	TOOLACHEE-35
6912.0	83.0	18.2	3085	73-0	0.0	210.39	TOOLACHEE-36
6915.0	73.0	10.3	3120	73-0	0.4	210.39	TOOLACHEE-36
6919.0	83.0	13.6	3088	73-0	0.1	210.39	TOOLACHEE-36
6941.0	75.0	11.5	2407	73-5	0.1	210.39	TOOLACHEE-36
6947.0	77.0	12.1	2395	73-5	0.1	210.39	TOOLACHEE-36
7224.0	78.0	12.8	3229	73-0	0.3	211.28	TOOLACHEE-38
7322.0	76.0	11.8	3396	74-4	0.2	211.28	TOOLACHEE-38
7322.0	76.0	11.8	3389	74-4	0.2	211.28	TOOLACHEE-38
7363.0	72.0	8.7	3540	74-6	0.4	211.28	TOOLACHEE-38
7369.0	76.0	10.8	2491	74-6	0.3	211.28	TOOLACHEE-38
7380.0	77.0	12.5	2474	74-6	0.1	211.28	TOOLACHEE-38
7383.0	78.0	10.7	2493	74-6	0.1	211.28	TOOLACHEE-38
7384.0	81.0	15.0	2477	74-6	0.1	211.28	TOOLACHEE-38
7386.0	73.0	11.6	2476	74-6	0.1	211.28	TOOLACHEE-38

7527.0	70.0	9.4	2407	73-0	0.1	254.60	TOOLACHEE-39
7532.0	71.0	9.7	2385	73-0	0.1	254.60	TOOLACHEE-39
7538.0	72.0	10.0	2316	73-0	0.1	254.60	TOOLACHEE-39
7552.0	78.0	12.2	3308	73-0	0.1	254.60	TOOLACHEE-39
7553.0	80.0	12.7	3306	73-0	0.1	254.60	TOOLACHEE-39
7581.0	71.0	9.2	3342	73-5	0.1	254.60	TOOLACHEE-39
7713.0	71.0	9.0	3119	74-6	0.1	254.60	TOOLACHEE-39
7717.0	71.0	9.0	3042	74-6	0.2	254.60	TOOLACHEE-39
7721.0	70.0	8.6	3091	74-6	0.1	254.60	TOOLACHEE-39
7738.0	69.0	8.3	3494	74-6	0.2	254.60	TOOLACHEE-39
7813.0	67.0	7.2	2176	75-6	0.1	254.60	TOOLACHEE-39
7827.0	65.0	5.9	2007	75-6	0.0	254.60	TOOLACHEE-39
7862.0	68.0	7.3	2930	76-4	0.1	254.60	TOOLACHEE-39
7891.0	69.0	8.0	2666	76-4	0.0	254.60	TOOLACHEE-39
7902.0	67.0	6.4	2663	76-4	0.1	254.60	TOOLACHEE-39
7923.0	79.0	13.0	2624	76-4	0.0	254.60	TOOLACHEE-39
8158.0	76.0	11.3	3580	81-6	0.3	254.60	TOOLACHEE-39
8160.0	78.0	13.3	3528	81-6	0.1	254.60	TOOLACHEE-39
8163.0	78.0	13.3	3537	81-6	0.1	254.60	TOOLACHEE-39
7190.0	80.9	14.6	3120	74-4	0.0	214.53	TOOLACHEE-41
7190.0	80.9	14.6	3119	74-4	0.0	214.53	TOOLACHEE-41
7200.0	82.8	15.7	3120	74-4	0.0	214.53	TOOLACHEE-41
7200.0	82.8	15.7	3119	74-4	0.0	214.53	TOOLACHEE-41
7206.0	80.2	14.6	3120	74-4	0.2	214.53	TOOLACHEE-41
7206.0	80.2	14.6	3119	74-4	0.2	214.53	TOOLACHEE-41
7228.0	76.6	12.4	2864	74-6	0.1	214.53	TOOLACHEE-41
7228.0	76.6	12.4	2863	74-6	0.1	214.53	TOOLACHEE-41
7236.0	76.1	12.2	2867	74-6	0.1	214.53	TOOLACHEE-41
7236.0	76.1	12.2	2866	74-6	0.1	214.53	TOOLACHEE-41
7244.0	78.5	13.6	2863	74-6	0.1	214.53	TOOLACHEE-41
7244.0	78.5	13.6	2862	74-6	0.1	214.53	TOOLACHEE-41
7226.0	82.4	15.9	3209	73-0	0.2	237.00	TOOLACHEE-42

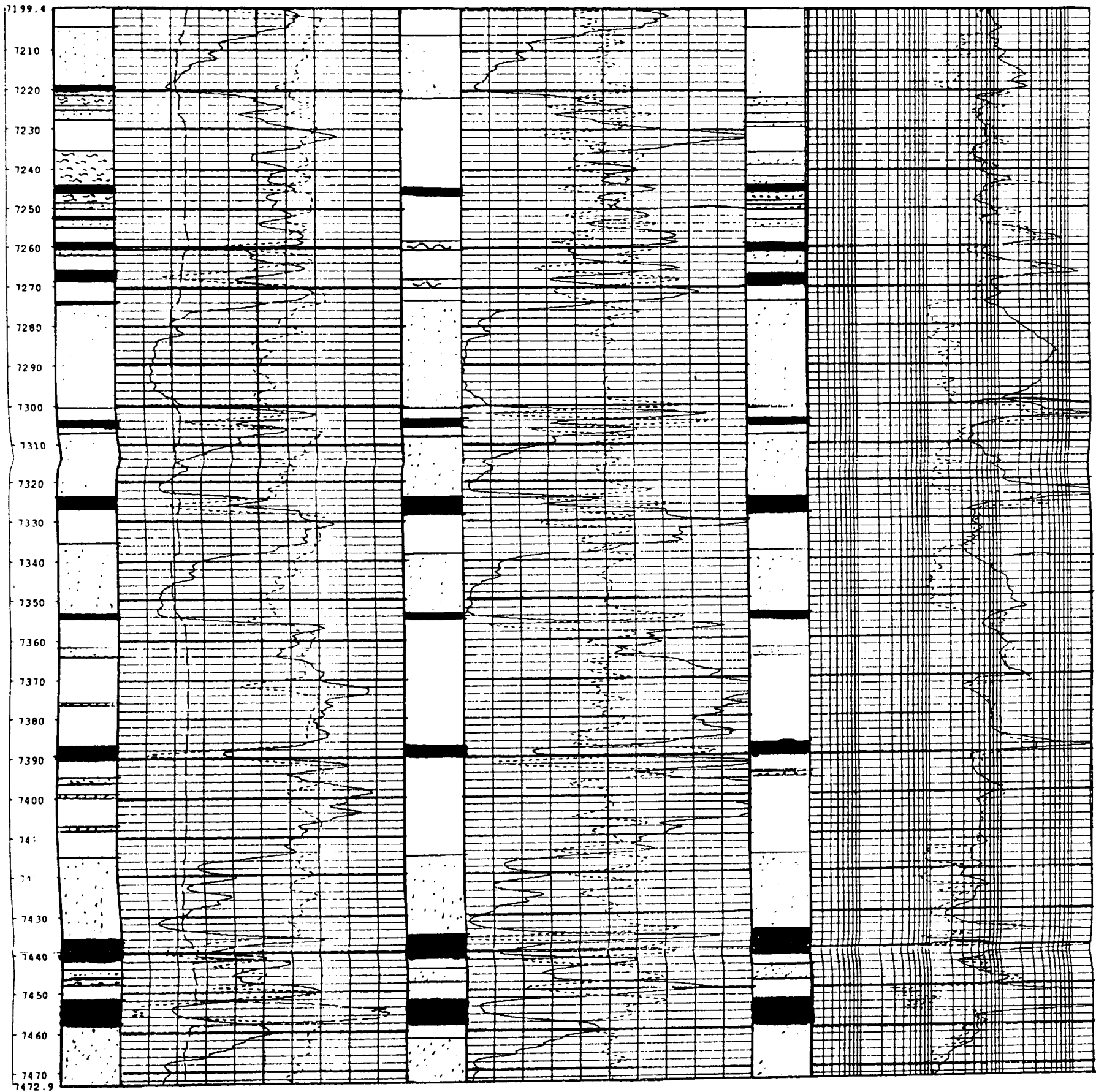
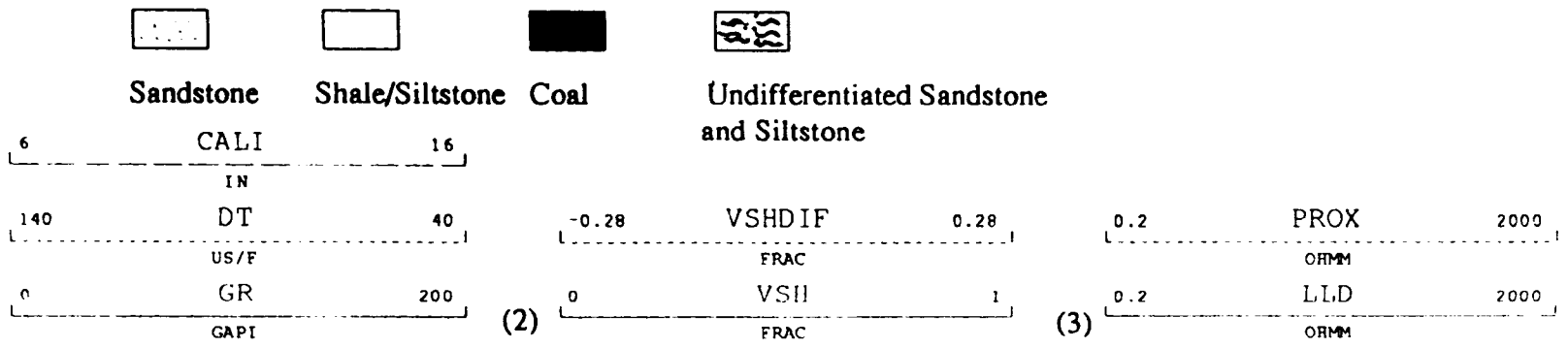
7228.0	80.9	14.7	3221	73-0	0.2	237.00	TOOLACHEE-42
7369.0	80.0	14.5	1699	74-6	0.1	237.00	TOOLACHEE-42
7373.0	79.5	14.1	1700	74-6	0.1	237.00	TOOLACHEE-42
7408.0	73.4	10.6	3287	75-5	0.1	237.00	TOOLACHEE-42
7409.0	72.9	10.3	3283	75-5	0.2	237.00	TOOLACHEE-42
7445.0	73.8	13.5	1454	76-4	0.1	237.00	TOOLACHEE-42
7456.0	78.1	13.0	1453	76-4	0.0	237.00	TOOLACHEE-42
7458.0	74.6	11.1	1452	76-4	0.0	237.00	TOOLACHEE-42
7466.0	79.9	14.0	1452	76-4	0.0	237.00	TOOLACHEE-42
7482.0	76.1	11.7	1453	76-4	0.0	237.00	TOOLACHEE-42
7495.0	78.0	13.1	1456	76-4	0.0	237.00	TOOLACHEE-42
7514.0	71.5	9.4	1471	76-4	0.1	237.00	TOOLACHEE-42
7309.0	76.8	12.4	3262	73-0	0.1	237.63	TOOLACHEE-43
7311.0	75.0	11.5	3271	73-0	0.0	237.63	TOOLACHEE-43
7312.0	77.6	13.0	3268	73-0	0.1	237.63	TOOLACHEE-43
7379.0	82.8	15.9	3307	73-5	0.2	237.63	TOOLACHEE-43
7442.0	80.5	14.8	3114	74-6	0.0	237.63	TOOLACHEE-43
7448.0	78.4	14.5	3116	74-6	0.0	237.63	TOOLACHEE-43
7456.0	78.4	13.5	3119	74-6	0.0	237.63	TOOLACHEE-43
7459.0	77.6	13.0	3117	74-6	0.0	237.63	TOOLACHEE-43
7173.0	79.1	13.7	1380	73-0	0.0	211.15	TOOLACHEE-45
7177.0	76.0	11.9	1379	73-0	0.0	211.15	TOOLACHEE-45
7210.0	79.1	13.9	1649	73-5	0.1	211.15	TOOLACHEE-45
7214.0	77.0	12.7	1500	73-5	0.1	211.15	TOOLACHEE-45
7264.0	77.4	12.9	3229	73-5	0.1	211.15	TOOLACHEE-45
7265.0	76.4	12.5	3229	73-5	0.1	211.15	TOOLACHEE-45
7323.0	78.3	13.4	2571	74-6	0.1	211.15	TOOLACHEE-45
7330.0	87.3	18.6	2566	74-6	0.0	211.15	TOOLACHEE-45
7412.0	76.2	12.2	1763	75-6	0.1	211.15	TOOLACHEE-45
7426.0	78.7	13.7	1752	75-6	0.1	211.15	TOOLACHEE-45
7448.0	73.2	10.5	2892	76-4	0.2	211.15	TOOLACHEE-45
7456.0	76.4	12.3	2928	76-4	0.1	211.15	TOOLACHEE-45

7476.0	84.0	16.5	2777	76-4	0.0	211.15	TOOLACHEE-45
7506.0	83.2	16.2	2690	76-4	0.0	211.15	TOOLACHEE-45
7195.0	71.7	9.4	3348	73-5	0.1	212.42	TOOLACHEE-46
7253.0	88.3	19.4	2752	74-4	0.1	212.42	TOOLACHEE-46
7207.0	74.3	11.4	1501	73-0	0.2	221.11	TOOLACHEE-47
7229.0	74.9	11.4	1568	73-5	0.1	221.11	TOOLACHEE-47
7231.0	78.9	13.8	1568	73-5	0.1	221.11	TOOLACHEE-47
7253.0	72.6	9.9	3311	73-5	0.2	221.11	TOOLACHEE-47
7260.0	77.6	13	3209	73-5	0.1	221.11	TOOLACHEE-47
7330.0	76.5	12.3	3238	74-5	0.2	221.11	TOOLACHEE-47
7350.0	78.2	13.2	2508	74-6	0.1	221.11	TOOLACHEE-47
7353.0	79.7	13.4	2509	74-6	0.3	221.11	TOOLACHEE-47
7400.0	74.3	11.1	3275	75-5	0.1	221.11	TOOLACHEE-47
7434.0	77.1	12.6	1770	75-6	0.0	221.11	TOOLACHEE-47
7446.0	75.6	11.8	1775	75-6	0.0	221.11	TOOLACHEE-47
7452.0	72.9	10.1	1778	75-6	0.0	221.11	TOOLACHEE-47
7475.0	80.2	15.2	2869	76-4	0.0	221.11	TOOLACHEE-47
7481.0	78.2	13.3	2869	76-4	0.0	221.11	TOOLACHEE-47
7494.0	76.2	12.2	2471	76-4	0.1	221.11	TOOLACHEE-47
7506.0	74.9	11.4	2474	76-4	0.0	221.11	TOOLACHEE-47
7517.0	70.5	8.8	2770	76-4	0.2	221.11	TOOLACHEE-47
7532.0	74.1	10.8	2760	76-4	0.0	221.11	TOOLACHEE-47
7274.0	71.0	9.1	1060	73-0	0.2	243.94	TOOLACHEE-48
7277.0	68.0	7.3	1063	73-0	0.2	243.94	TOOLACHEE-48
7426.0	75.0	10.3	2105	74-6	0.3	243.94	TOOLACHEE-48
7436.0	75.0	10.2	2105	74-6	0.3	243.94	TOOLACHEE-48
7498.0	70.0	8.5	1798	75-6	0.1	243.94	TOOLACHEE-48
7518.0	71.0	9.1	1799	75-6	0.1	243.94	TOOLACHEE-48
7547.0	72.0	8.6	2477	76-4	0.3	243.94	TOOLACHEE-48
7570.0	73.0	9.2	2491	76-4	0.2	243.94	TOOLACHEE-48
7592.0	80.1	14.4	2410	76-4	0.1	243.94	TOOLACHEE-48
7199.0	75.0	11.5	3259	73-0	0.2	209.83	TOOLACHEE-49

7267.0	71.0	9.1	2758	73-5	0.3	209.83	TOOLACHEE-49
7268.0	70.0	9.0	2760	73-5	0.3	209.83	TOOLACHEE-49
7325.0	77.0	11.3	2625	74-4	0.2	209.83	TOOLACHEE-49
7331.0	78.0	11.5	2605	74-4	0.2	209.83	TOOLACHEE-49
7369.0	82.0	15.6	2222	74-6	0.1	209.83	TOOLACHEE-49
7295.0	78.0	13.2	2508	73-0	0.1	257.01	TOOLACHEE-50
7299.0	82.0	15.6	2542	73-0	0.2	257.01	TOOLACHEE-50
7350.0	76.0	12.1	3303	73-5	0.1	257.01	TOOLACHEE-50
7389.0	73.0	10.3	2155	74-4	0.2	257.01	TOOLACHEE-50
7408.0	78.0	13.2	2151	74-4	0.1	257.01	TOOLACHEE-50
7444.0	80.0	14.5	2118	74-5	0.1	257.01	TOOLACHEE-50
7447.0	80.0	14.5	2118	74-5	0.1	257.01	TOOLACHEE-50
7474.0	63.0	4.4	2246	74-6	0.1	257.01	TOOLACHEE-50
7524.0	71.0	9.1	2779	75-5	0.1	257.01	TOOLACHEE-50
7526.0	70.0	8.5	2781	75-5	0.1	257.01	TOOLACHEE-50
7544.0	79.0	13.9	2613	75-6	0.1	257.01	TOOLACHEE-50
7559.0	81.0	15.0	2622	75-6	0.1	257.01	TOOLACHEE-50
7613.0	78.0	13.2	2682	76-4	0.1	257.01	TOOLACHEE-50
7637.0	74.0	10.9	2694	76-4	0.1	257.01	TOOLACHEE-50




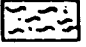
ENCLOSURE ONE

Comparison of lithology interpretation using binary and conventional methods with core lithology in the Patchawarra Formation in Toolachee 3 from 7199.4 to 7472.9 ft (Logger's depth, KB 221 ft). (1) Core lithology (from Alsop, 1990). (2) Conventional log-derived lithology (from Toolachee 3 composite log profile). (3) Binary lithology interpretation method (this study). Scale: 1 inch = 30 ft



ENCLOSURE THREE

Comparison of lithology interpretation using binary and conventional methods with core lithology in the Patchawarra Formation in Toolachee 6 from 7346.1 to 7652.6 ft (Logger's depth, KB 225 ft). (1) Core lithology (from Alsop, 1990). (2) Conventional log-derived lithology (from Toolachee 3 composite log profile). (3) Binary lithology interpretation method (this study). Scale: 1 inch = 30 ft

			
Sandstone	Shale/Siltstone	Coal	Undifferentiated Sandstone and Siltstone

6	CALI	16						
IN								
140	DT	40	-0.19	VSHDIF	0.25	0.2	PROX	2000
US/F								
0	GR	200	0	VSH	1	0.2	LLD	2000
GAPI								
(1)				(2)				(3)
			FRAC			OHMM		

